

How Do Amino Acids Transport Electrons Through Peptides?

Inaugural Dissertation

zur

Erlangung der Würde eines Doktors der Philosophie

vorgelegt der

Philosophisch-Naturwissenschaftlichen Fakultät

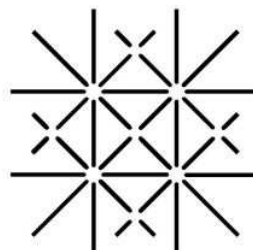
der Universität Basel

von

Meike Cordes

aus Mülheim an der Ruhr (Deutschland)

Basel 2008



**UNI
BASEL**

Genehmigt von der Philosophisch-Naturwissenschaftlichen Fakultät der Universität Basel
auf Antrag von

Prof. Dr. Bernd Giese

Prof. Dr. Helma Wennemers

Basel, den 25.03.2008

Prof. Dr. Hans-Peter Hauri

Dekan

Cover Picture: Cordes, M., Köttgen, A., Jasper, C. Jacques, O., Boudebous, H., Giese, B.: Influence of Amino Acid Side Chains on Long-Distance Electron Transfer in Peptides: Electron Hopping via "Stepping Stones", *Angew. Chem. Int. Ed.* 2008, 47, 3461.; Der Einfluss von Aminosäureseitenketten auf weitreichenden Elektronentransfer in Peptiden: Elektronenhopping mit Zwischenstationen, *Angew. Chem.* 2008, 120, 3511., Copyright Wiley-VCH Verlag GmbH & Co. KGaA. Reproduced with permission.

The work presented here was initiated and supervised by Prof. Bernd Giese at the Chemistry Department of the University of Basel, during the time period October 2004 to Februar 2008.

Excerpts from this work are published in:

Cordes, M., Jacques, O., Köttgen, A., Jasper, C., Boudebous, H., Giese, B.: **Development of a Model System for the Study of Long Distance Electron Transfer in Peptides**, *Adv. Synth. Cat.*, in press.

Cordes, M., Köttgen, A., Jasper, C. Jacques, O., Boudebous, H., Giese, B.: **Influence of Amino Acid Side Chains on Long-Distance Electron Transfer in Peptides: Electron Hopping via "Stepping Stones"**, *Angew. Chem. Int. Ed.* **2008**, *47*, 3461.; **Der Einfluss von Aminosäureseitenketten auf weitreichenden Elektronentransfer in Peptiden: Elektronenhopping mit Zwischenstationen**, *Angew. Chem.* **2008**, *120*, 3511.

The work was supported by:

Stiftung Stipendien Fonds, Verband der chemischen Industrie e.V.

Diese Arbeit ist meinem Freund Christian Wetter gewidmet.

einander zudrehen

einanderzudrehen und
aufeinandereinstellen

ineinandergreifen und
einandermitteilen

miteinanderdrehen und
voneinanderlösen

auseinanderkreisen und
einanderzudrehen

aufeinandereinstellen und
ineinandergreifen

einandermitteilen und
miteinanderdrehen

voneinanderlösen und
auseinanderkreisen

einanderzudrehen und

(Eugen Gomringer)

Ein Gleichnis

Wie wenn da einer, und er hielte
ein frühgereiftes Kind, das schielte,
hoch in den Himmel und er bäte:
„Du hörst jetzt auf den Namen Käthe!“ —
Wär dieser nicht dem Elch vergleichbar,
der tief im Sumpf und unerreichbar
nach Wurzeln, Halmen, Stauden sucht
und dabei stumm den Tag verflucht,
an dem er dieser Erde Licht ...
Nein? Nicht vergleichbar? Na, dann nicht!

(Robert Gernhardt)

Acknowledgements

I want to thank my supervisor Prof. Dr. Bernd Giese for providing me with a fascinating research topic and creating a work climate, which was governed by confidence, optimism and scientific curiosity. I would also like to thank Prof. Dr. Helma Wennemers for helpful discussions and for co-refereeing this thesis.

I am grateful to all former and present members of the Giese group, who contributed to this work: Dr. Christian Jasper and Dr. Agnieszka Köttgen were a tremendous help in the development of the syntheses of the building blocks. So was Dr. Olivier Jacques, who also had a patient ear and a helping hand for all technical and synthetical questions. Dr. Hassen Boudebous introduced me to the field of laser flash photolysis.

I would also like to thank Michael Kümin from the Wennemers group for his assistance with the peptide synthesizer and the CD spectrometer.

I want to thank the technical staff at the Departement of Chemistry, especially Dr. Klaus Kulicke for NMR-analysis, Dr. Heinz Nadig, who recorded the EI and FAB mass spectra, Werner Kirsch, who measured the elemental analyses and Dr. Sigmund Gunzenhauser for the tedious maintenance of the ESI mass spectrometer. I would like to thank the complete team of "Werkstatt" and "Materialausgabe" and also the secretaries, for furnishing the infrastructure of the departement.

My thanks go to the past members of the Giese group for leaving not only a tremendous amount of chemicals, but also of scientific knowledge behind and building up a friendly and cooperative tradition - and to the present members of the Giese group for keeping this tradition alive. It was a great pleasure to work with you.

I am especially grateful to my lab colleagues Stephan Buergi and Michael Graber who made lab work enjoyable and solved any upcoming problem, no matter if it concerned synthesis, office work or just motivation.

To Christian Wetter:

not only the correct angles in my schemes would be missing in this work, if you had not been there to help and support me during the last 3.5 years. Thank you.

Table of Contents

1	Introduction.....	3
2	Electron Transfer.....	4
2.1	Marcus Theory.....	4
2.2	Distance Dependence of Electron Transfer.....	5
2.3	Electron Transfer through Peptides.....	6
2.3.1	Superexchange.....	6
2.3.2	Hopping.....	10
3	Research Project.....	17
4	Spectroscopic Sensors for the Observation of Transients in ET through peptides.....	19
4.1	Introduction.....	19
4.2	Laser Flash Photolysis.....	21
4.3	Amino Acids as Spectroscopic Sensors.....	22
4.3.1	Synthesis and Properties of Methoxysubstituted Phenylalanine-Derivatives.....	26
5	Stability of Radical Cations.....	31
6	Occurrence of Oxidized Intermediates in ET through peptides.....	37
6.1	Introduction.....	37
6.2	Synthesis of Enantiopure Non-natural Amino Acids.....	38
6.3	Synthesis of Peptides.....	39
6.4	Data Collection and Analysis.....	42
6.4.1	Limitations.....	43
6.4.2	Analysis of the Data.....	46
6.5	Results and Discussion.....	48
7	Improving Charge Injection.....	57
7.1	Synthesis of a New Charge Injector.....	58
7.2	Synthesis of Peptides.....	60
7.3	Results and Discussion.....	63
8	Influence of Amino-Acid Side Chains on ET.....	67
8.1	Introduction.....	67
8.2	Structure.....	70
8.3	Results and Discussion.....	72
8.3.1	Mechanism of Electron Transfer.....	72
8.3.2	Electron Transfer Rates.....	79
9	The Phenylalanine Effect.....	83
10	Summary and Outlook.....	87
11	Experimental Part.....	89

Table of Contents

11.1	Conditions of Measurements	89
11.2	Synthesis	91
11.2.1	Materials, Solvents and Reagents.....	91
11.2.2	Notation.....	92
11.2.3	General Procedures (GP).....	93
11.2.4	Characterisation of Peptides.....	95
11.3	Compounds	96
11.4	List of LFP Experiments.....	135
12	Abbreviations	140
13	References	144

Introduction

Long range electron transfer (ET), i.e. the transfer of electrons across distances of 10 Å and more, is essential in all biological systems. In 1941 Szent-Györgyi reported a transfer of electrons between enzymes in the oxidation system.^[1] Yet regarding the insulating properties of the peptide matrix described by Evans and Gergely,^[2] with an energy gap between filled and empty bands in a polypeptide structure far too large for semiconductive properties at physiological temperatures, no simple explanation for the ability of living organisms to translocate electrons through enzymes could be found. Twenty years later, the importance of biological long range ET for the metabolism was confirmed by Mitchell, who proposed in his chemiosmotic hypothesis that during photosynthesis and respiration a flow of electrons is directed across the membrane dielectric, spanning a range of 35 Å.^[3] All living cells are therefore powered by the translocation of electrons - "the flow of electrons on oxidation-reduction reactions is responsible directly or indirectly for all of the work done in living organisms".^[4]

By now many examples for ET not only in enzymes involved in photosynthesis and respiration, e.g. photosystem II^[5] (PSII) and fumarate reductase,^[6] but also in metabolic catalysis, like prostaglandin H synthase^[7] and ribonucleotide reductase,^[8] are known and have been investigated in detail. Yet many questions remain to be answered regarding the factors that govern fast and selective distal ET in peptides.^[9] There is an ongoing discussion about the relative importance of superexchange and sequential mechanisms in biological ET. And while some information about the identity of the "stepping stones" in sequential ET could be obtained from molecular biology experiments, there is still not much known about the specific abilities of the 20 different natural amino acids to mediate protein ET.

1 Electron Transfer

1.1 Marcus Theory

A first theoretical model for the reaction of an electron donor D with an electron acceptor A was established by Marcus in the late 1950's.^[10, 11] In this model, the factors that control the ET reaction are the driving force $-\Delta G^0$, arising from the difference in the oxidation potentials of D and A, and the reorganization energy λ needed for the nuclear rearrangements that accompany ET. The ET rate k_{ET} can then be estimated as:

$$k_{ET} = k_{ET}(0) \exp\left[\frac{-(\lambda + \Delta G^0)^2}{4\lambda RT}\right]$$

Equation 1: classical Marcus theory, ET transfer rate k_{ET} as a function of reorganization energy λ and driving force ΔG^0 .

The factor $k_{ET}(0)$ represents the rate for activationless ET ($-\Delta G^0 = \lambda$). A graphical outline of the Marcus theory is given in Figure 1, showing a rate increase with increasing driving force in the Marcus normal region. A maximum rate is reached at $-\Delta G^0 = \lambda$. This contains the central lesson of the Marcus theory: for an ET event to occur in an efficient manner, available driving force and necessary reorganization energy have to be balanced. The energy needed to bring the nuclei from the equilibrium position of the reactants to the equilibrium position of the products (λ) has to be compensated by the driving force.

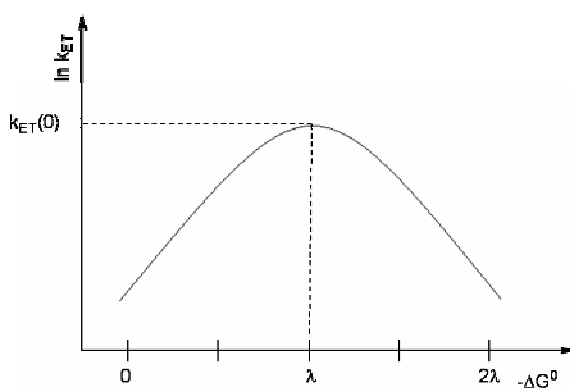


Figure 1: Dependence of ET rates on driving force and reorganisation energy according to the Marcus theory.

In addition to this intuitive coherency, the Marcus theory also predicts an "inverted region". For $-\Delta G^0 > \lambda$, the rate decreases with increasing driving force. Excess free energy has to be dissipated in order to allow ET.

1.2 Distance Dependence of Electron Transfer

The Marcus theory explains ET in cases, where electron donor D and electron acceptor A are in close contact. For cases, in which D and A are separated by a distance r , the occurrence of non-adiabatic ET can be explained by electronic coupling of D and A. An additional factor, the electronic coupling matrix element H_{AD} , was introduced into the Marcus theory by Levich.^[12] This changes Equation 1 to the following expression:

$$k_{ET} = \left(\frac{4\pi^3}{h^2 \lambda k_B T} \right)^{\frac{1}{2}} H_{AD}^2 \exp \left[-\frac{(\lambda + \Delta G^0)^2}{4\lambda RT} \right]$$

Equation 2: Marcus-Levich equation for non-adiabatic ET, describing the rate of electron transfer k_{ET} as a function of reorganisation energy λ , driving force ΔG^0 and electronic coupling between donor and acceptor H_{AD} .

with the square of the electronic coupling H_{AD}^2 giving the probability that an electron tunnels through the potential barrier between D and A. Since the height of the barrier is dependent on D/A-distance, the electronic coupling matrix element introduces a distance dependence into ET theory. The strength of electronic coupling of D and A decays exponentially with increasing D/A separation (Equation 3):

$$H_{AD} = H_{AD}^0 e^{-\beta(r_{DA} - r_0)}$$

Equation 3: Distance dependence of the electronic coupling element H_{AD} , with r_0 representing the close-contact donor/acceptor distance.

The importance of the separating medium for the strength of electronic coupling is expressed by the exponential factor β in Equation 3. When D and A are separated by a matrix, the ability of this matrix to mediate the electronic coupling influences the efficiency of ET. The importance of the exponential factor β increases with increasing D/A-distance.

1.3 Electron Transfer through Peptides

As could be seen in paragraph 1.2, the characteristics of a matrix separating electron donor (D) and electron acceptor (A) are of great importance for the efficiency of ET processes between D and A. The distance decay factor β in the extended Marcus theory for non-adiabatic ET is a measure for the ability of the matrix to mediate electronic coupling between D and A. In vacuum β is estimated to $3 - 5 \text{ \AA}^{-1}$, in water to 1.65 \AA^{-1} .^[13] With β -values of this order, the tunneling of electrons across distances of 10 \AA would take several million years, according to the classical theory. Since electrons are transferred through active enzymes across distances of 20 \AA and more with rates in the millisecond range,^[14] it can be concluded that the peptide matrix is able to support ET between distal redox-partners in a highly efficient manner. Two major models are discussed to explain the specific ET properties of peptides: the superexchange and the hopping model.^[15]

1.3.1 Superexchange

Already in 1949 Evans and Gergely^[2] pointed out that semiconductivity can be excluded as an explanation for ET through peptides since the energy gap is far too large to be overcome at physiological temperatures. An alternative explanation for efficient ET through enzymes was suggested by DeVault and Chance, who measured the temperature dependence of cytochrome oxidation in *Chromatium vinosum*,^[16] and found the reaction rates to show a very weak temperature dependence. They proposed a mechanism based on electron tunneling. A model for the kinetics of ET between proteins by a thermally activated tunneling process was then described by Hopfield,^[17] who predicted a distance decay constant β of 1.44 \AA^{-1} .

The superexchange - or tunneling - model is based on the idea that the orbitals of the bridge molecules are mixed with the donor and acceptor orbitals to increase electronic coupling between donor and acceptor. A simple model for ET across a bridge consisting of n identical repeat units was developed by McConnell. In this model, the charge transfer from the electron donor D to the electron acceptor A occurs in a single-step via a virtual intermediate state, constructed by mixing of the orbitals of D, bridge elements B, and A (Figure 2). The coupling element H_{DA} (see 1.2) thus is a function of the coupling between the redox sites and the bridge, the coupling between the bridge elements, and the energy gap between the tunneling electron and the reduced bridge states δE .^[18]

Mixing of all available electronic states lowers the potential barrier and thereby increases the tunneling probability H_{AD}^2 . The ET rate is increased, as compared to the transfer rate in vacuum, by an improved electronic coupling, which is expressed by a lowered value of the distance-decay factor β (see Equation 3).

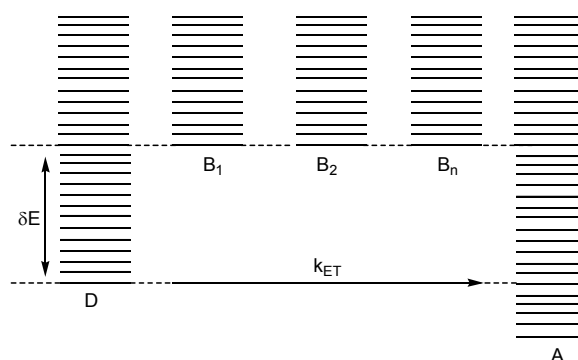


Figure 2: energy diagram for superexchange ET across a bridge of n identical units B_n (McConnell)

Since peptides can be built up from 20 different amino acids, the simple McConnell model cannot be applied in this case. A semiempirical approach by Dutton is based on the observation that ET rates through different types of proteins (reaction centres of different photosynthetic bacteria and several synthetic and semisynthetic proteins) are almost identical for similar D/A-distances. Dutton therefore concludes that the influence of peptide sequence is small and that ET pathways are optimized only in terms of distance, not in terms of peptide structure. In consequence, he regards the peptide matrix as a uniform barrier and estimates the β -value to 1.4 \AA^{-1} .^[19, 20] A rough estimate of structural differences has been taken up into a refined version of Dutton's uniform barrier model, which includes the packing density of the protein matrix as an additional factor.^[21] Yet bioinformatic investigations revealed no major difference in protein packing density between long-distance and short-distance electron transfers. This leads back to the central hypothesis of Dutton's model: the belief, that in the course of evolution large effects of structural changes in ET proteins would have been highly unfavourable and that nature therefore preferred ET-proteins to be robust when it comes to structural and sequence changes. As a consequence of this demand, the peptide matrix is equipped with a mainly uniform ET behaviour, controlled by cofactor distances, and not optimized with respect to ET properties in special enzymes.^[22]

This view has been challenged by Gray and Winkler, who measured ET rates in modified proteins.^[14, 23] They used naturally occurring metalloproteins with copper (azurin)^[24] or iron (cytochrome)^[25] cofactors and with known crystal structures and attached a ruthenium-complex to specific histidine residues at defined distances. ET was then induced by photoexcitation of the ruthenium chromophore, and subsequent rapid oxidation by an external acceptor (flash-quench-technique). The rates of ET from the metal cofactor to the oxidized ruthenium complex were measured by absorption spectroscopy of the transient metal complexes. The original oxidation state was then recovered by a slow reaction with the reduced quencher (Figure 3). This method spans a wide time frame for the measurement of ET rates ranging from sub-microseconds to seconds.^[13]

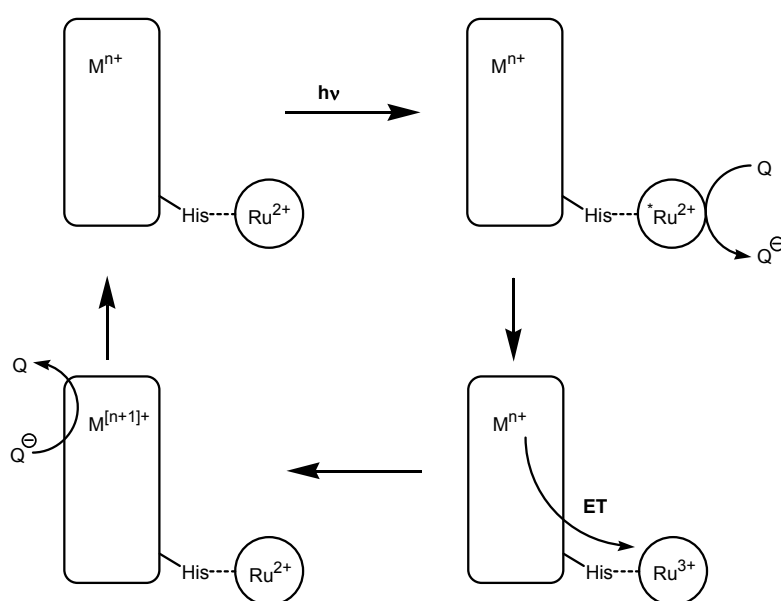


Figure 3: Flash-quench technique for the induction and observation of ET in Ru-modified metalloproteins

The method was used to gain a large collection of experimental data from different classes of modified metalloproteins. From the azurin series, a timetable for ET through proteins that proceeds according to the tunneling model, with rates in the microsecond range for ET across 15-20 Å and a β -value of 1.1 \AA^{-1} for a β -strand, was derived.^[13] Nevertheless, in several cases, ET velocities cannot be explained by D/A distances alone: ET rates for similar D/A distances can differ by several orders of magnitude and similar rates can be observed for distances that differ by as much as 5 Å.^[26] Gray and Winkler therefore concluded, that the structure of the peptide matrix is the main factor controlling ET rates.

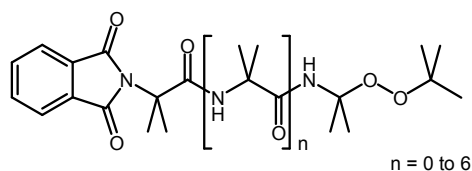
Based on the experimental data, a more complex theoretical model, which takes protein secondary structure into account, has been proposed by Beratan and Onuchic.^[27-29] It is built on the assumption, that pathways of optimized electronic coupling exist, which are composed of covalent bonds, H-bridges and through-space contacts. For each of these links a specific coupling decay (ϵ_c , ϵ_H , ϵ_S) is assigned and the electronic coupling element H_{AD} can be determined as the product of all couplings in a specific pathway (Equation 4).

$$H_{AD} \propto \prod \epsilon_C \prod \epsilon_H \prod \epsilon_S$$

Equation 4: The electronic coupling element in the pathway model is given as the product of coupling through covalent bonds ϵ_C , H-bonds ϵ_H and through space contacts ϵ_S .

Modern computational techniques in combination with available protein structure data allow a search of all possible pathways to identify the optimum pathway. Using this method, a good agreement between theory and the experimental data for the ET rates observed in modified metalloproteins can be achieved.^[30] The model also allows predictions concerning the ET properties of secondary structure motifs. In recent work, the pathway model has been further refined by taking the effects of protein dynamics into account.^[14, 31-33] The key determinant of biological ET in the pathway model, as opposed to the uniform-barrier model, is the protein fold.

Electrochemical measurements of oligopeptidic systems with α -aminoisobutyric acid (Aib) as the peptide matrix, a phthalimid as N-terminal electron donor and peroxide as C-terminal electron acceptor (Scheme 1), carried out by Maran and coworkers, support the pathway theory.^[34] They found increasing rates with increasing number n of spacer amino acids and attributed this unexpected effect to an increase in intramolecular H-bonding, leading to an improved electronic coupling. Following their argumentation, an increase in n does not only lead to an increased donor/acceptor separation, but also to a concomitant increase in the number of intramolecular H-bonds in the 3_{10} -helix formed by Aib-oligomers.^[35]



Scheme 1: Oligopeptidic model system designed for electrochemical measurement of ET rates by Maran et al.

In summary, in superexchange ET, migration of the charge from the donor to the acceptor is enhanced by bridge-mediated mixing of donor and acceptor wave functions, and occurs in a single step. The

exponential decrease of ET rates with increasing D/A distance is characteristic of the superexchange mechanism, with the magnitude of the exponential decay constant β depending on the ability of the bridging matrix to mediate electronic coupling. The coupling strength of peptides is either regarded as the result of a network of covalent bonds, H-bridges and through-space contacts (pathway model) or as a structure-independent feature of these organic supramolecules (uniform barrier).

1.3.2 Hopping

Since the driving forces in naturally occurring ET are relatively low, a practical upper distance-limit for the superexchange mechanism exists. Dutton regards a distance of 14 Å as the upper limit of efficient ET by superexchange.^[20] Gray and Winkler set the maximum tunneling distance to 20Å.^[13] Dutton proposes the alignment of metal-containing redox-cofactors, especially Fe-S-clusters and hemes, in enzymes involved in ET cascades, as a possible solution to allow transfer steps of more than 14 Å overall distance.^[20] If the distances between these cofactors stay below the limit of superexchange ET, a sequence of tunneling steps can be used to transfer the electron. Such a stepwise process is known as multistep tunneling or electron hopping.

The hopping model for ET has first been developed for DNA. It stems from the observation that DNA is a very efficient charge-carrier and that the efficiency of charge transfer scales with the number of guanine base pairs. The experimental data on ET through DNA double strands, collected by Barton and coworkers,^[36] Giese and coworkers,^[37, 38] and Lewis and Schuster and coworkers,^[39, 40] could not be explained by the superexchange theory. The electron coupling properties of DNA are in a range expected for organic matrices, with β -values from 0.6 to 1.2 Å⁻¹ and cannot rationalize the highly efficient distal ET. However, the guanine base pairs with their low oxidation potential, offer the possibility to form oxidized chemical intermediates in the ET process. ET between D and A can thus proceed in a multistep process with the DNA-bases serving as stepping stones, which allows short distances (and thus high transfer rates) for each step. This results in overall ET rates for which the exponential D/A-distance dependency, predicted from the superexchange theory, does not apply. Instead, the rate scales algebraically with distance and is a function of the number of intervening base pairs n . The theoretical treatment of Bixon and Jortner:^[41-43]

$$k_{ET} \propto k_{ib} n^{-1}$$

Equation 5: Hopping model for DNA. The rate of electron transfer k_{ET} as a function of the number of intervening base pairs n .

with k_{ib} giving the rate of interbase ET and η taking values between 1 and 2, has been confirmed experimentally by work of Giese and coworkers.^[44]

The main characteristic of sequential electron transfer (hopping) is the occurrence of chemical intermediates, oxidized (or reduced) relays R. The charge is transferred from the donor D to a localized relay site R on the bridge, then passed through the bridge by a number of adjacent oxidation/reduction reactions, before it finally reaches the acceptor A. An important characteristic of this model is the possibility of endergonic transfer steps (Figure 4).^[20, 45]

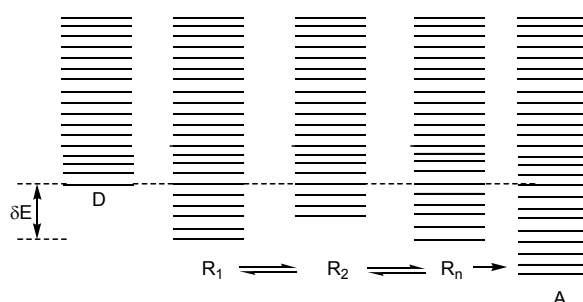


Figure 4: Energy diagram for sequential ET with relays R that allow the occurrence of oxidized intermediates.

A sequential ET mechanism is now generally accepted for electron transport during photosynthesis, with the electron hopping from the reaction-centre (P680) to chlorophyll and subsequently to pheophytin. Similar sequential transfer chains, using redox cofactors as relays, have been proposed for other ET pathways in biology,^[21] e.g. in *E. coli* fumarate reductase electrons are relayed over more than 30 Å, presumably using a chain of Fe-S clusters.^[6]

But in a number of proteins, electrons have to be transferred across large distances without the presence of specially designed redox cofactors. An intensively studied enzyme is the class I ribonucleotide reductase (RNR), which catalyses the conversion of nucleotides into the deoxynucleotides needed for the construction of DNA, and is therefore essential in all organisms. In this enzyme, an electron is transferred between two homodimeric subunits across a distance of more than 35 Å, from a cysteine residue (Cys439) in the active site of subunit R1 to a diiron-tyrosyl (Tyr122) radical cofactor in subunit R2, generating the thiyl-radical responsible for the catalytic activity of RNR (Figure 5).^[46]

A transfer of the electron by a single-step superexchange mechanism can be excluded, since it would be slow and limit the rate of nucleotide-conversion to $10^{-4} - 10^{-9} \text{ s}^{-1}$, whereas the observed turnover number for class I RNRs are measured to $2-10 \text{ s}^{-1}$.^[46] An ET hopping pathway, using aromatic amino acids as relays, has been proposed in this enzyme.^[47, 48]

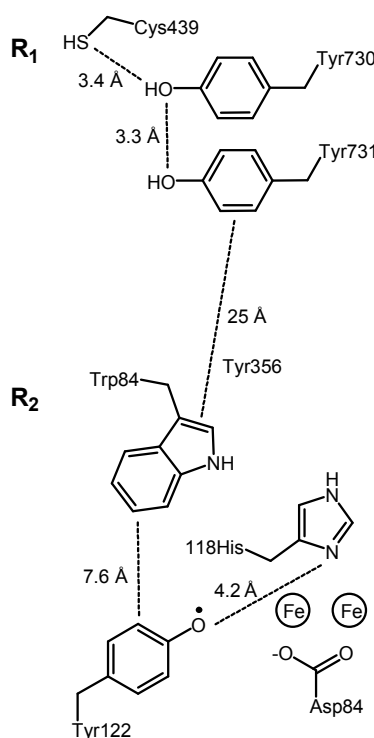


Figure 5: Aromatic residues possibly involved in ET through RNR.

In vitro and in vivo mutagenesis studies have proven the aromatic amino acids depicted in Figure 5 to be essential for enzyme function.^[49] Substitution of Tyr356 by fluorinated tyrosine residues of higher oxidation potential led to a loss of enzyme function.^[50] This is a strong argument in favor of a sequential mechanism, since the energy needed to form oxidized intermediates in the bridge is the main factor determining the relative magnitude of superexchange versus hopping mechanism.^[15, 45]

The enzyme DNA photolyase is another example, in which aromatic amino acid side chains are thought to operate as "stepping stones" in electron hopping.^[51, 52]

In short-time spectroscopic studies of *E. coli* type I photolyase, the tryptophane residues Trp382, Trp359 and Trp306 have shown to be oxidized during electron transfer from the flavine adenine nucleotide (FAD) cofactor in the enzyme active site to a second redox active cofactor located close to the protein surface (Figure 6).^[53]

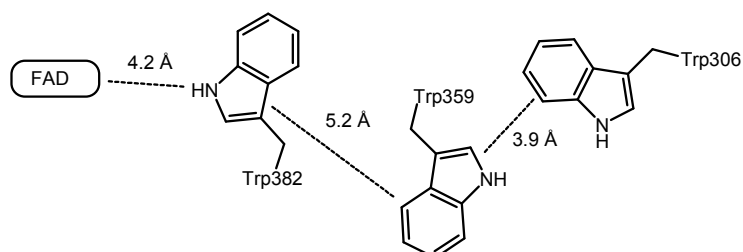


Figure 6: Tryptophane residues participating in ET through type I DNA photolyase

From this experimental data it can be concluded that amino acid side chains possibly operate as relays in sequential ET and that, in consequence, not only secondary structure but also amino acid sequence has to be considered in the explanation of protein ET. Aromatic amino acids as oxidized intermediates might thus expand the theory of specifically designed sequential redox-chains^[20] to enzymes that lack the redox-active metal containing cofactors present in photosynthesis and respiration. Even in enzymes with a high cofactor-density, like PSII, aromatic amino acid residues are discussed as additional intermediates in ET processes.^[54] From the relay stations assumed in the DNA photolyase (Figure 6), it can moreover be deduced that sequential ET might already come into play at distances that are in principle short enough to be overcome by monostep tunneling.

Whether electron hopping does also occur in peptides without aromatic residues as relays, is a question still under discussion. Peptide bonds have been proposed as possible relay sites by Schlag. He developed a model for stepwise ET through peptide bonds, in which the bond-angles, i.e. peptide dynamics, are of central relevance.^[55, 56]

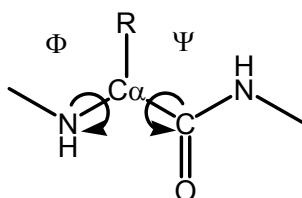
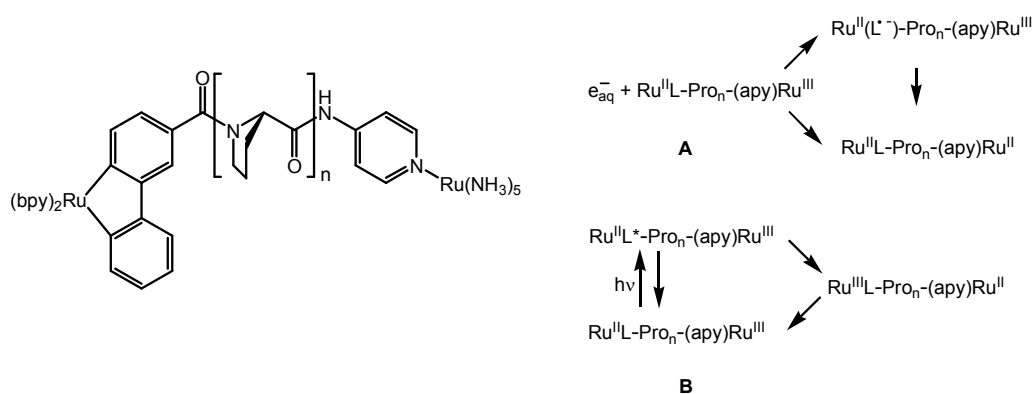


Figure 7: Ramachandran angles in a peptide

He observed facile migration of a positive charge, generated by photosensitization of an aromatic chromophore, through small peptides in the gas phase. The distance and direction of charge migration depended strongly on the ionization potentials of the individual amino acids in the peptide chain – not

on the overall ionization potential of the supramolecule. Based on these observations, Schlag concluded that the charge is transferred via a stepwise mechanism. He calculated the energy barriers for ET between adjacent amino acid residues and found them to be strongly dependent on the torsional angles of the peptide bond, Φ and Ψ , the Ramachandran angles (Figure 7). According to his theory, ET through a peptide chain is preceded by the arrangement of adjacent peptide bonds into a favorable angle, which minimizes the distance between neighbouring CO groups to 2.8 Å and allows a subsequent fast oxidation reaction (firing).^[55, 57]

The experiments on oligopeptides synthesized by Isied and coworkers also point towards the possibility of electron hopping, even without the presence of oxidizable aromatic side chains. They have developed an experimental system to measure the distance dependence of ET rates in oligoproline, in which ET in a Creutz-Taube analogon containing two ruthenium centres, is induced by pulse radiolysis **A** or flash photolysis **B** (Scheme 2). The ET reaction can be monitored by absorption spectroscopy of the transient metal complexes. From the measured rate differences upon variation of spacer length, Isied concluded, that a mechanistic transition from superexchange (exponential distance dependence) to hopping (linear distance dependence) takes places, starting from a length of 5 proline residues.^[58]



Scheme 2: Oligoproline model synthesized by Isied for distance dependent ET measurements

A linear distance dependence for ET has also been observed by Kraatz and coworkers in oligoglycine self-assembled monolayers, in which ET rates between ferrocene and a gold-electrode were measured electrochemically.^[59, 60] Yet though there is, in addition, spectroscopical data available, that points towards amide participation in ET through peptides,^[61] the occurrence of oxidized peptide bonds as intermediates seems to be unfavourable, due to the high activation energy needed to permit such an oxidation reaction.^[13]

An explanation for the observation of unexpected ET behaviour upon peptide-spacer elongation, is through-space electron transfer. In contrast to the superexchange theory discussed in paragraph 1.3.1, the peptide bridge orbitals are not involved in mediating ET in this model.^[62] Instead, ET occurs directly between D and A, either by direct D/A orbital overlap, or by participation of solvent molecules. Through-space ET has been discussed especially in the context of experiments on small peptides in solution. Peptide models for the measurement of ET based on oligoproline units as spacers have been developed among others by Meyer^[63, 64] and Giese.^[65] The weak dependencies of ET rates on the number of separating proline units observed in those systems, point to through-space ET as the dominant pathway.

In summary, the sequential or hopping mechanism for ET is characterized by the temporary localization of the electron on the bridge, i.e. it requires the existence of oxidized chemical intermediates. ET rates exhibit only a weak (linear) distance dependence and are strongly dependent on the oxidation potentials of the bridging units (relays). Endergonic steps are possible in sequential ET. Traveling of the electron between the possible redox-sites can occur via through-bond or through-space steps. Metal-cofactors are known to assist in long-range peptide electron transfer through enzymes involved in photosynthesis and respiration. Long-range ET is, however, also observed in enzymes that do not possess suitable cofactor-arrangement. A hypothesis currently studied is the function of aromatic amino acid side chains as hopping relays in such enzymes.

2 Research Project

The aim of this work was to contribute to the investigation of sequential ET via oxidizable amino acid side chains. Information about the role of individual amino acid side chains in ET through peptides should be gained. The advantage of a small model systems in this context is the modular design, that allows the fast synthesis of peptides which differ in parameters relevant for ET, like distances and driving forces. And, in comparison with molecular biology approaches, the possibility to replace individual amino acids without completely shutting down ET activity. Moreover, the spectroscopic observation of intermediates is less restricted by a smaller matrix.

For these reasons, an oligopeptidic model should be designed, that allows the site selective injection of a charge into a peptide, generating an electron acceptor site A, and the subsequent observation of charge migration to an electron donor site D. An amino acid, suitable to serve as a relay for stepwise ET should be placed between D and A (Figure 8). So far, the differentiation between superexchange and hopping mechanism in model peptides has been achieved by measurement of distance dependencies, which are expected to be exponential for superexchange and linear for sequential ET. Yet the structural flexibility of small peptides in solution is a limitation of this approach, since D/A edge-to-edge distances vary significantly for different peptide conformers. A straightforward approach to overcome this problem is the incorporation of an additional spectroscopic sensor into the model, that allows the detection of chemical intermediates and thus provides direct proof of the hopping mechanism.

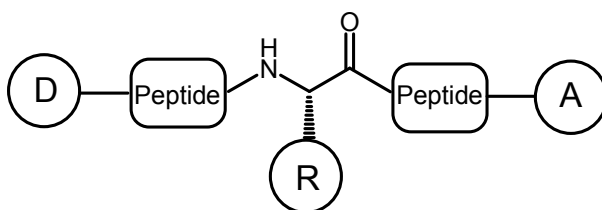


Figure 8: Schematic design of a peptide model for the observation of sequential ET via the relay R

We designed an aromatic amino acid R, to function as a central redox relay and spectroscopic sensor. Using this approach, a peptide should be developed, in which stepwise intramolecular ET can be induced and subsequently observed time-dependently, using orthogonal spectroscopic properties of D, R and A. This design results in a number of experimental restrictions concerning the electrochemical and spectroscopical properties of D, A and R, that will be discussed in detail in chapter 3.3. Another difficulty stems from the fact that the concentration of the intermediate depends on the relative rates of the transfer steps $D \rightarrow R$ and $R \rightarrow A$. The synthesis of peptides with different D/R and R/A distances was therefore likely to be necessary in the search for a system with appropriate rate ratios to observe the

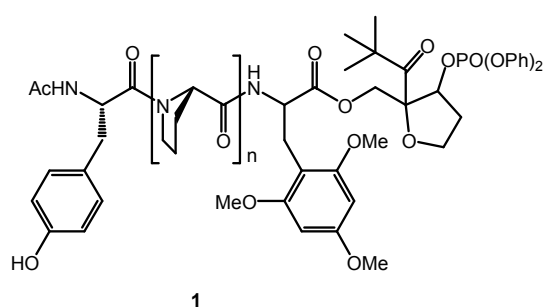
oxidized intermediate. Replacement of R by side chains, which can not serve as relays and/or do not produce observable intermediates, should then yield information about the importance of the relay for ET. This leads to additional restrictions concerning the structure of the peptides. Structural uniformity among a peptide series with different relays R has to be guaranteed to allow comparability of the results. In other words: replacing R should show only minor effects on the overall structure, yet allow the observation of effects on intramolecular ET efficiency. A system, in which those conditions can be met, allows the investigation of the role of amino acid side chains in ET through peptides. In addition, quantitative information about the individual rates might be derived from the spectroscopic measurements.

In summary, a peptide model should be developed, in which a) sequential ET can be directly observed, b) the role of individual amino acid side chains in this transfer can be investigated, c) information about ET rates can be gained.

3 Spectroscopic Sensors for the Observation of Transients in ET through peptides

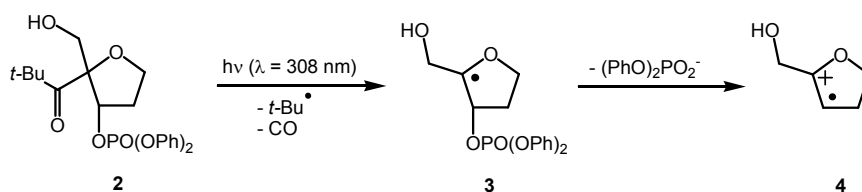
3.1 Introduction

A peptide model **1** that allows the site selective generation of an oxidized aromatic amino acid side chain at the C-terminus of an oligopeptide and the subsequent time-resolved spectroscopical observation of ET from an N-terminal electron donating amino acid, was synthesized in the Giese group by Napp (Scheme 3).^[65, 66]



Scheme 3: Napp-system for the observation of ET through peptides

In this peptide, a charge injection system **2**, similar to the one developed in the Giese group to study the transfer of a positive charge through DNA,^[67, 68] was placed at the C-terminus of the oligopeptide via ester-linkage. Irradiation of **2** with a laser flash of 308 nm leads to Norrish-type-I photocleavage of the ketone functionality. The resulting radical **3** subsequently undergoes heterolytic β -elimination of the phosphate group and yields radical cation **4** (Scheme 4). A major advantage of this injection system is the generation of radicals in the electronic ground state. ET reactions can thus be observed without side reactions stemming from photoexcited intermediates.

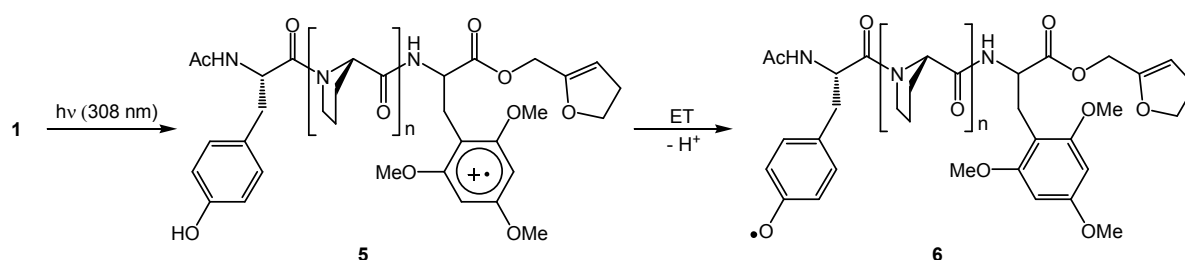


Scheme 4: Photoinduced radical cation generation

The mechanism of the injection reaction leads to several requests regarding the reaction conditions for laser flash photolysis (LFP) measurements. They have to be carried out in an oxygen-free environment, because oxygen addition to radical **3** is a fast side reaction, leading to formation of the peroxide and quenching the intended radical cation formation. Moreover polar solvents are necessary,

to ensure a fast dissociation of the phosphate leaving group from the remaining radical cation **4**.^[69, 70] A 3:1 mixture of acetonitrile and water has been found to offer optimum reaction conditions with respect to injector function and peptide solubility.

With an oxidation potential of estimated 1.29 – 1.44 V vs. NHE,^[71] radical cation **4** is able to oxidize the aromatic side chain of the adjacent amino acid in peptide **1** and thus generate an electron acceptor in the oligopeptide, yielding the transient **5**. Radical cation **5** can be observed by transient absorption spectroscopy, with an absorption maximum at 550 nm. This signal vanishes by ET from tyrosine, which deprotonates upon oxidation and yields a tyrosyl radical **6**, with an absorption maximum around 410 nm^[72] (Scheme 5).



Scheme 5: Electron transfer through an oligoproline chain in the Napp-model

Napp noticed, that the introduction of non redox-active amino acid residues between the trimethoxysubstituted phenylalanine and the injection moiety leads to a severe drop in signal intensities. This can be explained by a side reaction of radical cation **4**, the water-addition reaction, which comes into play when ET between **4** and the aromatic ring is slower than $8 \cdot 10^6 \text{ s}^{-1}$. A short linkage between the oxidizable amino acid and the injector is therefore needed to ensure fast injection and prevent side reactions of **4**.^[66] Peptide model **1** was used for time-resolved measurements of ET **5** → **6** in molecules with different oligoproline spacers ($n = 0, 1, 3, 5$). As a result, the rates for intramolecular ET, extracted from the decay of the transient absorption at 550 nm (**5**), depended only weakly on the spacer length, with rates ranging from $8.6 \cdot 10^6$ for direct D/A linkage ($n = 0$) to $2.7 \cdot 10^5$ for $n = 5$. This led to the conclusion, that ET occurs in a through-space mechanism, not via through-bond tunneling (cf. paragraph 1.3, page 15). The small effect of spacer-elongation on the rate might be rationalized by the flexibility of the peptide structure, due to rotational freedom around the C_α - CH_2 -bond of the aromatic residues and the resulting existence of peptide conformers with short D/A-distances. Molecular modeling experiments for **1** with $n = 5$, with the peptide backbone conformation fixed to the all-*trans* polyproline II structure, showed distance variations for the aromatic residues of more than 5 Å.^[66]

In summary, peptide model **1** can be used for the direct observation of ET through a peptide matrix. ET can be assumed to occur in a through-space mechanism.

3.2 Laser Flash Photolysis

The method of laser flash photolysis (LFP) offers several advantages for the analysis of photogenerated ET reactions through peptides. Since peptides with specific absorption properties can be designed by the choice of amino acid side chains, the rates of ET can be derived directly from the transient spectra. Neither photoproduct analysis nor the comparison of observed rates with competing side reactions is necessary.^[73] ET processes were induced by irradiation of peptide solutions with a laser flash of 308 nm wavelength, 20 ns pulse duration and an energy of 100 – 130 mJ. The flash was generated by a XeCl-excimer laser and directed to a UV-cuvette (Figure 9), that allowed for degassing of the sample and storage under vacuum. Orthogonal to the laser a pulsed Xe-lamp provided the light needed to record a UV-Vis spectrum of the sample.

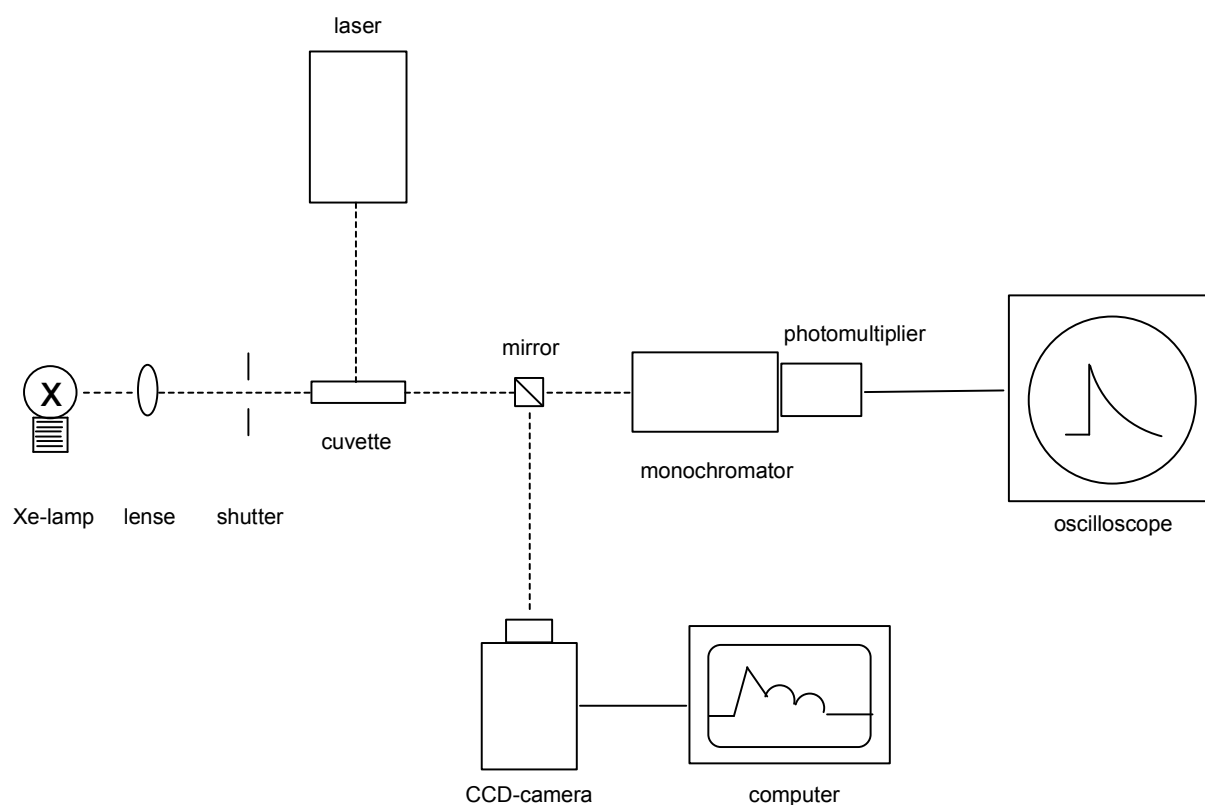


Figure 9: Experimental setup for laser flash photolysis.

Two detection systems could be used: a photomultiplier allowed time-resolved measurements of absorption at a defined wavelength. Processes with rates up to $3 \cdot 10^7 \text{ s}^{-1}$ could be resolved. With a CCD-camera and a fast electronic shutter the complete transient absorption spectrum between 300 and 650 nm could be measured after a defined time-delay.^[74-76]

The concentration of the sample may not exceed 8 mM because the optical density (OD), i.e. the UV-absorption of the peptide sample at the wavelength of laser-irradiation, should be below 0.5 to guarantee homogeneous photoreaction properties. Because of the low efficiency of Norrish-

photocleavage of the *tert*-butylketone injection moiety, the signal intensities dropped below detection limits at sample-concentration of less than 1 mM. Therefore, the experiments discussed in this work were carried out at concentrations of 1 – 8 mM.

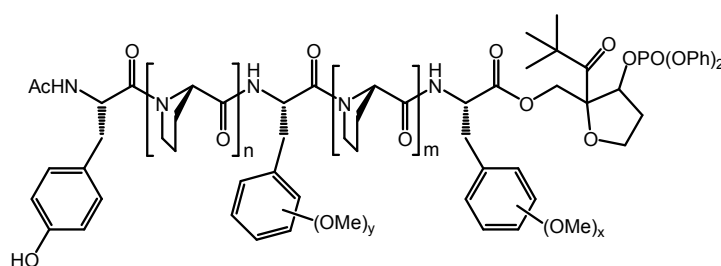
3.3 Amino Acids as Spectroscopic Sensors

A model peptide should be designed, in which the oxidation of three residues, functioning as inducible electron acceptor A, final electron donor D and relay amino acid R, leads to observable transients. To this end, model system **1** (Scheme 3), should be extended by an additional oxidizable amino acid residue (Figure 8, page 17).

Tyrosine was kept as a suitable final electron donor, because oxidation of tyrosine is accompanied by an irreversible deprotonation reaction. The long-lived tyrosyl radical with its low oxidation potential (0.93 V vs. NHE)^[77] thus provides a thermodynamic sink for the electron hole, suppressing back ET and reducing intermolecular side reactions. In addition, the transient absorption spectrum of tyrosyl radical shows a sharp band,^[78] leaving a broad spectral range for the detection of other intermediates.

Oligoprolines served as spacing units, since proline oligomers are known to form stable helices starting already from 3 units,^[79] and prolines do not form H-bridges, so that electronic coupling properties depend on the number of spacer units in a less complex way than in the Aib-system used among others by Maran (see 1.3.1, Scheme 1).

Electron acceptor and relay amino acid were chosen to be methoxysubstituted phenylalanines, because the radical cations of those aromatic systems are known to give absorption signals in the UV-Vis region^[80, 81] and can thus be monitored by laser flash photolysis (LFP) experiments as described in paragraph 3.2.



Scheme 6: Design of the extended peptide model.

The design of the resulting peptide is depicted in Scheme 6: tyrosine as the N-terminal donor is separated from the C-terminal injection system by a peptide matrix, containing the electron acceptor precursor situated close to the injection system as the C-terminal amino acid, an additional central aromatic amino acid, and two oligoproline spacers, separating the aromatic rings.

To choose the right substitution pattern for the non-natural methoxysubstituted phenylalanines, several conditions have to be taken into account:

1. the redox potentials of the aromatic rings should be between 1.3 V vs. NHE (injector radical cation **4**)^[71] and 0.93 V vs. NHE (Tyr).^[77] Though endergonic steps are in principle possible in electron hopping,^[20, 45, 51] the transfer chain should be designed as a sequence of downhill steps. Thus, attention had to be paid to the relative oxidation potentials of acceptor and relay as well.
2. The transient absorption maxima of the generated oxidized species should be located at different wavelengths, to allow the simultaneous observation of all oxidized intermediates. In addition, the extinction coefficients of acceptor and relay radical cation as well as the tyrosyl radical should be of comparable magnitude, so that good resolution of all three signals is possible.
3. The amino acids used in the construction of the peptide model should be transparent at the wavelength of laser irradiation, 308 nm, to avoid a loss in photocleavage efficiency as well as possible side reactions of photoexcited intermediates.

2,4,6-Trimethoxyphenylalanine has already served as a sensor in ET through peptides and is thus known to meet conditions **1** and **3**. Dimethoxybenzenes with 1,3 and 1,4 substitution pattern were examined on their suitability to supplement the tyrosine/trimethoxyphenylalanine system, with focus on the conditions described above.

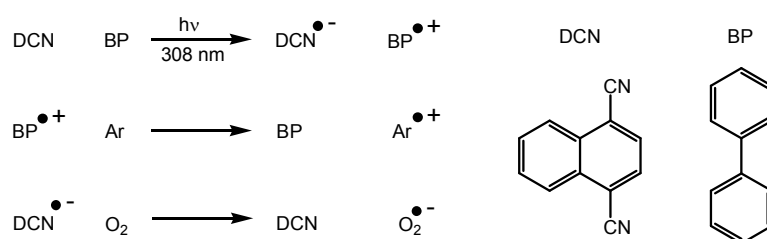
ad 1: The redox potentials of methoxysubstituted benzenes could be extracted from the literature. The oxidation potential of 1,3,5-trimethoxybenzene, the side chain of the amino acid used by Napp in the model system **1**, is given with 1.46 - 1.49 V vs. SCE;^[82-84] 1,3-dimethoxybenzene with 1.49 V - 1.6 V vs. SCE^[82, 85, 86] and 1,4-dimethoxybenzene with values ranging from 1.34 to 1.51 vs. SCE.^[82, 83, 85, 86] So the oxidation potentials of all possible candidates fall in a range suitable to serve as relays in ET between the injector radical cation **4** (1.54 vs. SCE) and tyrosine (1.17 vs. SCE).

ad2:

In addition to the literature values available for the absorption maxima of the radical cations (1,3-dimethoxybenzene: 477 - 505 nm, 1,4-dimethoxybenzene: 443 - 475 nm),^[82] photosensitization experiments were carried out to allow direct comparison of the radical cation absorptions. For this purpose, 1 mM concentrations of 1,3-dimethoxybenzene and 1,4-dimethoxybenzene were irradiated with dicyanonaphthalene (DCN) as a photosensitizer and biphenyl (BP) as a codonor in air saturated acetonitrile. Electron rich aromatic compounds can be photooxidized under these conditions.^[81, 87]

The reaction starts with the excitation of DCN. Subsequent fast ET from BP generates the BP radical cation, which is able to oxidize electron rich aromatic compounds (Ar). DCN is then regenerated by

reaction with oxygen (Scheme 7). The transient absorption spectra of the formed aromatic radical cations were measured after a delay of 500 ns. (Figure 10).



Scheme 7: Photosensitization to generate aromatic radical cations Ar^{•+} from the respective aromates.

While the absorption maximum of the para substituted dimethoxybenzene radical cation (grey line) stretches from 430 nm to 460 nm, the meta substituted derivative (black line) has its maximum absorption between 445 and 475 nm.

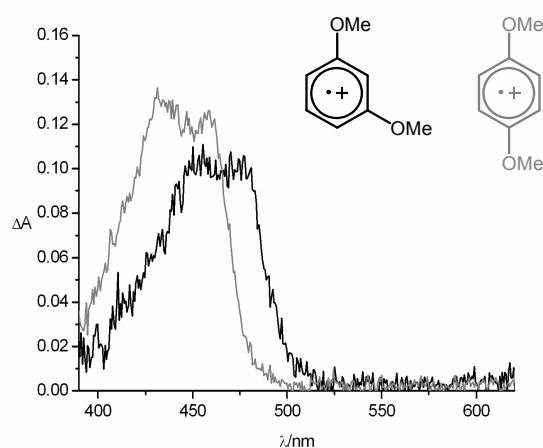


Figure 10: Transient absorption spectra recorded after oxidation of 1,3-dimethoxybenzene (black) and 1,4-dimethoxybenzene (grey) by photosensitized electron transfer with 1,4-dicyanonaphthalene as a sensitizer and biphenyl as a codonor.

Both radical cations yield a transient absorption spectrum that can be differentiated from the spectrum of the tyrosyl radical ($\lambda_{\text{max}} = 410$ nm) and the trimethoxyphenylalanine radical cation ($\lambda_{\text{max}} = 550$ nm).

ad3: Since peptide concentrations in the LFP measurements have to be in the millimolar range, due to the low absorption coefficient of the injector chromophore, the transparency of the chosen amino acid residues at the wavelength of laser irradiation is of crucial importance. UV-spectra of 1,3-dimethoxybenzene and 1,4-dimethoxybenzene were therefore recorded at 8 mM concentrations in acetonitrile.

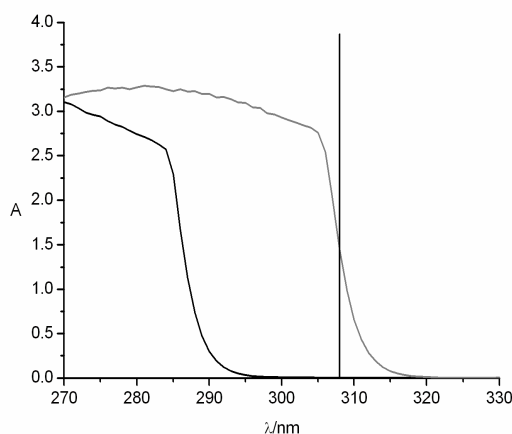
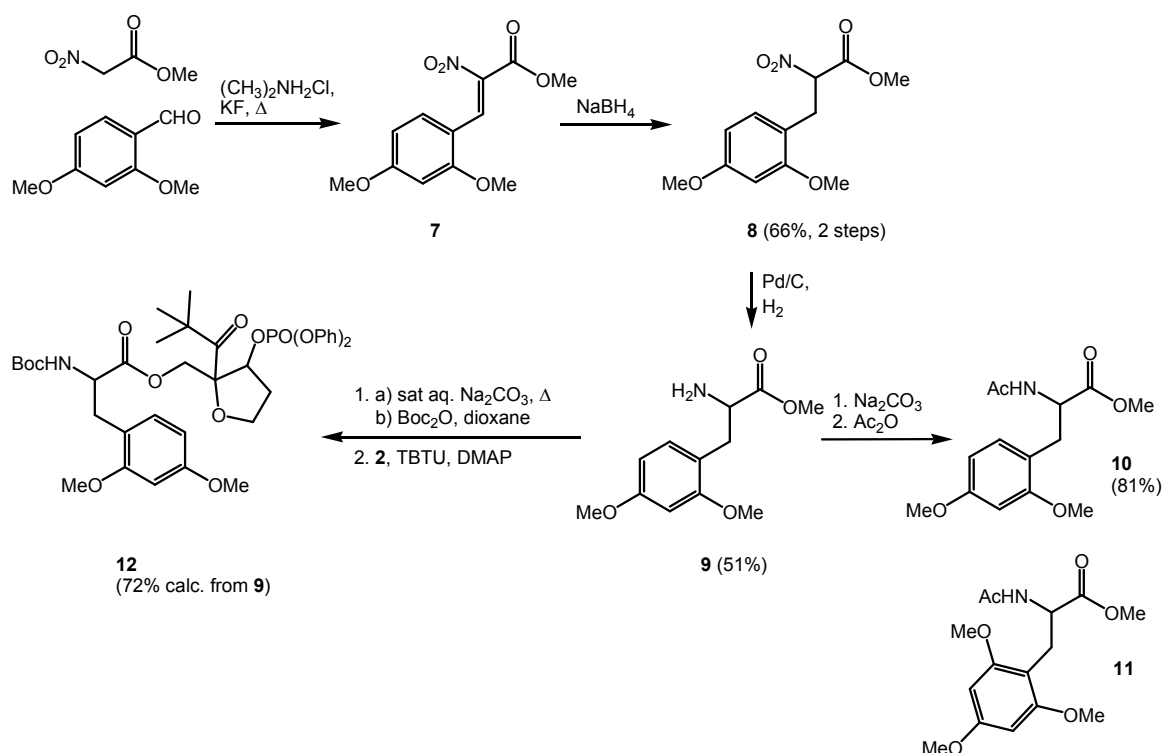


Figure 11: UV-spectra of 1,3-dimethoxybenzene (black) and 1,4-dimethoxybenzene (grey) 8 mM in acetonitrile.

The vertical line in Figure 11 indicates 308 nm. It is obvious from the graphs that the para substituted dimethoxybenzene has to be excluded as a candidate for one of the non-natural amino acids needed to construct a peptide model containing three oxidizable spectroscopic sensors (Scheme 6). 1,3-dimethoxybenzene was therefore chosen together with the already established 1,3,5-trimethoxybenzene as an appropriate aromatic side chain for the acceptor resp. relay amino acid.

3.3.1 Synthesis and Properties of Methoxysubstituted Phenylalanine-Derivatives

To check, whether the electrochemical and spectroscopical data available for the substituted benzenes does also apply to the corresponding amino acids, a fast synthetic route to the racemic substituted phenylalanines,^[88] established by Napp,^[66] was used.



Scheme 8: Synthesis of racemic 2,4-dimethoxyphenylalanine and coupling to the injector moiety.

Condensation of substituted aromatic aldehyde with nitro-acetic acid-methylester in the presence of dimethylaminhydrochloride leads to *E/Z*-mixtures of α -nitro-acrylic acid-methylester **7**, which was reduced with NaBH_4 without further purification to yield nitropropionic acid **8** in 66% yield. Subsequent reduction of the nitrofunction leads to the methyl ester **9** of the substituted phenylalanine in 51% yield. The fully protected amino acid derivative **10** used for cyclovoltammetry and photosensitization experiments could be synthesized by acetylation with acetic anhydride and sodium carbonate as a base. The synthesis of the trimethoxysubstituted analogue **11** is described in detail in ref. [88] and [66]. Saponification of **9** in saturated aqueous sodium carbonate solution at 40 °C and subsequent *tert*-butyloxycarbonyl (Boc) protection gave the N-protected free acid, which could be coupled to primary alcohol **2**, in an esterification reaction, using 2-(1H-benzotriazole-1-yl)-1,1,3,3-tetramethyluronium tetrafluoroborate (TBTU) and 4-(dimethylamino)-pyridine (DMAP) as activators, to yield **12** in 72%.

The injector moiety **2** was prepared in 7 steps starting from pivaldehyde with a 1,3 dipolar cycloaddition of a nitrileoxide to furane as the key step, according to synthesis protocols developed in the Giese group.^[66, 89, 90]

The redox potentials of the aromatic amino acids were measured by differential pulse cyclovoltammetry, using acetonitrile as a solvent and ferrocene as internal standard (Figure 12).

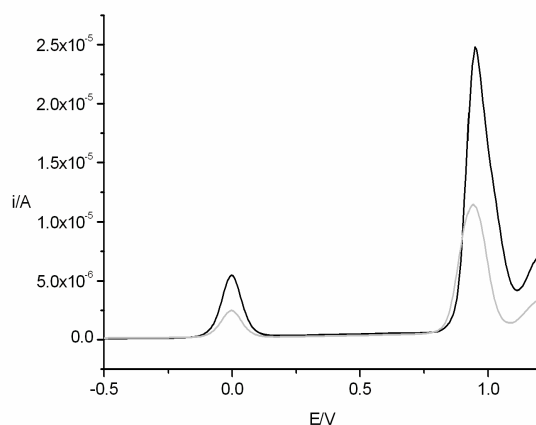


Figure 12: Differential pulse cyclovoltammetric measurement of Ac-2,4-dimethoxyphenylalaninemethylester **10** (black) and Ac-2,4,6-trimethoxyphenylalaninemethylester **11** (grey) 2mM in acetonitrile with 100 mM tetrabutylammonium hexafluorophosphate (TBAPF₆) as electrolyte and ferrocene as internal standard.

The potentials referring to ferrocene are 0.95 V for 2,4-dimethoxyphenylalanine **10** and 0.94 V for 2,4,6-trimethoxyphenylalanine **11**. In comparison, we measured the potential of N-Acetyl-tyrosine-methylester to amount to 0.85 V vs. the ferrocene redox couple. This equals the value determined by Harriman in water (pH 7) of 0.93 V vs. NHE.^[77]

The UV-Vis spectra of compounds **10** and **11** in acetonitrile (Figure 13) clearly show, that there are no absorption bands above 300 nm, so that peptide absorbance will not interfere with photocleavage of the injector.

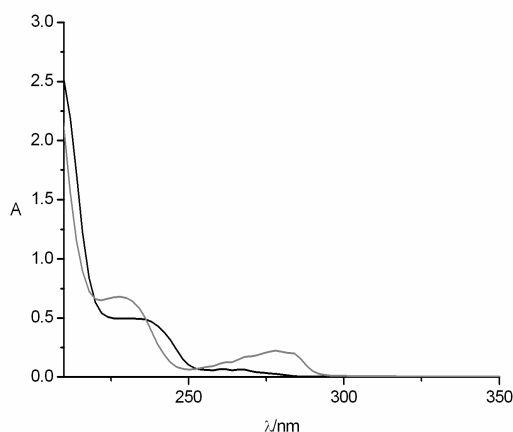


Figure 13: UV-Vis spectra of Ac-2,4-dimethoxyphenylalaninemetylester **10** (black) and Ac-2,4,6-trimethoxyphenylalaninemetylester **11** (grey); 20 μM in acetonitrile.

To investigate the spectroscopical properties of the radical cation of the newly introduced 2,4-dimethoxyphenylalanine, photosensitization experiments with the protected amino acid **10** were carried out in acetonitrile. They show an absorption band with a maximum around 450 nm (Figure 14, left graph).

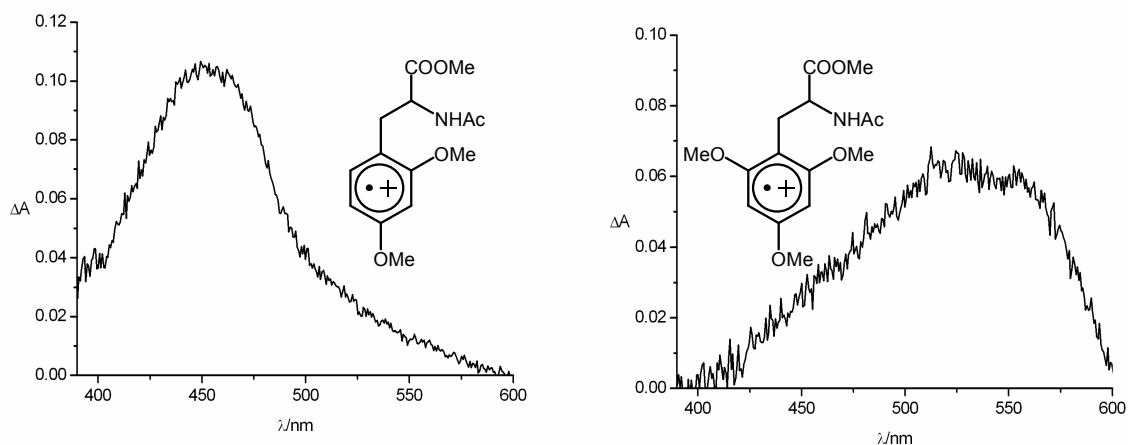
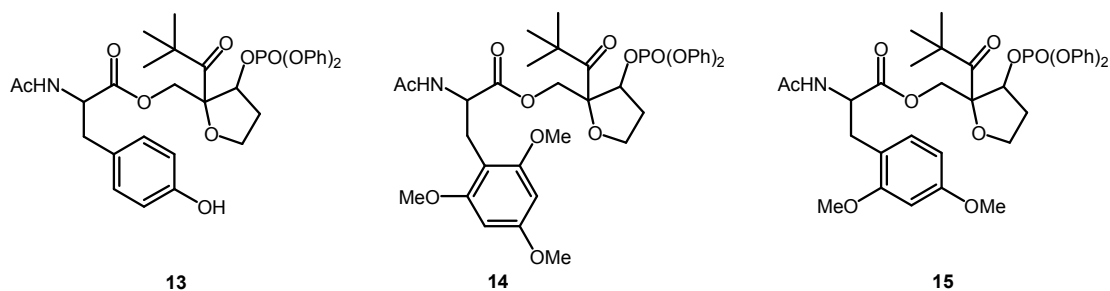


Figure 14: Transient absorption spectra recorded after oxidation of Ac-1,4-dimethoxyphenylalaninemetylester **10** (left) and Ac-2,4,6-trimethoxyphenylalaninemetylester **11** (right) by photosensitized electron transfer with 1,4-dicyanonaphthalene as a sensitizer and biphenyl as a codonor.

For comparison, the spectrum of the trimethoxyphenylalanine **11** used in previous experiments (see also ref. [66] and [65]) was also recorded, showing a maximum at 550 nm (Figure 14, right graph).

As an additional control, to guarantee the functioning of all electron donors used in the model peptide under the reaction conditions of the LFP measurements, compounds **15**, **14** and **13** in which the donors were connected to the injection unit via ester linkage (Scheme 9) were synthesized by deprotection and acetylation of **12** and the respective compounds (Scheme 8).



Scheme 9: All electron donors directly linked to the injection system for control experiments.

Degassed solutions of **13**, **14** and **15** in a 3:1 mixture of acetonitrile and water were then irradiated with a laser flash of 308 nm and the transient spectra were recorded after a delay of 40 ns. As can be seen in Figure 15, the absorption maxima are clearly distinct and allow, in principle, observation of all three oxidized species at the same time.

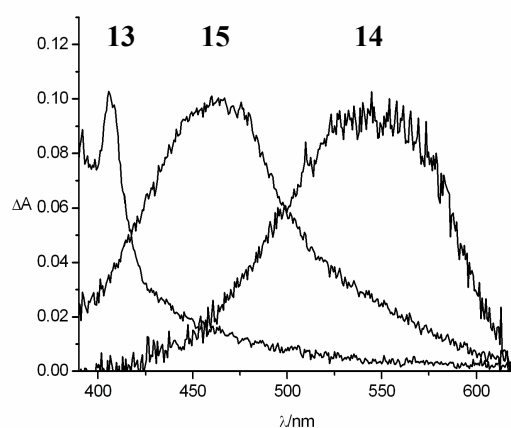


*Figure 15: Overlay of the transient absorption spectra of **15**, **14** and **13** recorded 100 ns after the laser flash.*

The spectroscopical and electrochemical data collected on the racemic amino acids as well as a first test in LFP experiments confirmed the suitability of the chosen phenylalanine derivatives to function as charge carriers and spectroscopic sensors in ET through peptides. From the oxidation potentials cited in the literature for the aromatic systems, no explicit trend could be derived with respect to the order of the side chains preferred in ET. But the pulsed cyclovoltammetry measurements carried out on the amino acids, indicated a slightly higher potential for the dimethoxysubstituted ring.

4 Stability of Radical Cations

The small difference in oxidation potential between the two non-natural aromatic amino acids led to the question, if 2,4-dimethoxyphenylalanine radical cation can oxidize 2,4,6-trimethoxyphenylalanine in the absence of tyrosine, which provides the driving force for ET in a peptide model containing all three redox sites. Therefore, quenching experiments were carried out with the small model **15**. Time-resolved measurements of the absorption intensity at 450 nm, the maximum absorption of 2,4-dimethoxyphenylalanine radical cation (see above), were carried out with **15** alone, and after addition of equimolar amounts of Ac-2,4,6-trimethoxyphenylalaninemethylester (**11**), resp. Ac-tyrosine-methylester. The curves depicted in Figure 16 show a considerable quenching effect upon addition of trimethoxyphenylalanine (red line), demonstrating that ET from the trimethoxysubstituted aromatic ring to the oxidized dimethoxy derivative is possible in an intermolecular reaction. As expected, a large radical cation quenching effect is observed in the presence of tyrosine (green line).

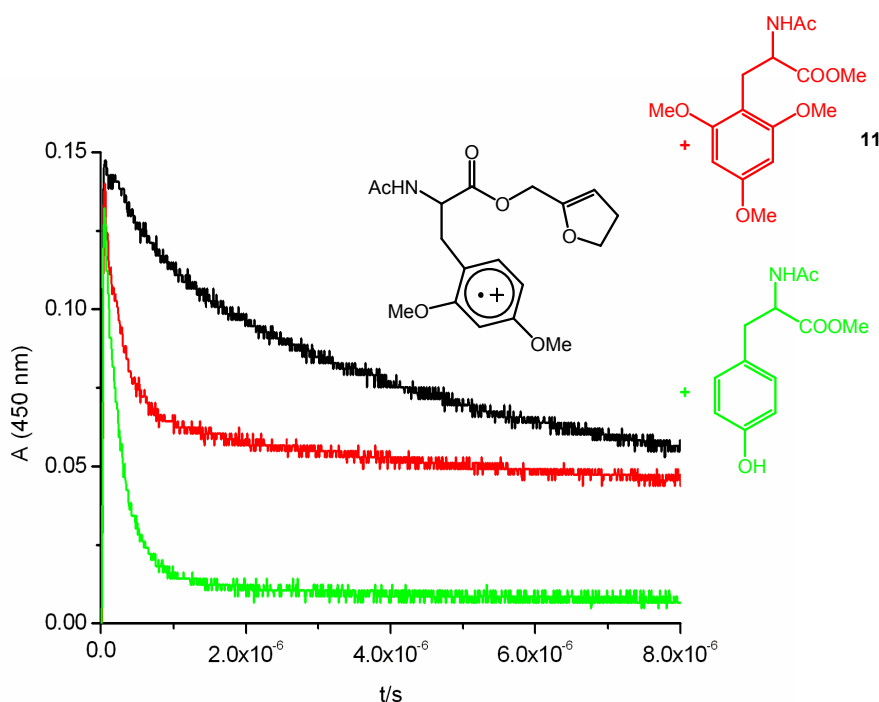
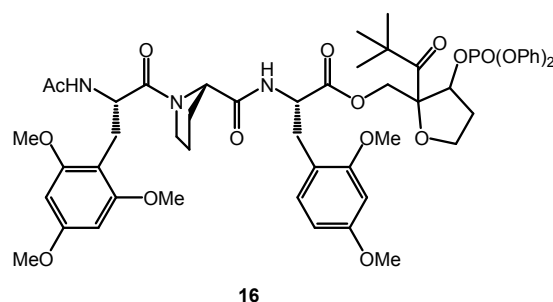


Figure 16: Time-resolved LFP measurements of the absorption at 450 nm of small model **15** alone (black line) and upon addition of Ac-2,4,6-trimethoxyphenylalanine-methylester (red line) resp. Ac-tyrosine-methylester (**11**) (green line) as a quencher.

In a next experiment, the question should be answered, to which extent ET between electron acceptor and relay amino acid occurs, when those two are assembled in one peptide (for a detailed description of peptide synthesis protocols see chapter 5.3.). In peptide **16**, only the two methoxysubstituted phenylalanine derivatives, separated by one proline unit, are present; no driving force is induced by a final irreversible ET step (Scheme 10).



Scheme 10: Peptide 16 contains electron acceptor and relay amino acid in close proximity but no final donor functioning as a thermodynamic sink.

The transient absorption spectrum, recorded 40 ns after laser irradiation of **16**, clearly shows the simultaneous presence of both radical cations with two absorption bands at 450 nm (2,4-dimethoxyphenylalanine radical cation) and 550 nm (2,4,6-trimethoxyphenylalanine radical cation). Thus, in a peptide containing aromatic residues of similar oxidation potentials, a distribution of the charge across the aromatic rings is observed.

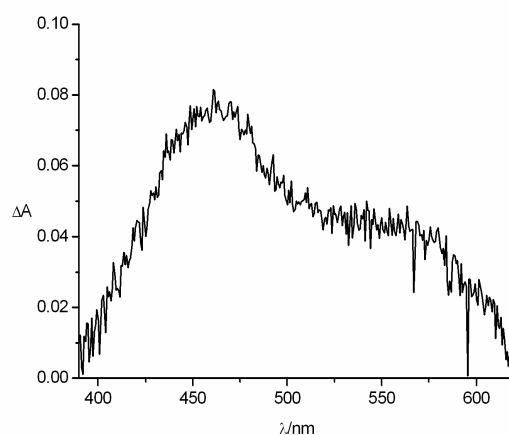


Figure 17: Transient absorption spectrum recorded 40 ns after laser irradiation of 16.

For comparison, the spectrum of peptide **17** containing the final electron donor tyrosine at the N-terminal position, separated from 2,4-dimethoxyphenylalanine as electron acceptor precursor by one proline unit, was recorded.

In this peptide, the electron transfer step can be assumed to be irreversible, due to deprotonation of tyrosine upon ET. The transient absorption spectrum, recorded 40 ns after the laser flash, clearly shows, that the charge has almost completely been transferred to the final electron donor ($\lambda_{\text{max}} = 410 \text{ nm}$) within this delay, with just a small residual absorption intensity around 450 nm (Figure 18).

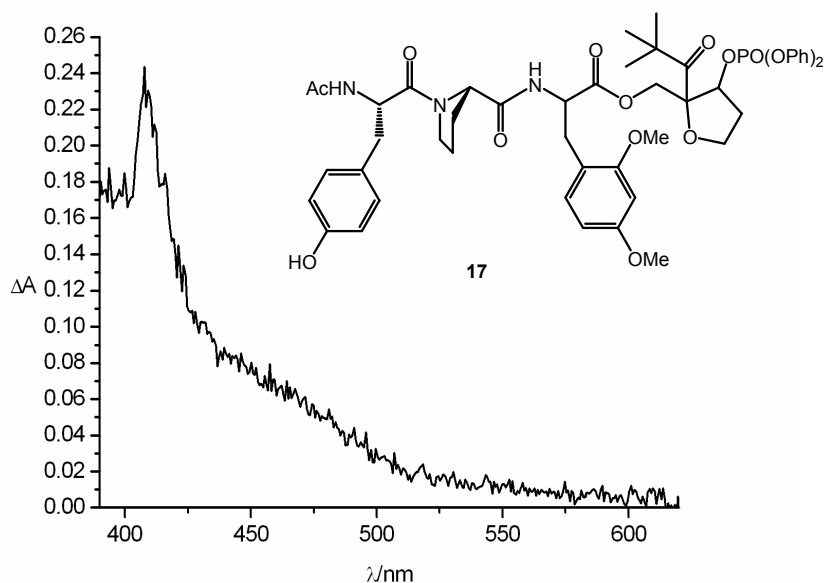


Figure 18: Transient absorption spectrum recorded 40 ns after laser irradiation of **17**.

This result is in accordance with the difference in driving forces for ET in peptides **16** and **17**, resulting from the oxidation potentials of the participating redox partners. While a contribution of the charge between dimethoxy and trimethoxybenzene in **16** might be achieved in an equilibrium reaction, due to their similar oxidation potentials, tyrosine is deprotonated upon oxidation to the tyrosyl radical in an irreversible reaction in **17**.

In an additional quenching experiment, the stability of the electron acceptor in peptide **16** was investigated. Surprising results were obtained from time-resolved measurements of 450 nm absorption in this peptide. A slower decay of the dimethoxyphenylalanine radical cation (black line, Figure 19) is observed, compared to the respective decay in small model **15**, in which no second amino acid is present (black line, Figure 16, page 31). This points to an increase in stability, possibly induced by the formation of a charge transfer complex between the two aromatic sites. Upon addition of equimolar amounts of trimethoxyphenylalanine derivative **11** as a quencher to the solution of **16**, no substantial effect on the radical cation decay could be measured (red line). Addition of tyrosine, however, led to the expected acceleration in signal decay (green line).

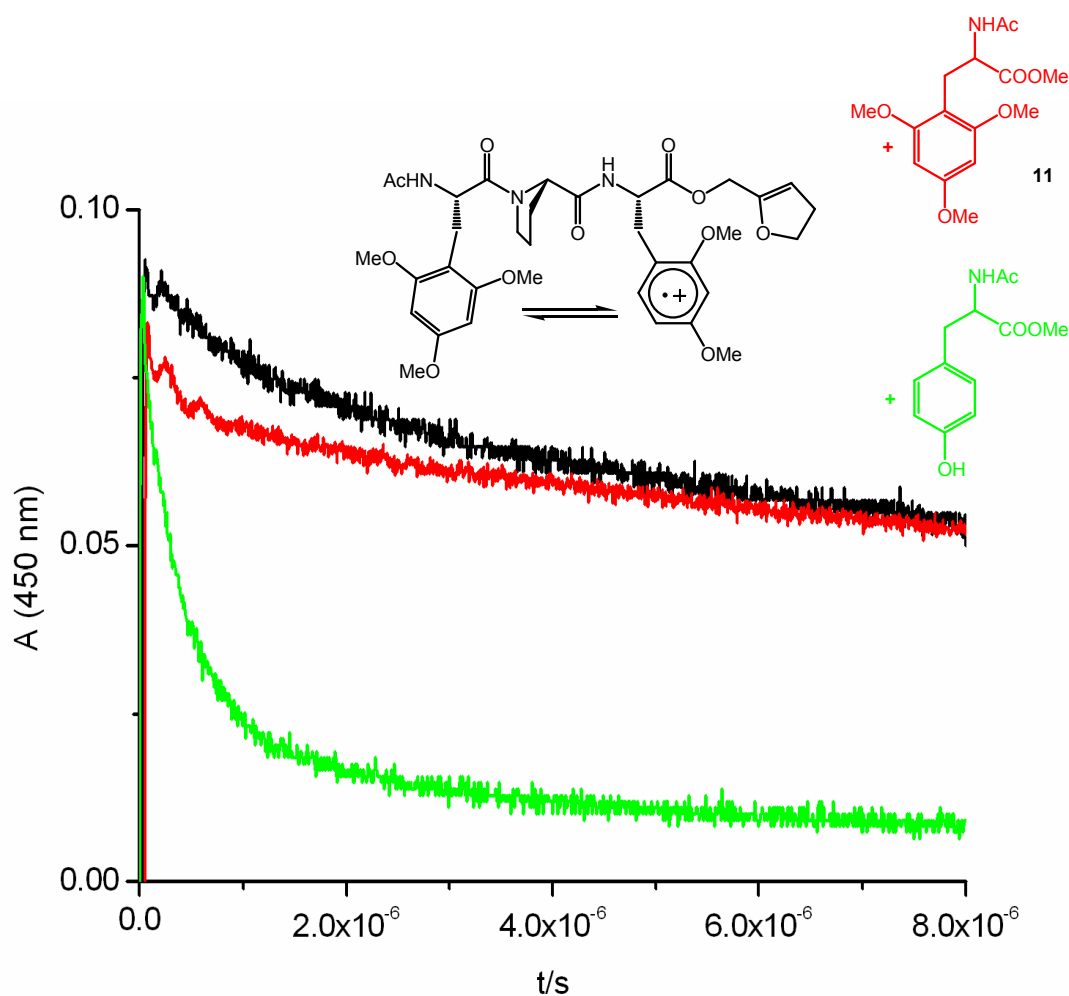


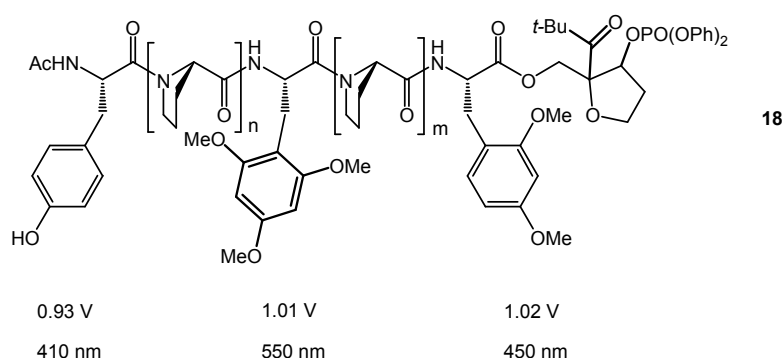
Figure 19: Time-resolved LFP measurements of the absorption at 450 nm of peptide **16** alone (black line) and upon addition of Ac-2,4,6-trimethoxyphenylalaninemethylester (grey line) resp. Ac-tyrosinemethylester (light grey line) as a quencher.

To summarize the results, 2,4-dimethoxyphenylalanine radical cation is able to oxidize 2,4,6-trimethoxyphenylalanine, as could be presumed from CV measurements (cf. paragraph 3.3.1), which revealed a difference in oxidation potential of 10 mV between the two aromatics. If the two redox sites are situated in close proximity, the stability of 2,4-dimethoxyphenylalanine radical cation is increased and the formed radical cation complex is not reduced by an external donor of similar oxidation potential. Tyrosine, as an electron donor of substantially lower oxidation potential (100 mV difference), is able to rapidly reduce the radical cation of 2,4 dimethoxyphenylalanine, as well as the radical cation complex formed by the two methoxysubstituted aromatics.

5 Occurrence of Oxidized Intermediates in ET through peptides

5.1 Introduction

A peptide model should be constructed, in which sequential ET through a peptide chain containing three aromatic amino acid side chains as redox sites, was possible and could be observed by transient absorption spectroscopy. The natural amino acid tyrosine as an irreversible electron donor should be situated at the N-terminus. Two methoxysubstituted phenylalanines, 2,4-dimethoxyphenylalanine and 2,4,6-trimethoxyphenylalanine were chosen as additional redox sites, because of their suitable electrochemical and spectroscopic properties. The information regarding the possibility of ET between 2,4,6-trimethoxyphenylalanine and 2,4-dimethoxyphenylalanine radical cation, obtained by cyclic voltammetry measurements and quenching experiments, lead to the decision to place the dimethoxy phenylalanine derivative at the acceptor and the trimethoxy derivative at the relay position. The resulting peptide model is depicted in Scheme 11.



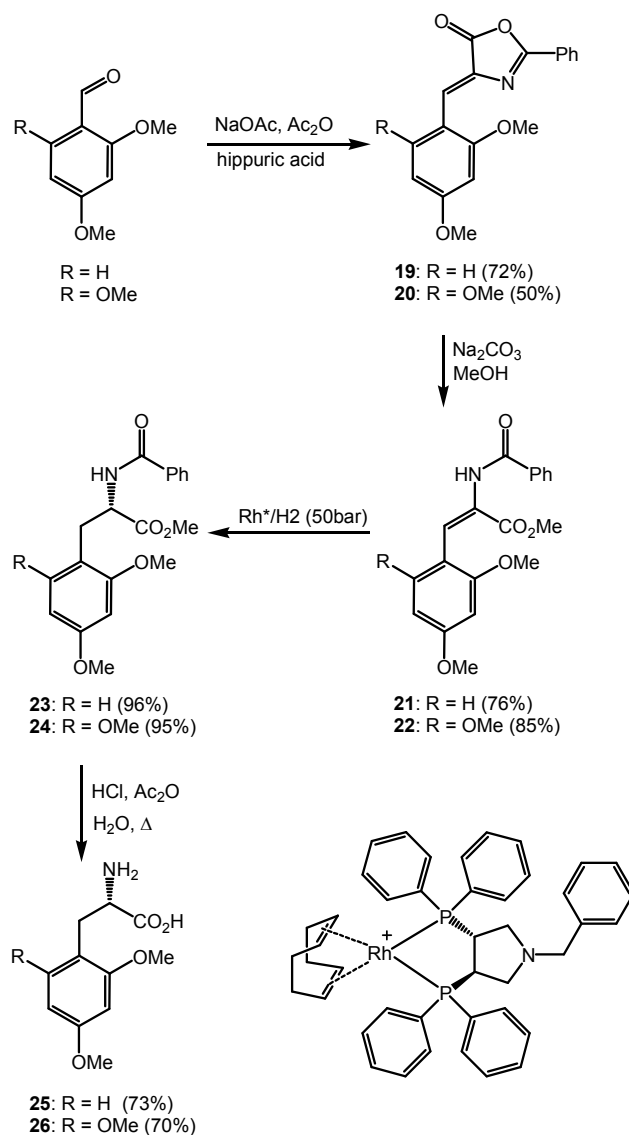
Scheme 11: Peptides suitable for the observation of intermediates in a sequential ET process with the oxidation potentials (vs. NHE) and the wavelengths of maximum absorption of the oxidized side chains indicated below the respective aromatic rings.

In peptides of type **18** an electron hole can be generated by laser irradiation, according to the reaction depicted in Scheme 4 (page 9). Oxidation of the C-terminal amino acid, generating an electron acceptor, will lead to a transient absorption signal at 450 nm. Subsequent ET from the N-terminal electron donor tyrosine will be observable by an absorption at 410 nm. If ET occurs in a sequential mechanism via oxidation of the relay amino acid, an additional signal with a maximum at 550 nm should be visible in the absorption spectrum (see also Scheme 16).

5.2 Synthesis of Enantiopure Non-natural Amino Acids

To guarantee a higher degree of structural homogeneity in the investigated peptide models, and to synthesize peptides similar to naturally occurring structures, the non-natural amino acids in peptides **18** should be synthesized as enantiopure molecules.

For this purpose, a synthetic route to the amino acids was developed, based on an Erlenmeyer azlactone procedure,^[91, 92] with an asymmetric hydrogenation using a commercially available Rhodium Deguphos^[93] catalyst that has been used before in the enantioselective hydrogenation of acrylates,^[94] as the key step (Scheme 12).

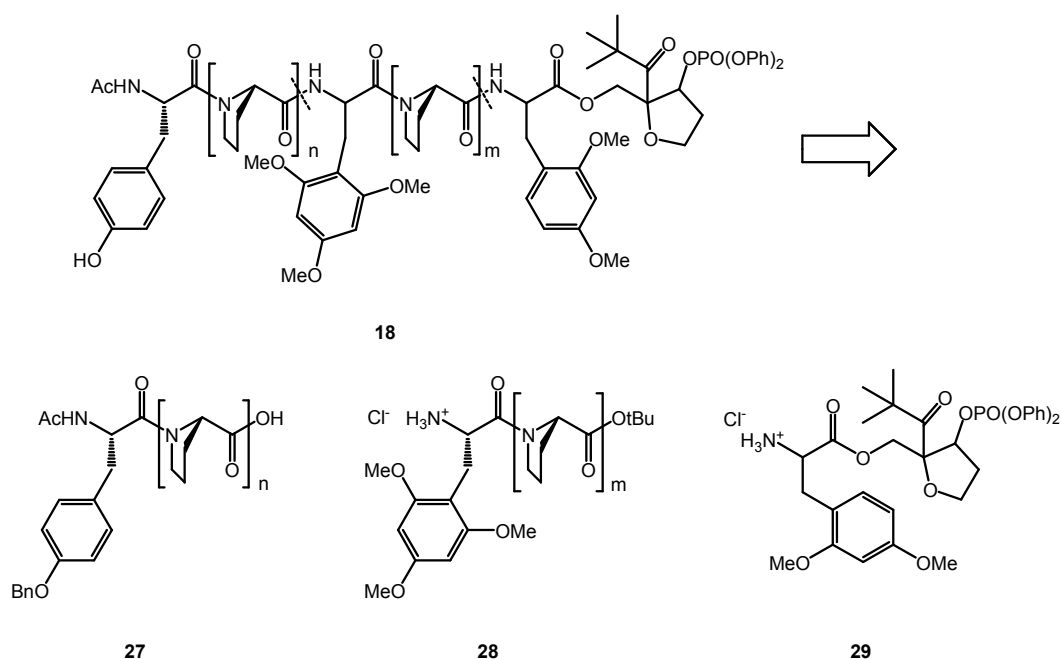


Scheme 12: Synthesis of 2,4-dimethoxyphenylalanine and 2,4,6-trimethoxyphenylalanine.

Condensation of the commercially available methoxy substituted benzaldehydes with the adequate substitution pattern, led to the corresponding azlactones **19** and **20**. This reaction, as well as the basic opening of the lactones to the acrylic acid derivatives **21** and **22** could be carried out on a multigram scale in moderate to good yields. Subsequent asymmetric hydrogenation at 50 bar hydrogen pressure with 3R,4R-(+)-bis(diphenylphosphino)-1-benzylpyrrolidine(1,5-cyclooctadiene) rhodium(I) as a catalyst gave the (S)-configured amino acid derivatives **23** and **24** in more than 90% yield and >95% *ee*. Deprotection under strongly acidic conditions and subsequent purification via ion exchange chromatography yielded free amino acids **25** and **26** (70%).

5.3 Synthesis of Peptides

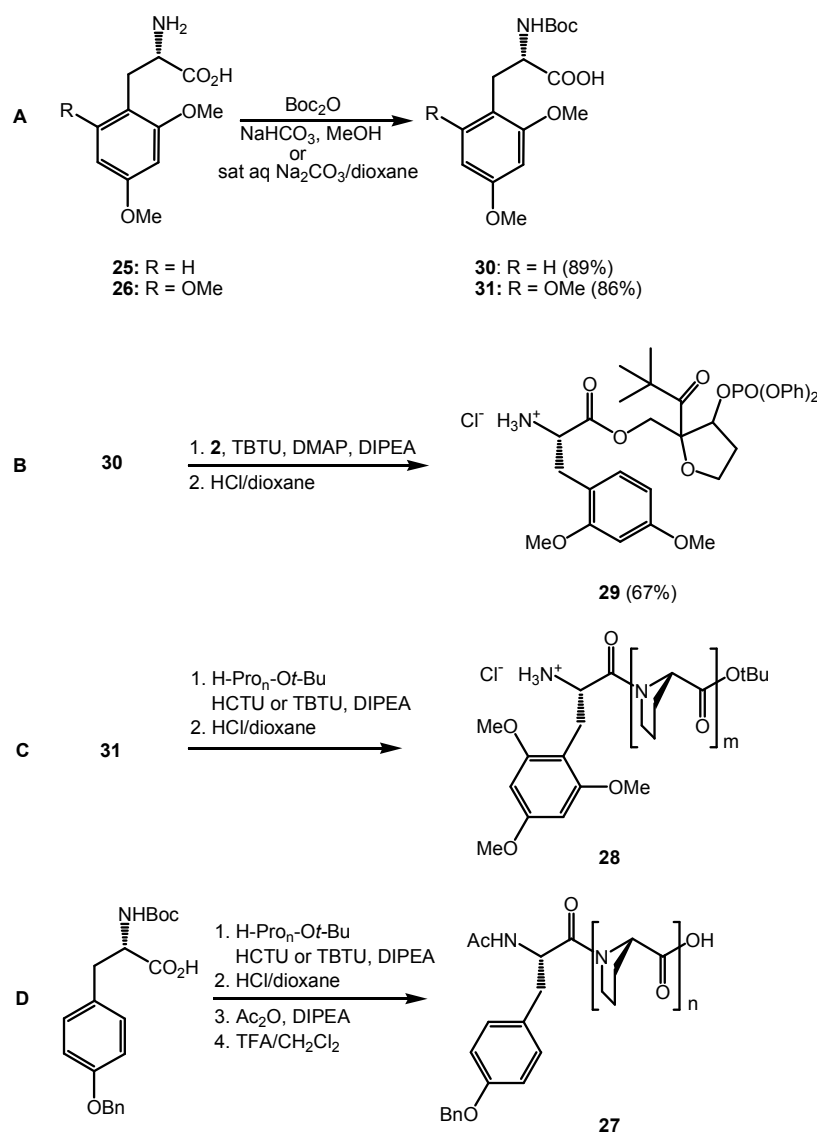
For the assembly of peptides **18**, we chose to work in solution, using the Boc-strategy, to avoid the use of high excess of our non-natural amino acids. The peptides were synthesized in a convergent strategy from the fragments indicated in Scheme 13.



Scheme 13: Synthetic strategy for the assembly of peptide models of type **18**.

To synthesize the fragments **28** and **29**, conversion of the non-natural amino acids **26** and **25** to the respective Boc-protected residues **30** and **31** was possible in good yields using di-*tert*-butyldicarbonate (Boc₂O) and carbonate bases (Scheme 14, A). Esterification of Boc-2,4-dimethoxyphenylalanine **30** with injection system **2** (cf. also Scheme 8, page 26) was then followed by acidic deprotection with HCl in dioxane to give the amine hydrochloride **29** of the C-terminal electron acceptor precursor

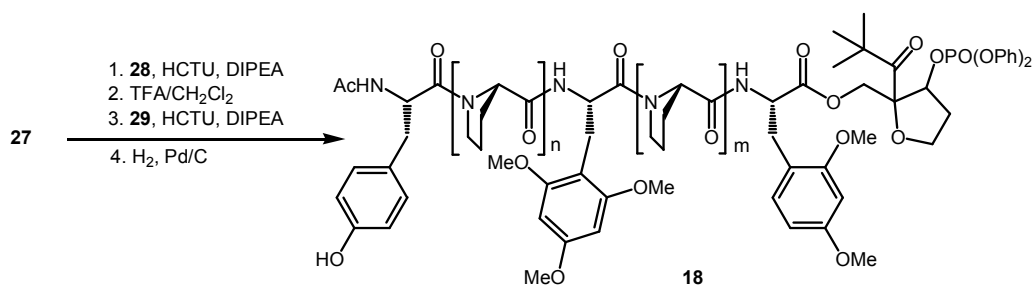
(Scheme 14, **B**). Fragment **28**, containing the relay amino acid, was obtained by peptide coupling in solution, of amino acid derivative **31** to an oligoproline unit of the requested length, with 2-(1H-benzotriazole-1-yl)-1,1,3,3-tetramethyluronium tetrafluoroborate (TBTU) or 2-(6-chloro-1H-benzotriazole-1-yl)-1,1,3,3-tetramethyluronium hexafluorophosphate (HCTU) as coupling reagents and *N,N'*-diisopropylethylamine (DIPEA) as base, and subsequent acidic Boc-deprotection (Scheme 14, **C**). Commercially available benzyl-protected Boc-tyrosine was used as starting material in the analogous synthesis of the N-terminal electron-donor fragment **27**, depicted in Scheme 14, **D**.



Scheme 14: Synthesis of the peptide fragments needed for the assembly of model peptide **18**.

For the proline spacers, commercially available *N*-Boc protected proline, the free amine of proline-*tert*-butylester and *N*-Boc protected diproline were used as building blocks. Peptide couplings (not depicted) were then carried out in solution with HCTU or TBTU as coupling reagents and DIPEA as base. Deprotection of the Boc group was achieved under acidic conditions (HCl in dioxane).

Assembly of the building blocks **27**, **28** and **29** to peptides **18** was achieved starting with the HCTU-mediated coupling of the N-terminal fragment **27** to the central fragment **28**, followed by acidic deprotection to yield the free acid, and subsequent coupling to the amine hydrochloride **29** of the C-terminal fragment. As a final step, the benzyl-protection group at the N-terminal tyrosine residue was cleaved via hydrogenation with palladium on activated charcoal as a catalyst and 1 bar hydrogen pressure (Scheme 15).

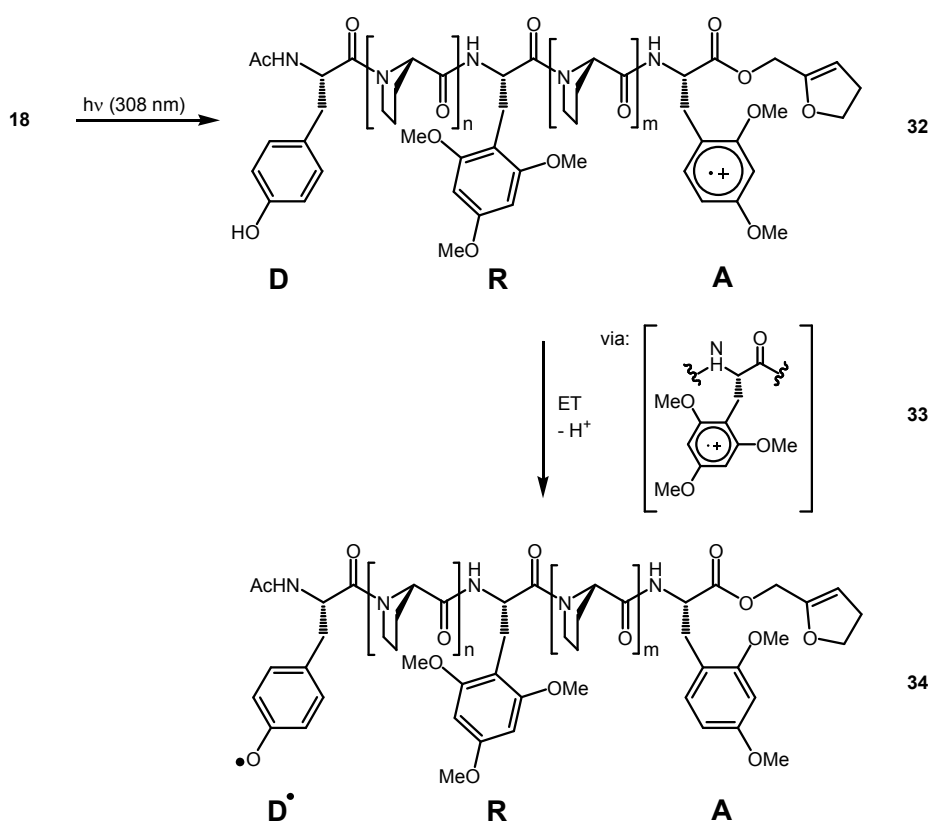


Scheme 15: Assembly of the fragments to oligopeptides 18.

All reactions were controlled by thin layer chromatography (TLC) and ESI-mass-spectrometry (ESI-MS). All intermediates in the synthesis that wore protection groups at the N- and C-terminus were purified by flash chromatography, but used in the next step without complete characterization. The yields of the peptide couplings ranged from 60% to 80%. Deprotection steps were quantitative.

5.4 Data Collection and Analysis

The experimental setup for Laser Flash Photolysis (LFP) experiments is described in chapter 3.2. LFP should be used to detect the appearance of oxidized intermediates during ET through peptides **18** (Scheme 16). Induced by the laser flash, an electron acceptor **A** was generated at the C-terminus, giving peptide **32** which absorbs around 450 nm. Subsequent transfer of electrons from the N-terminal electron donor tyrosine (**D**), resulting in the formation of a tyrosyl radical (**D[•]**) **34** leads to the build-up of a second absorption maximum at 410 nm.



Scheme 16: ET from D to A through the peptide chain might occur via oxidation of the relay amino acid R.

Special attention should be paid to the role of the aromatic amino acid **R**, separating the proline matrix into two spacers with defined numbers of residues n and m , which is in principle able to serve as a relay in sequential ET between D and A, yielding an oxidized intermediate **33** (**R^{•+}**), with an absorption maximum at 550 nm.

5.4.1 Limitations

Some limitations regarding the LFP measurements result from the design of the model.

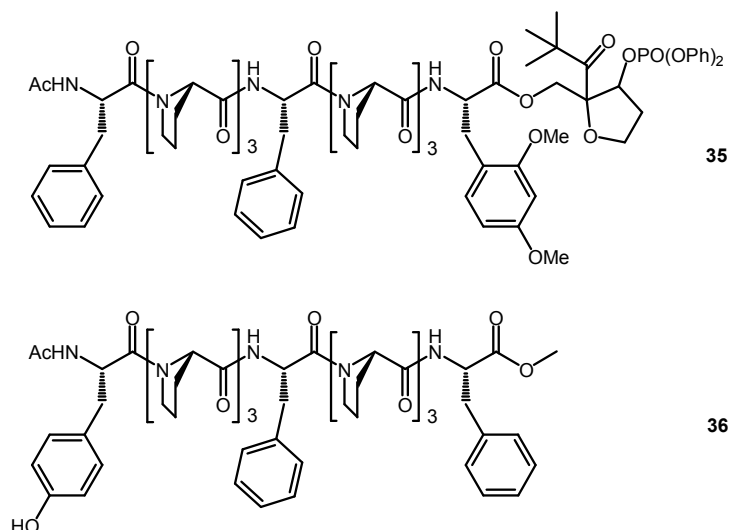
Time-resolved measurements

While the signals of all three oxidized intermediates can be clearly distinguished in the transient absorption spectrum (see 3.3.1), rate measurements at the respective maxima will suffer from errors due to significant signal-overlap (cf. Figure 15). Moreover, a reliable rate detection at 410 nm (wavelength of tyrosyl radical absorption), is complicated by a strong fluorescence band at that wavelength, emitted from the pivaloyl chromophore. This negative absorption saturates the photomultiplier, which takes 200 – 300 ns to recover. Detailed analysis of the kinetic data is, in addition, only possible if assumptions are made about the mechanism of radical cation decay. We therefore decided not to rely on time-resolved measurements at a specific wavelength, but to use the complete transient absorption spectra to gain information about the course of the reaction depicted in Scheme 16. The CCD-camera used to record the transient absorption spectra is not hampered by the fluorescence, since it can be triggered to a 40 ns delay after irradiation and the fluorescence signal itself decays within 20 ns, as could be estimated by single photon counting experiments.

Intermolecular ET

Since photocleavage of the injector moiety is based on a quantum-mechanically forbidden $n-\pi^*$ transition, the extinction coefficient of the respective band at the wavelength of laser irradiation is low (ϵ (308 nm) approx 30 – 40 $\text{M}^{-1}\text{cm}^{-1}$).^[95] Therefore, LFP experiments have to be carried out in millimolar concentrations of peptide, to gain sufficient signal intensities. At concentrations in this range, *intermolecular* reactions can already play a role. As a rough estimation, from the rate coefficient for diffusion controlled reactions in acetonitrile (10^9 s^{-1}), rates of *intermolecular* ET at millimolar peptide concentrations can be expected to be in the range of 10^6 s^{-1} . Dilution measurements performed by Napp on peptide models of type **1** (Scheme 3, page 19), allow a more precise determination of intermolecular ET rates. He measured a rate coefficient of $3 \cdot 10^8 \text{ s}^{-1}$ for *intermolecular* ET between the C-terminal 2,4,6-trimethoxyphenylalanine radical cation and an N-terminal tyrosine in peptides with 5 and 7 amino acid residues.^[65] This value results in intermolecular ET rates of $1 - 2.5 \cdot 10^6 \text{ s}^{-1}$ for the 3 - 8 mM concentrations used in LFP. Thus, intensity changes of around 4% - 10% after a time delay of 40 ns can be expected to be caused by *intermolecular* contributions, whereas the error caused by *intermolecular* reactions reaches already 50% after 500 ns.

To check experimentally, whether these estimations apply in the new system **18**, a control experiment was carried out, using a peptide **35** that contains only the acceptor amino acid, and a second peptide **36** with just tyrosine as a redox-active aromatic side chain. To keep the structure similar to peptides of type **18**, all other aromatic rings were exchanged by phenylalanine (Scheme 17).



Scheme 17: Peptide designed for a control experiment to estimate the contribution of intermolecular ET.

When the transient absorption spectra of peptide **35**, are recorded 40 ns and 500 ns after laser irradiation, no major difference between the two spectra is observed (Figure 20, left graph). The radical cation of the 2,4-dimethoxyphenylalanine side chain is stable for at least 500 ns, as could be expected from previous experiments (cf. Figure 16, page 31).

When peptide **36** is added in equimolar amounts as an intermolecular electron donor (Figure 20, right graph), the spectrum changes from almost entirely electron acceptor (35^{*+}) 40 ns after the flash (black line) to a significant amount of tyrosyl radical (36^{\bullet}) formed already 500 ns after the flash (red line, $\lambda_{\max}[\text{tyr}^{\bullet}] = 410 \text{ nm}$). This result is in accordance with the considerations described above, and with quenching experiments performed on small peptides (cf. chapter 4).

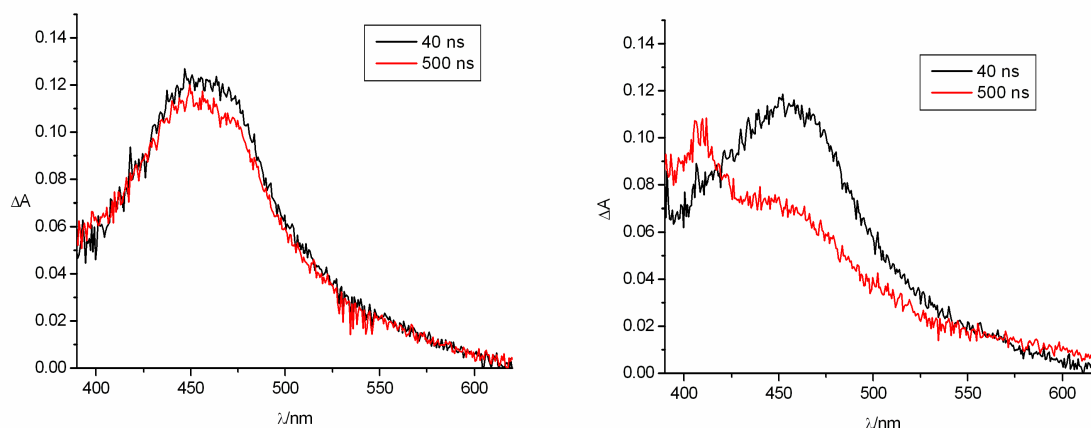


Figure 20: left graph: Transient absorption spectra of peptide **35** recorded 40 ns (black line) and 500 ns (red line) after laser irradiation.; right graph: Transient absorption spectra of an equimolar solution of peptides **35** and **36** recorded 40 ns (black line) and 500 ns (red line) after laser irradiation.

As a consequence of these considerations, it was decided, that the transient absorption spectra of peptide models of type **18**, gained 40 ns after laser irradiation, should be used for analysis. In these spectra, the amount of *intermolecular* ET is low ($\leq 10\%$) and thus does not hamper the observation of *intramolecular* processes. Shorter delays are not useful, since the rate for the β -fragmentation of the injector radical **3** to give the charged intermediate **4** that initiates the ET cascade (see Scheme 4, page 19), has been determined by competition experiments to $2 \times 10^8 \text{ s}^{-1}$,^[66] resulting in a half-life time of approximately 20 ns for electron acceptor generation.

5.4.2 Analysis of the Data

A first, qualitative analysis of the obtained spectra reveals directly, which aromatic side chains are present in the oxidized form, since the three spectroscopic sensors, indicating the electron acceptor, the oxidized relay and the oxidized donor, yield different absorption spectra. For a quantification of the analysis, reference curves obtained from measurements of the respective side chains coupled directly to the injector (Figure 14, page 28), were used, representative of the transient species **32**, **33** and **34**. Fitting of these curves, so that the sum of the spectrum of the tyrosyl radical **D**[•] (blue, $\lambda_{\text{max}} = 410$ nm), the 2,4-dimethoxyradical cation **A** (red, $\lambda_{\text{max}} = 450$ nm), and the 2,4,6-trimethoxy-phenylalanine radical cation **R**^{•+} (green, $\lambda_{\text{max}} = 550$ nm) yields the measured overall absorption, allowed a graphical analysis of the contributions of the respective transients. An example is depicted in Figure 21.

The absorption values extracted from this analysis were then corrected by the extinction coefficients of the radical cations at their maximum absorption. The extinction coefficient of the phenoxyl radical is known to amount to $3000 \text{ M}^{-1}\text{cm}^{-1}$,^[78] while 1,3-dimethoxybenzene radical cation and 1,3,5-trimethoxybenzene radical cation have extinction coefficients of approx. $4000 \text{ M}^{-1}\text{cm}^{-1}$.^[80, 81] Thus, the values determined for tyrosine from the graphical analysis were multiplied with a factor of 1.33.

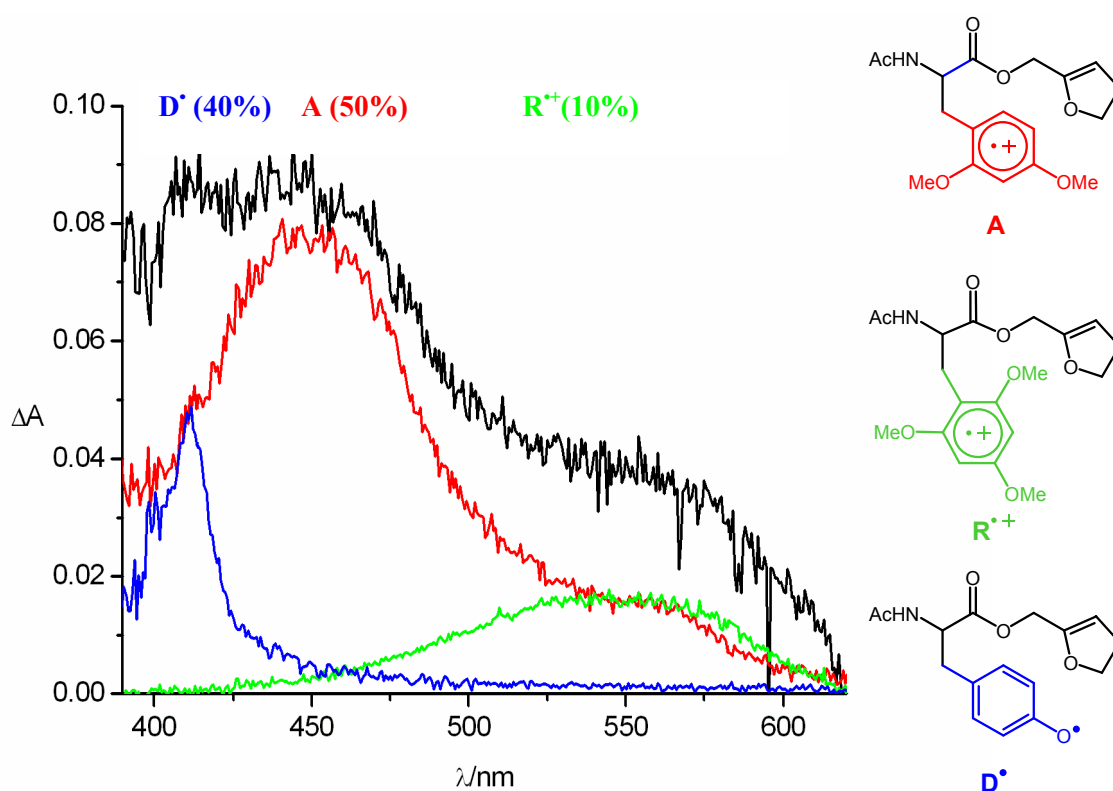


Figure 21: Decomposition of a recorded transient absorption spectrum (black) to reveal the contributions of tyrosyl radical (blue), 2,4-dimethoxyphenylalanine radical cation (red) and 2,4,6-trimethoxyphenylalanine radical cation (green).

Since the laser energy varies slightly between two flashes and significantly between different days of measurements, due to variations in the gas mixture, the absolute absorption values could not be used for the comparison of different molecules. The obtained values were therefore scaled to the sum of all absorption maxima, set to 100%.

5.5 Results and Discussion

As a first molecule, peptide **37** in which electron acceptor, relay amino acid and electron donor are assembled in close proximity, was synthesized and ET in this peptide was examined by LFP.

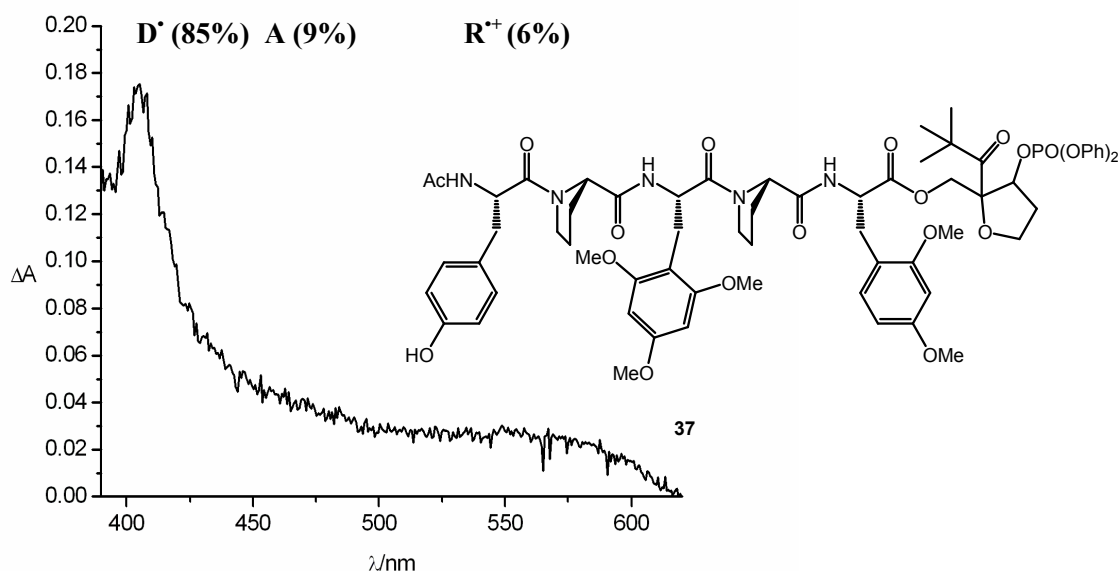


Figure 22: Transient absorption spectrum of **37** 40 ns after laser irradiation.

It is obvious from the resulting spectrum recorded 40 ns after the laser flash (Figure 22), that the main part of the charge has been transferred to the final electron donor tyrosine already within this short delay, yielding tyrosyl radical **34** (D^{\bullet} , $\lambda_{\text{max}} = 410$ nm). Around 550 nm, the wavelength of absorption of the relay radical cation **33** ($R^{\bullet+}$), a small absorption band is observed. Analysis of the spectrum by graphical decomposition of the curve (cf. Figure 21) reveals a distribution of oxidized species of 85% tyrosyl radical **34** (D^{\bullet}), 9% remaining electron acceptor **32** (A), and 6% oxidized relay **33** ($R^{\bullet+}$). Since *intermolecular* donor to acceptor ET has been estimated to cause effects of less than 10%, it can be concluded, that very fast *intramolecular* ET from tyrosine to 2,4-dimethoxyphenylalanine radical cation takes place in peptide **37**.

For comparison, ET was monitored in peptide **38** containing the same number of backbone peptide bonds between donor and acceptor, yet no relay amino acid. Instead, three prolines separate D and A.

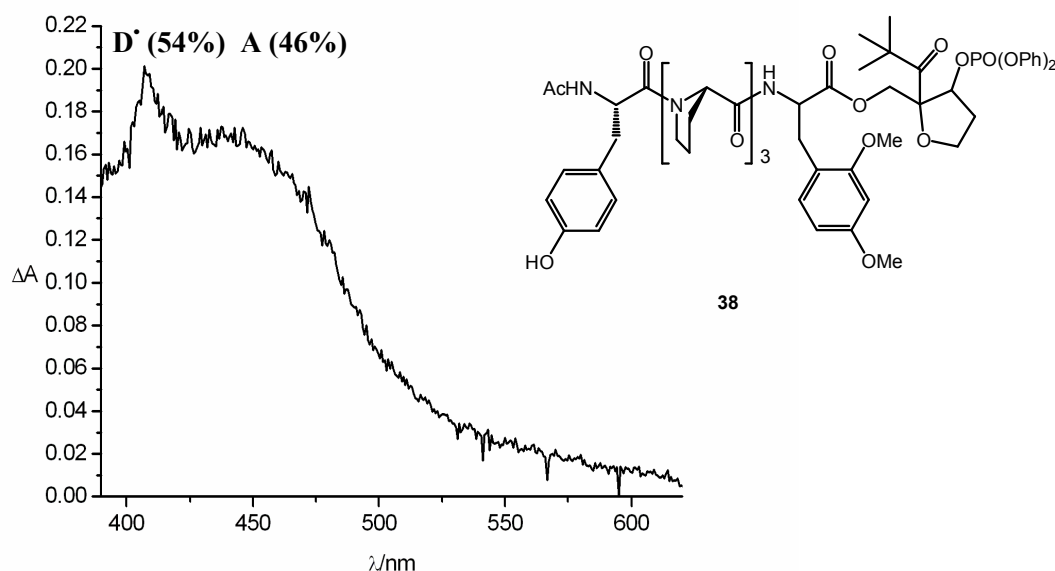


Figure 23: Transient absorption spectrum of **38** 40 ns after laser irradiation.

In this peptide, the charge is almost equally distributed between the electron acceptor (A, 46%) and the oxidized donor (D[•], 54%), 40 ns after the laser flash. ET to the acceptor is less efficient in this peptide. A charge distribution similar to that observed in peptide **37**, could however be detected in peptide **17**, similar to **38**, but with just one proline unit separating D and A. After 40 ns already 86% of the charge has been transferred to the donor, with 14% remaining at the acceptor site (Figure 18, page 33).

These findings confirm the results obtained by Napp: the bonds in the peptide backbone are not the main factor controlling ET. Instead, ET between donor and acceptor, separated by three amino acids, can occur with significantly different rates, depending on the amino acid sequence. And ET processes of equal efficiencies can be observed in peptides with one or three separating amino acids. This excludes through-bond ET as a mechanism responsible for ET through peptides **18**. Whether this effect is due to differences in D/A distance caused by the peptide structure, or due to participation of the relay, which is available in peptide **37**, cannot be answered by these experiments.

Since the ET process was very fast in peptide **37**, a peptide with longer proline spacers was synthesized. Three prolines were chosen as a separating unit, because this is the length of one repeat unit of the polyproline II (PPII) helical structure.^[96] In the resulting peptide **39** with the relay amino acid having a three-proline distance to each electron donor and electron acceptor, efficient ET between donor and acceptor (separated by 7 amino acids), did not take place within 40 ns. The main part of the charge is still located at the electron acceptor, indicated by a strong absorption band at 450 nm (Figure 24).

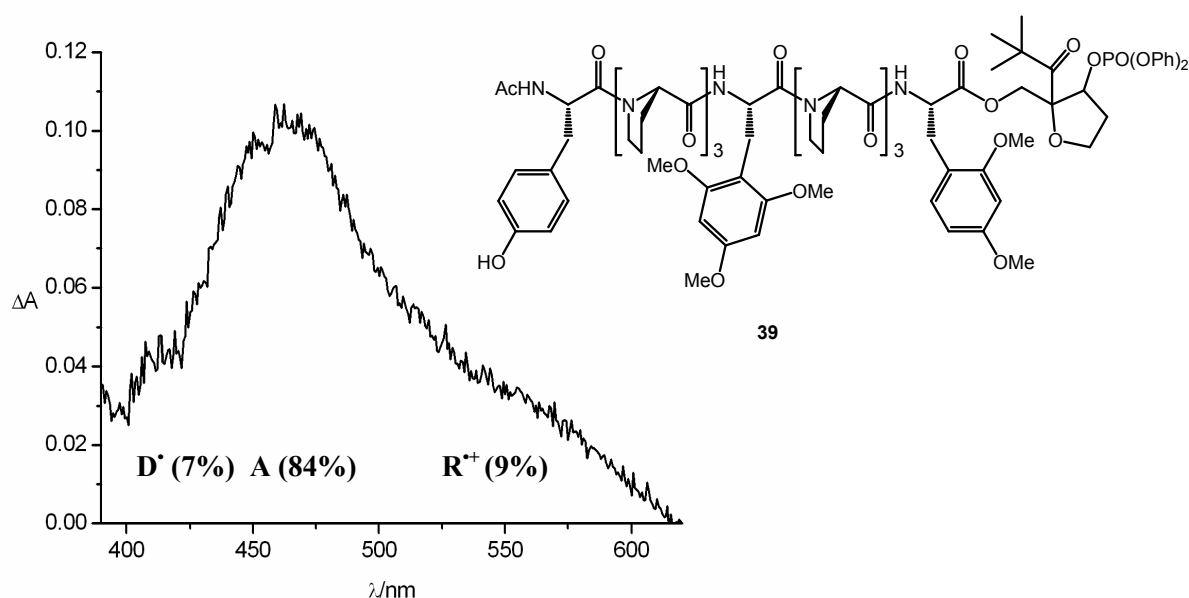
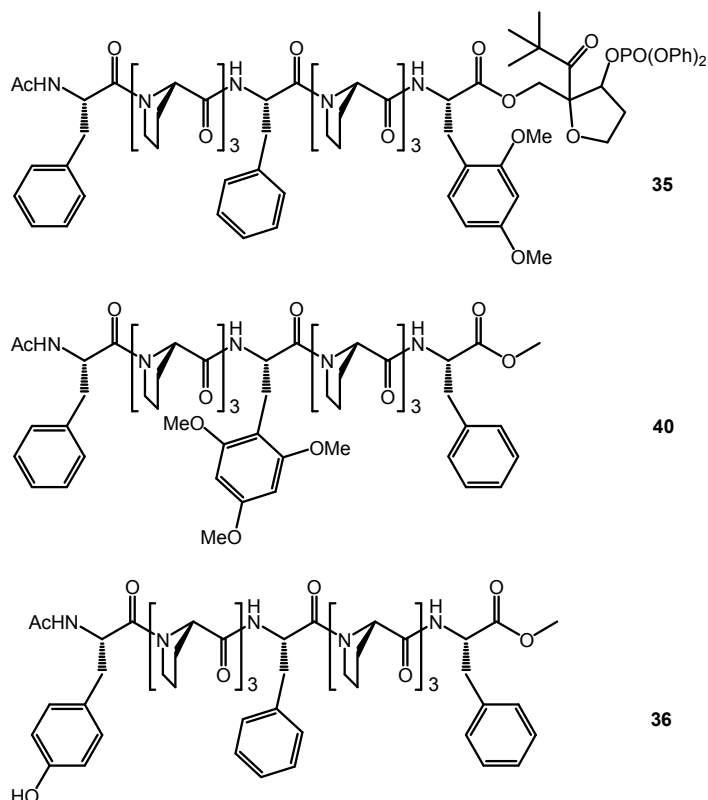


Figure 24: Transient absorption spectrum of **39**, 40 ns after laser irradiation.

However, an absorption band at 550 nm points to the existence of oxidized relay amino acid. The distribution of charge was determined to 7% oxidized electron donor (D^{\bullet} , 410 nm), 84% electron acceptor (A, 450 nm) and 9% oxidized relay ($R^{\bullet+}$, 550 nm). The amount of oxidized relay and donor is thus in an order of magnitude, that might be caused by *intermolecular* processes.

To answer the question, whether *intramolecular* ET takes place in peptide **39**, a control experiment was carried out. In addition to peptides **35** and **36**, used to estimate the effect of *intermolecular* transfer between donor and acceptor, a third peptide **40** was synthesized, containing only the relay amino acid as redox-active residue.



Scheme 18: Peptides used to estimate the role of intermolecular ET.

An equimolar mixture of **35**, **36** and **40** was investigated by LFP, and the spectrum obtained after 40 ns (Figure 25, black), was compared to the transient absorption spectrum of **39** (Figure 25, red). While the absorption band at 550 nm, stemming from the oxidized relay (**33**, R^+), is clearly visible in peptide **39** (red line), no significant amount of oxidized relay is formed in the control experiment (black line).

Since 2,4,6-trimethoxyphenylalanine can in principle be oxidized by the electron acceptor in an *intermolecular* reaction, as shown in quenching experiments (Figure 16, page 31), this result is attributed to the structure of the molecule, with the relay amino acid embedded in the proline matrix. However, as discussed before, ET from the N-terminal tyrosine to the C-terminal electron acceptor can take place *intermolecularly* in small amounts. Decomposition of the black curve in Figure 25 yielded a 9:1 ratio of acceptor to oxidized donor, i.e. a 10% efficiency of *intermolecular* donor to acceptor ET in peptides of type **18** can be assumed.

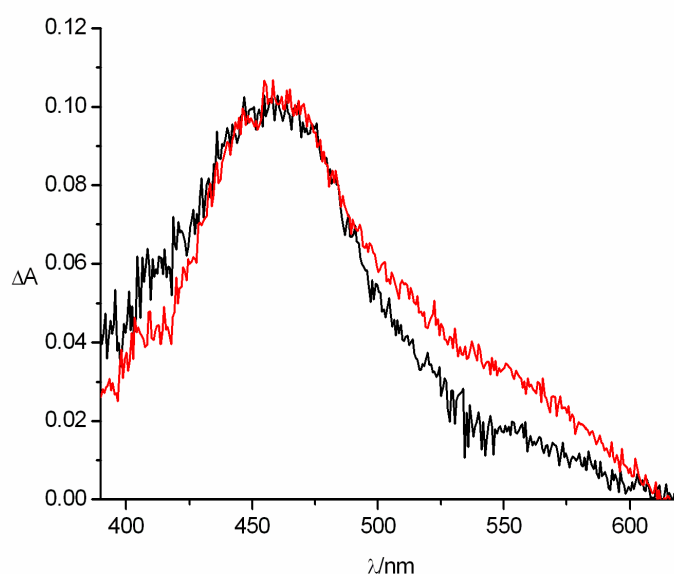


Figure 25: Transient absorption spectrum of an equimolar mixture of **35**, **36** and **40** (black) in direct comparison with the transient absorption spectrum of **39**, both recorded 40 ns after laser irradiation.

In conclusion, ET observed between the electron donor and the electron acceptor in compound **39** might be due to *intermolecular* reactions, while the formation of oxidized relay, 2,4,6-trimethoxyphenylalanine radical cation, can be traced back to *intramolecular* processes.

While in the nonapeptide **39**, containing two tripoline spacers, *intramolecular* donor to acceptor charge transfer does not occur within 40 ns, the amount of tyrosyl radical formed is significantly increased upon spacer-shortening. In peptide **41**, relay and acceptor are only separated by one proline, while the relay/donor distance is kept to three prolines (Figure 26). The ratio of oxidized species formed 40 ns after irradiation of **41**, amounts to 40% tyrosyl radical (D^{\bullet}), 50% remaining electron acceptor (A), and 10% oxidized relay ($R^{\bullet+}$). So the contribution of oxidized relay to the overall absorption does not differ from the value measured upon LFP of molecule **39** (around 10%, see above). But donor to acceptor electron transfer has increased and can no longer be explained by *intermolecular* reactions.

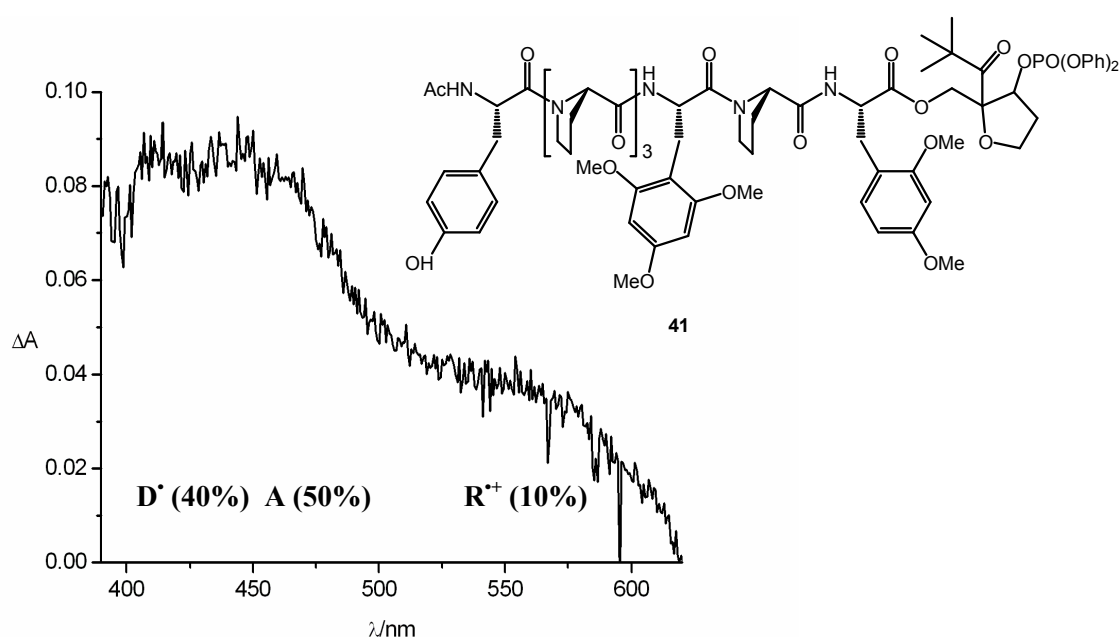


Figure 26: Transient absorption spectrum of **41**, 40 ns after laser irradiation.

Intramolecular donor to acceptor and relay to acceptor ET takes place in peptide **41**.

In peptide **42**, a proline matrix of the same overall length as **41** is arranged differently, with three prolines separating acceptor and relay and just one proline between relay and N-terminal donor. In this case, the overall efficiency of ET to the acceptor stays the same with around 50% of charge having left the acceptor after 40 ns. Yet the amount of observed oxidized relay is decreased by a factor of 2. The exact ratio of oxidized species is determined to 42% tyrosyl radical, 53% electron acceptor and 5% oxidized relay.

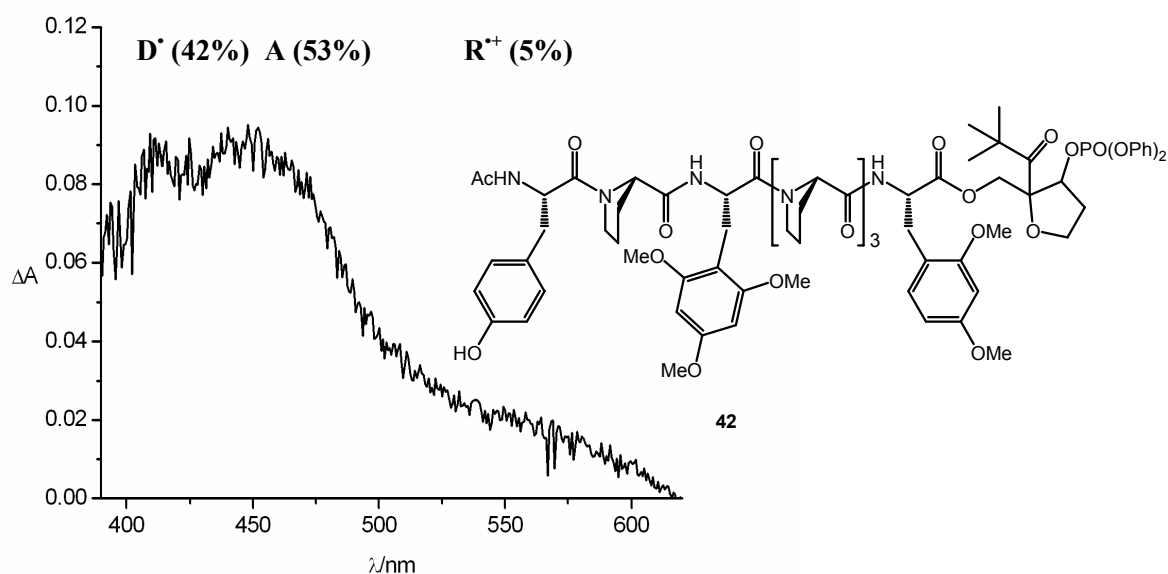


Figure 27: Transient absorption spectrum of **42** 40 ns after laser irradiation.

The sum of electrons transferred from the distal relay sites to the acceptor is thus dependent on the overall length of the peptide. The ratio of oxidized relay and donor can be deduced to depend on the relative length of the spacers.

Upon elongation of the separating matrix to a total of seven prolines with one proline between acceptor and relay and six prolines between relay and donor, as in peptide **43**, the amount of oxidized relay observed after 40 ns is increased to 35% of overall absorption. Around 50% of the charge has already left the electron acceptor after that delay. The graphical decomposition leads to a distribution of 19% oxidized tyrosine, 46% oxidized electron acceptor and 35% oxidized relay. However, the quality of the measured spectrum is low, due to a lower signal intensity.

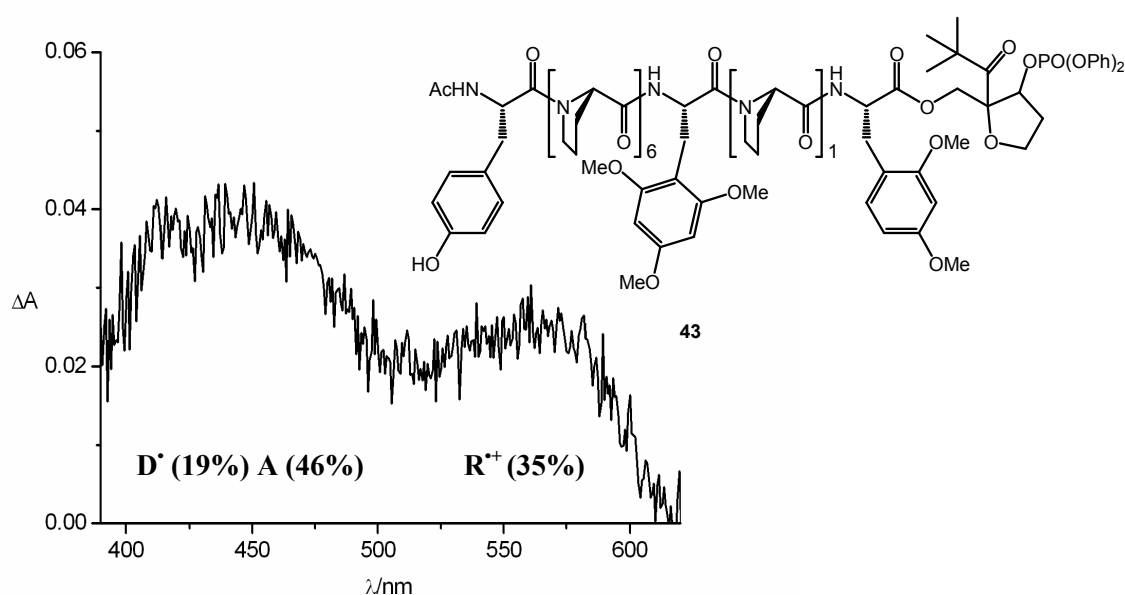


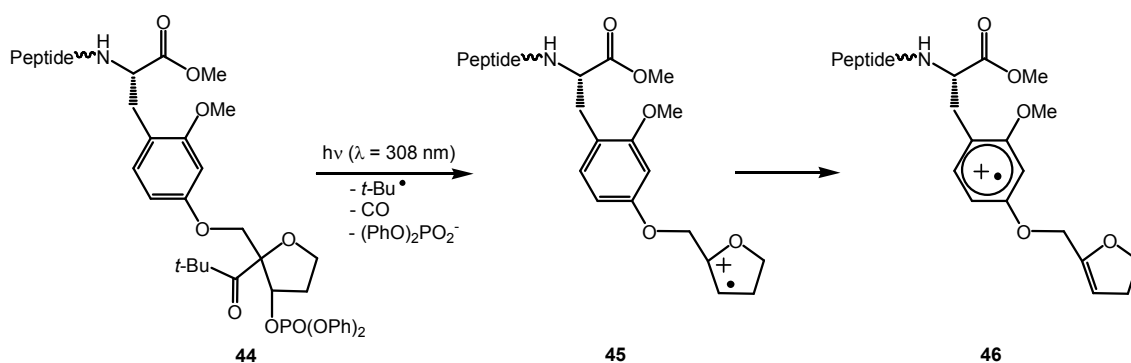
Figure 28: Transient absorption spectrum of **43** 40 ns after laser irradiation.

To summarize the results obtained in LFP of peptides of type **18**, signals of oxidized relay amino acids are observed in all experiments. A control experiment showed, that *intermolecular* reactions can be excluded as an origin of these oxidations. Therefore, *intramolecular* ET processes between relay amino acids and electron acceptors occur in peptides **18**. While a small amount of tyrosyl radical can be explained by *intermolecular* oxidation reactions, the efficient donor to acceptor ET observed in peptides **37**, **41** and **42**, can only be explained by *intramolecular* processes. This can be deduced from considerations referring to diffusion controlled reaction rates, as well as from a control experiment and from the consideration that diffusion controlled processes between the respective ends of two peptide chains should not depend on the length and structure of the peptide strong enough to explain the remarkable differences in ET efficiency in peptides **18** noted above. In conclusion, *intramolecular* ET between donor, relay and acceptor occurs in peptides of type **18**. The distribution of the charge across the three available redox sites depends on the length of the spacers separating those sites.

These experimental results leads to the interpretation, that ET in peptides **18** possibly occurs in a stepwise manner with ET efficiencies controlled by distance (dependent on the spacer length) and driving force of each, the donor to relay as well as the relay to acceptor transfer step. However, these conclusions have to be taken with care, because though all investigated peptides have been constructed from the same building blocks, with units of 1 proline resp. 3 or 6 prolines (one or two repeat units of the PPII-helix), not much is known about the structure of the peptides in solution and the resulting actual distances between the redox sites. An additional uncertainty exists concerning the mechanism of ET. It could be proven that ET occurs *intramolecularly*, and that oxidized intermediates of the relay site can be observed. But it is not clear, whether the electrons are passed successively through the available redox sites in those peptides, where all three transients are observed upon irradiation. A direct transfer of the charge from the injector radical cation **4** to the relay or donor site should be inefficient, due to competition with water addition, as could be proven by experiments of Napp (cf. paragraph 3.1), but could not be excluded completely so far. Additional experiments performed to check this possibility are described in the following chapter. It is moreover conceivable, that different members of the ensemble of peptide conformers in solution either allow oxidation of the final electron donor or of the relay amino acid and that the distribution of conformers is the crucial factor controlling the observed ET efficiencies. Since efficient donor to acceptor ET only takes place in peptides containing at least one short (monoproline) spacer, presumably resulting in significant structural flexibility, the discussed systems are not suited as a starting point for the replacement of the amino acid at the relay position. To solve the possible problem of direct injection into distal sites and to design a model suitable for the investigation of side-chain relevance, a new injection system was designed, as described in chapter 6.

6 Improving Charge Injection

To address the problem of possible direct ET to the injector radical cation **4** from a distal relay site, the distance between injection unit and aromatic amino acid should be shortened.

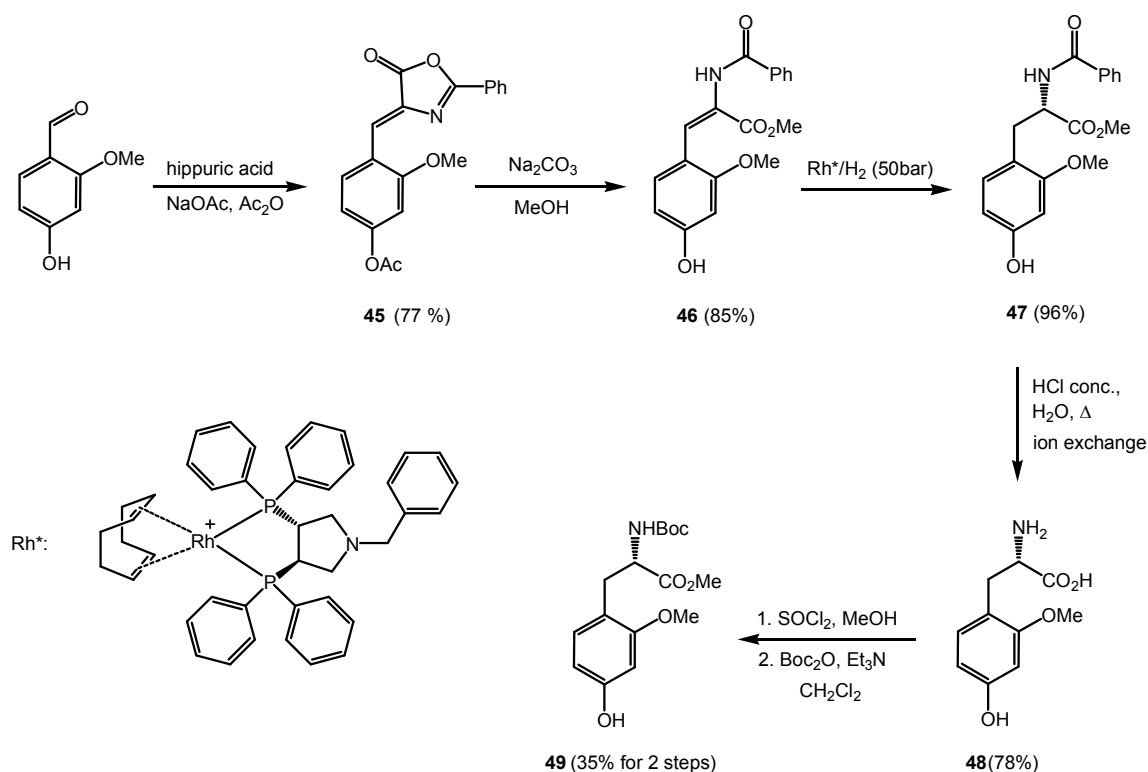


Scheme 19: New electron acceptor precursor with shortened linkage between injection moiety and aromatic side chain, to guarantee fast charge injection.

In the precursor **44**, the primary alcohol of the injection system **2** (Scheme 4, page 19) is connected directly, via an ether bond, to the aromatic side chain of a tyrosine derivative, carrying an additional methoxyfunction in *ortho*-position. Thus, the number of bonds separating the respective injector radical cation **45**, generated upon laser irradiation, from the adjacent aromatic has decreased from six to three, compared to the C-terminal ester linkage found in peptides **18**. This leads to fast electron acceptor generation (**45** → **46**) and renders a successful competition of distal charge injection highly improbable (Scheme 19).

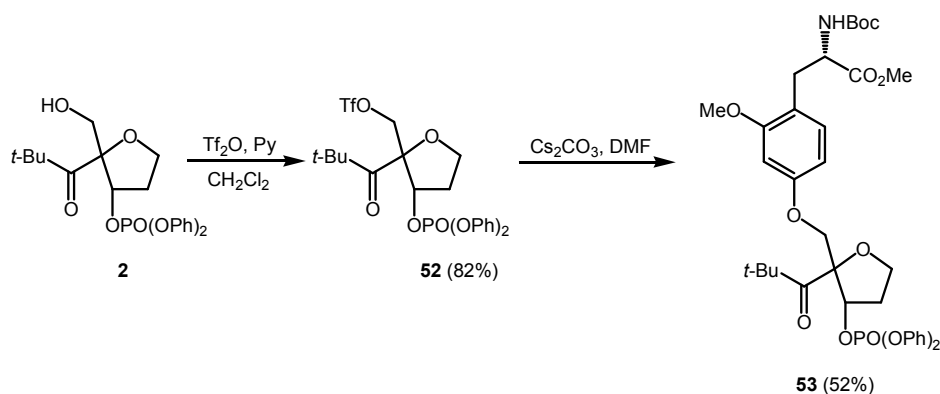
6.1 Synthesis of a New Charge Injector

The synthesis of non-natural amino acid **50** (Scheme 20) was possible analogous to the synthesis of the methoxysubstituted phenylalanines depicted in Scheme 12, starting from commercially available 4-hydroxy-2-methoxybenzaldehyde applying an Erlenmeyer azlactone procedure.^[25, 26] Basic opening of lactone **45** and asymmetric hydrogenation of acrylic acid **48** with a commercially available Rhodium Deguphos^[27] catalyst gave the (S)-configured amino acid derivative **49** in very good yield and >95% *ee*. Deprotection under strongly acidic conditions and purification via ion exchange chromatography yielded free amino acid **50** (78%), which could be converted to the N-Boc protected methyl ester **51** using standard conditions. However, a migration of the Boc-protection group to the hydroxy function of the aromatic ring lowered the yield in this reaction to 35%. Due to the instability of compound **51**, coupling to the injection moiety was carried out directly after the isolation.



Scheme 20: Synthesis of enantiopure 4-hydroxy-2-methoxyphenylalanine

The injector moiety was connected to the phenol of the newly synthesized phenylalanine derivative **51**. This was achieved by conversion of primary alcohol **2** into the triflate **52**, using triflic anhydride and pyridine (82%), and subsequent coupling of **52** to the protected 2-methoxysubstituted tyrosine **51** with caesium carbonate as a mild base to give the desired injector-modified aromatic amino acid **53** in 52% yield (Scheme 3).



Scheme 21: Coupling of the injector to 4-hydroxy-2-methoxyphenylalanine

Irradiation of an N-acetyl protected derivative of **53** yielded a transient absorption spectrum with a maximum absorption at 450 nm, as expected (Figure 29).

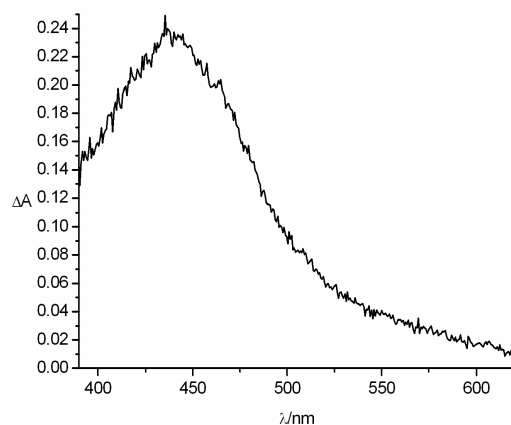


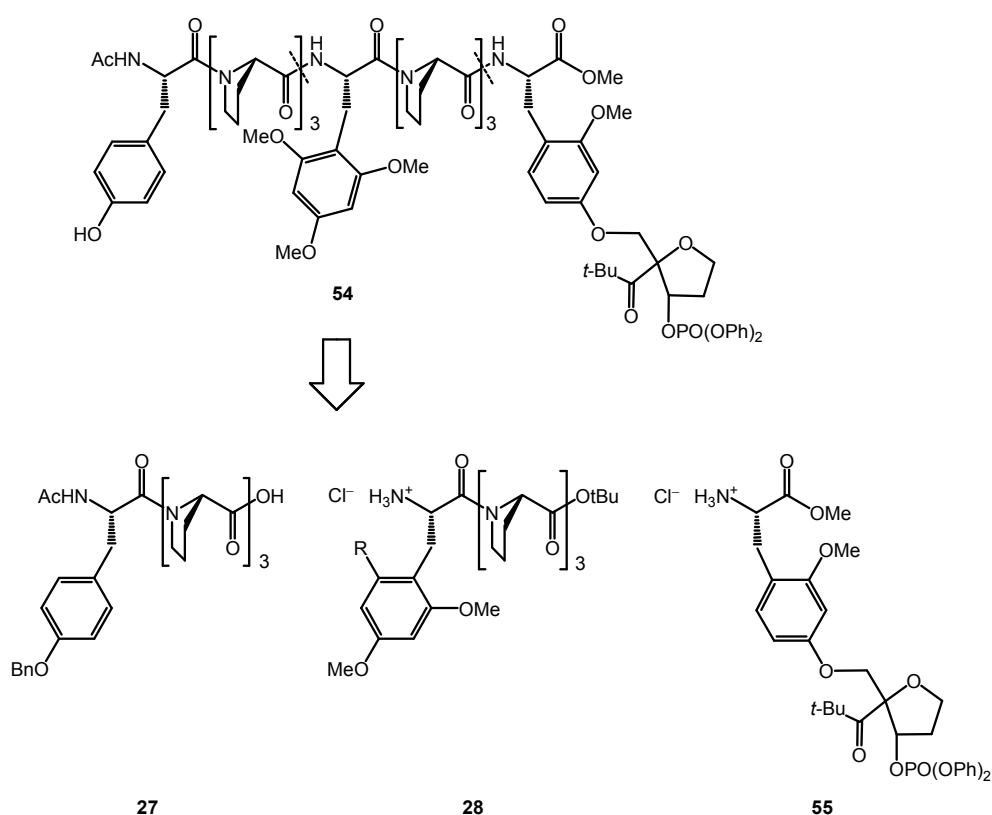
*Figure 29: Transient absorption spectrum recorded 40 ns after laser irradiation of N-acetyl protected **53**.*

The shape of the absorption band differs slightly from the respective spectrum of the 2,4-dimethoxyphenylalanine radical cation, generated from the precursor **15** (Figure 15, page 29). Therefore, the curve in Figure 29 was used for decomposition of transient absorption spectra of peptides containing the new electron acceptor precursor **44**, analogous to the method depicted in Figure 21 (page 47).

6.2 Synthesis of Peptides

Peptides containing the new electron acceptor precursor were assembled using two different strategies, dependent on the nature of the relay amino acid.

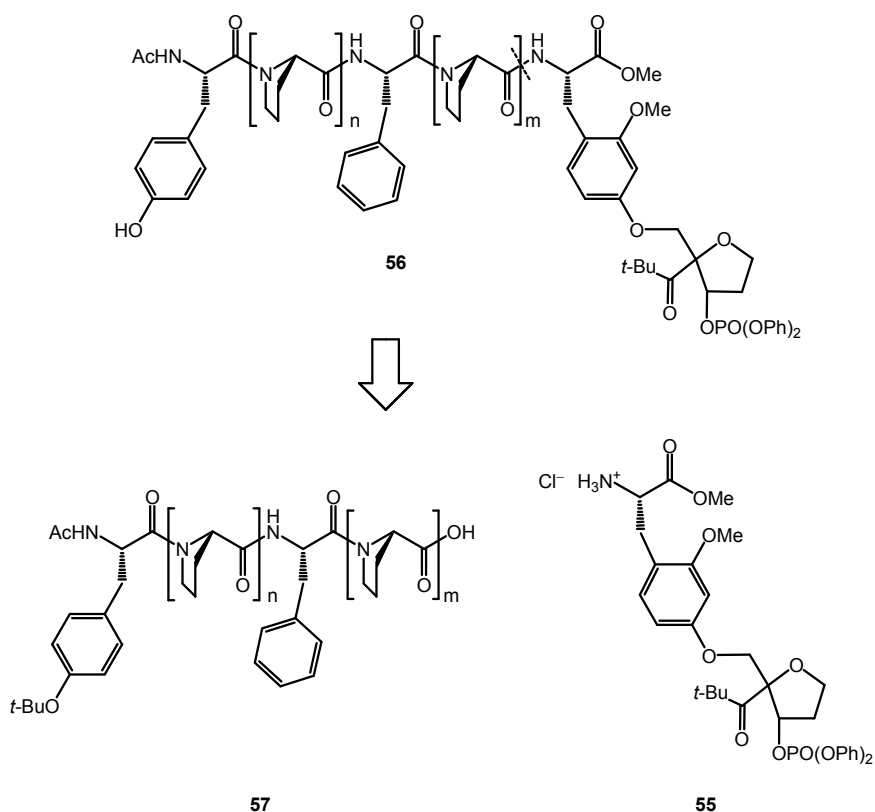
1.) If the relay amino acid, situated inside the proline matrix and separating it into two fragments of n and m units, was a non-natural amino acid (in this case 2,4,6-trimethoxyphenylalanine) peptides **54** were assembled by solution synthesis using the Boc-protection strategy, analogous to the peptide models of type **18** (cf. Scheme 13, page 39). The fragments used are indicated in Scheme 22. Synthesis of the respective fragments **27** and **28** is depicted in Scheme 14 (page 40). Fragment **55** can be obtained by acidic deprotection of **53**, using HCl in dioxane.



Scheme 22: Synthesis of peptides containing the new injection unit and a non-natural amino acid as relay.

Assembly of the peptide fragments is achieved analogous to the procedure depicted in Scheme 15 (page 41), by HCTU-mediated coupling and subsequent reductive benzyl-deprotection of the tyrosine hydroxy function with hydrogen and Pd on activated charcoal as a last step, yielding peptides **54**.

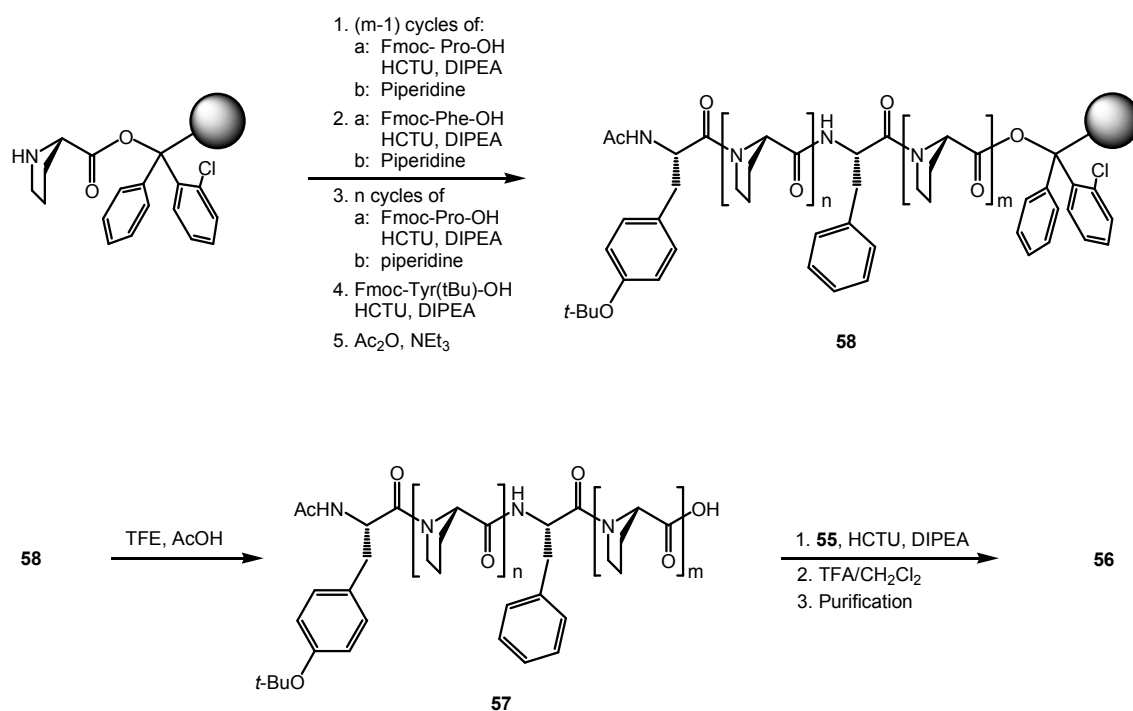
2.) If the central amino acid was a natural amino acid, in this case phenylalanine, peptides **56** were assembled from two fragments, one consisting of the N-deprotected electron acceptor precursor **55**. The second fragment, the free acid of the N-terminal peptide part **57**, was synthesized using solid phase peptide synthesis (SPPS) (Scheme 23).



Scheme 23: Fragments used for the synthesis of peptides containing the natura amino acid phenylalanine at the relay position.

The course of the SPPS is depicted in Scheme 24. It was carried out on a commercially available chlorotrityl-resin, charged with proline, using Fmoc strategy in a fully automatized peptide synthesizer. Cleavage of the resulting oligopeptide with trifluoroethanol and acetic acid yielded the free acid **57**, which was coupled to the deprotected electron acceptor precursor **55** in solution. The *tert*-butylether group protecting the tyrosine hydroxy function was subsequently cleaved with trifluoroacetic acid (TFA) in CH_2Cl_2 (Scheme 24).

To remove all UV-active impurities absorbing at 308 nm, a hydrogenation step with Pd/C as a catalyst was introduced in the purification procedure.

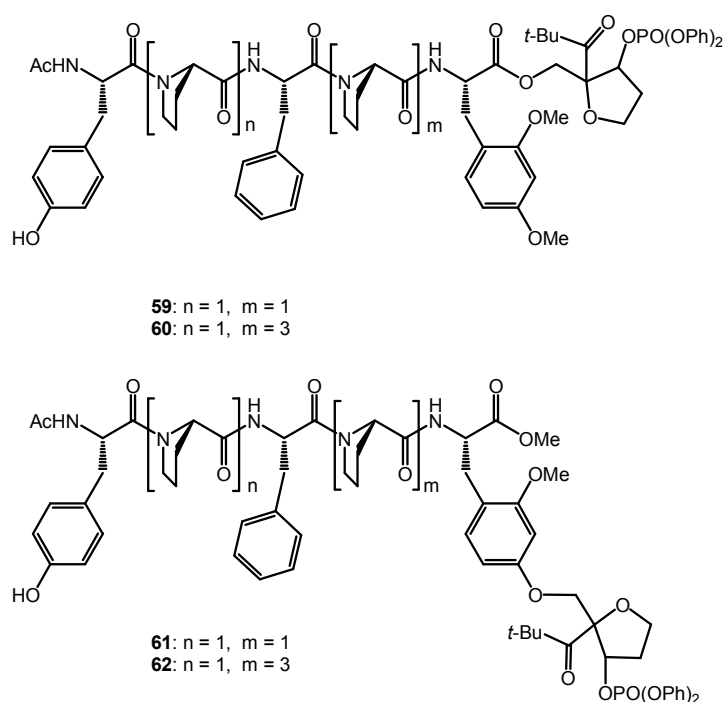


Scheme 24: SPPS strategy for the synthesis of fragment 57 and coupling to 55 in solution phase.

The resulting peptide models of type 54 and 56 were checked on their purity by HPLC analysis and UV-spectroscopy ($\epsilon_{308} < 60 \text{ M}^{-1} \text{ cm}^{-1}$).

6.3 Results and Discussion

To investigate the influence of the charge injection system on donor to acceptor ET, peptides **59** and **61** as well as **60** and **62** were synthesized according to the SPPS strategy depicted in Scheme 24 and their transient absorption spectra were recorded 40 ns after laser irradiation. Analysis of the spectra revealed an increased amount of tyrosyl radical formation in peptides **61** and **62**, containing the side-chain linked injection unit, as compared to **59** and **60**, in which charge injection into analogous sequences occurred across the C-terminal ester linkage.



Scheme 25: Peptides synthesized to estimate the influence of the charge injection system on donor to acceptor ET within 40 ns.

79% of tyrosine has already been oxidized 40 ns after the laser flash in peptide **61**, as compared to 68% in **59** and 41% tyrosyl was formed 40 ns after irradiation of **62**, compared to 30% in **60** (see Figure 30).

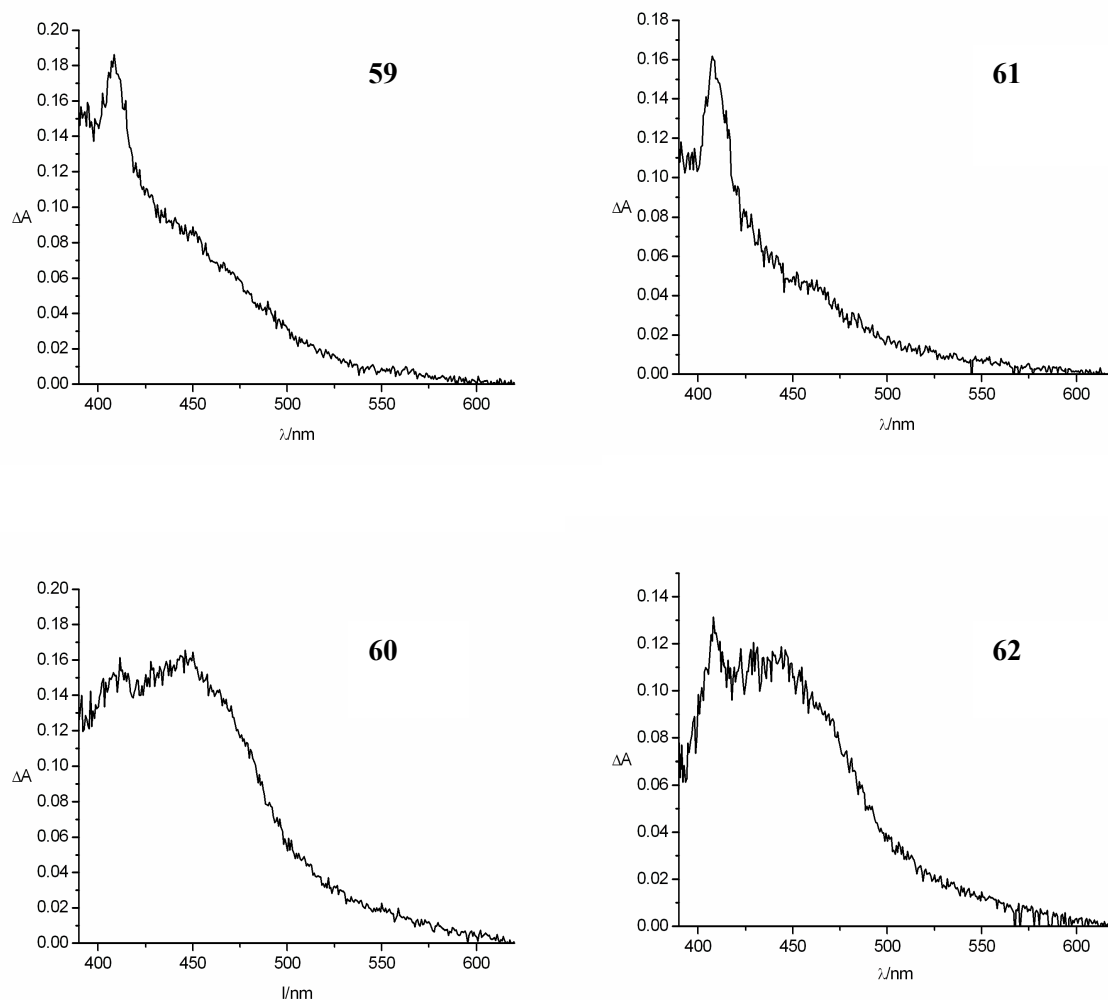
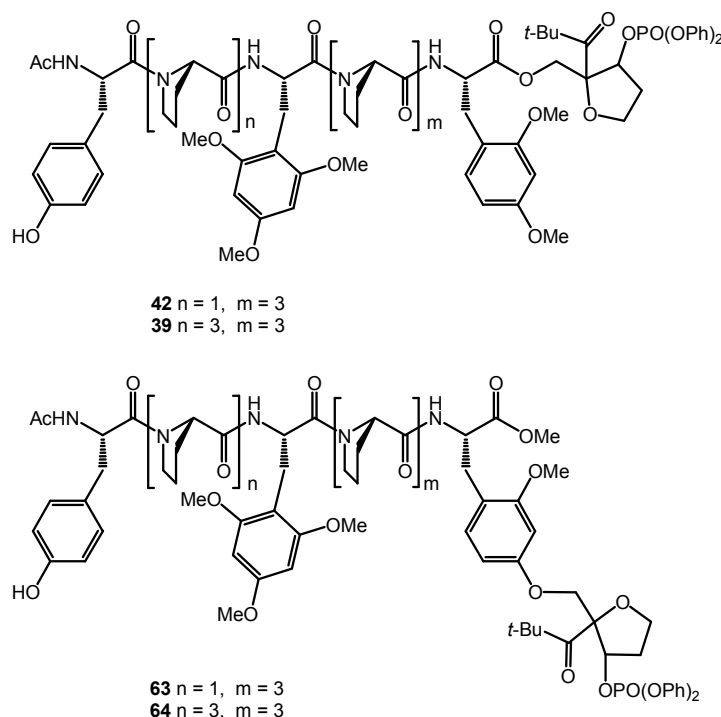


Figure 30: Transient absorption spectra of peptides **59**, **61** and **60**, **62** recorded 40 ns after laser irradiation.

If distal charge injection into tyrosine occurred in peptides featuring the ester-linked injection system (**59** and **60**), the tyrosine signal in those peptides should be increased by this reaction, compared to a system in which distal injection can be excluded (**61** and **62**). The results obtained with peptides **59-62** thus rule out direct donor (tyrosine) to injector radical cation (**4**) ET in peptides **18**.

To investigate the possibility of distal injection into the relay amino acid, the transient absorption spectra of peptides **42** and **63**, as well as **39** and **64** were compared.



Scheme 26: Peptides synthesized to estimate the influence of the charge injection system on relay to acceptor ET within 40 ns.

As a result of the measurement, the intensity of the relay amino acid signal is higher in **63**, containing the directly linked injection system (11% oxidized relay), than in **42** (5% oxidized relay). Distal charge injection into the relay amino acid in peptides **18**, containing the ester-linked C-terminal injector, can thus also be excluded.

Laser flash photolysis of peptides **39** and **64**, showed a similar yield of oxidized relay (9% and 10% respectively), yet a significant difference in the amount of donor to acceptor ET during 40 ns. While in **39** almost no tyrosine oxidation occurred within the time frame of the measurement, in **64** the tyrosyl radical amounts to 36% of overall oxidized species within that delay.

The increased donor to acceptor ET efficiency within a 40 ns delay, observed upon introduction of the directly linked injector, points to an increase in the injection rate. In this context, the observation of oxidized donor 40 ns after irradiation in the nonapeptide **64** is of special interest, since the ester-linked injection system did not allow the observation of donor to acceptor ET within 40 ns in a peptide of analogous sequence (**39**). The newly developed electron acceptor precursor **44** therefore also contributes to the construction of a suitable model for the investigation of side-chain influence on ET through peptides, as will be discussed in detail below.

7 Influence of Amino-Acid Side Chains on ET

7.1 Introduction

In chapter 6.3 it could be shown, that electron acceptor generation in peptide models of type **54**, containing the electron acceptor precursor **44** (Scheme 19, page 57), can be assumed to proceed faster than in the respective peptides of type **18**, discussed in chapter 5. The distance between the injector radical cation generated upon irradiation, and the C-terminal aromatic ring is substantially smaller in peptides **54** than in peptides **18**. As a consequence, one advantage of the electron acceptor precursor **44** is its lower susceptibility for side reactions of the respective precursor radical **45**. Much more important, it widens the number of possible candidates to observe intramolecular ET: The limitations of our model have been discussed extensively in chapter 5.4.1. One important point is the small time window available for the observation of *intramolecular* donor to acceptor ET, due to high peptide concentrations and the resulting high rates for bimolecular reactions. Significant results, yielding information about *intramolecular* ET, can be obtained by analyzing spectra recorded only 40 ns after the laser flash. This limits the possible distances between electron donor and acceptor, i.e. the length of the proline spacers. On the other hand, systems of high structural rigidity, and thus long proline spacers, are needed, if the influence of amino acid side chains on ET shall be investigated, because only if structural uniformity can be guaranteed, the ET-mediation properties of an individual amino acid can be observed as the key factor controlling the overall ET behaviour of the peptide. During the investigation of peptide models **18** no suitable system could be found. However, the faster charge injection in peptides **54**, caused by shorter injector/acceptor distance, allows longer spacers without blocking *intramolecular* ET in the available time window. Special care has to be taken to the observation of an oxidized intermediate during ET, because this proof is needed to confirm a sequential mechanism. The amount of intermediate formed in a consecutive reaction depends on the relative rates of the reaction steps. Therefore the structure of a peptide suited for the observation of oxidized intermediates has to be optimized also in this respect.

For these reasons, the finding, that in peptide **64**, with two triproline spacers separating the central 2,4,6-trimethoxyphenylalanine from C-terminal electron acceptor and N-terminal electron donor each, all three oxidized aromatic side chains can be detected after 40 ns (Figure 31), was highly encouraging to us.

The N-terminal donor getting oxidized within 40 ns, indicated by the maximum at 410 nm, points to *intramolecular*, donor to acceptor ET, as discussed extensively above.

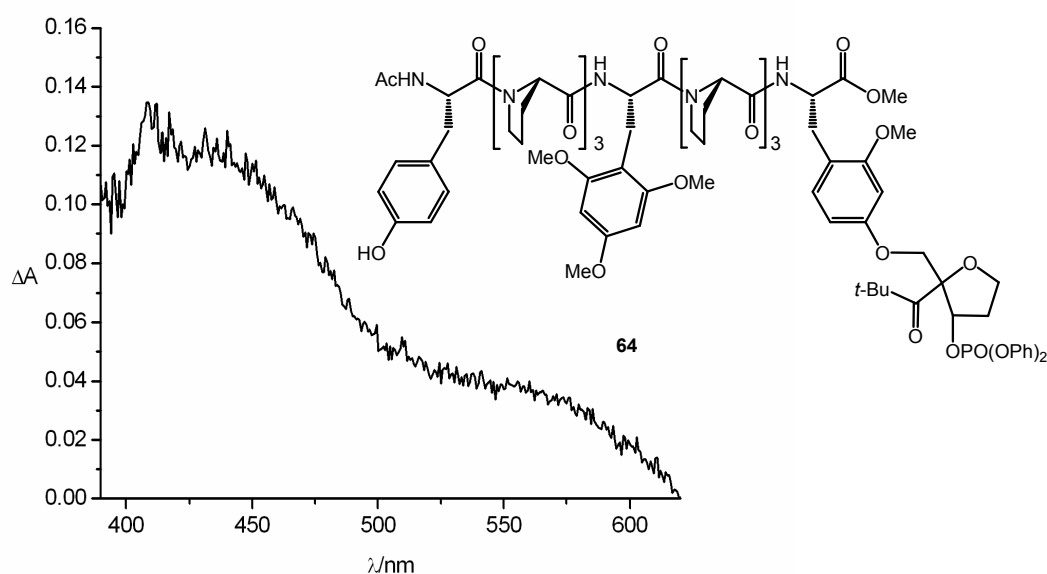
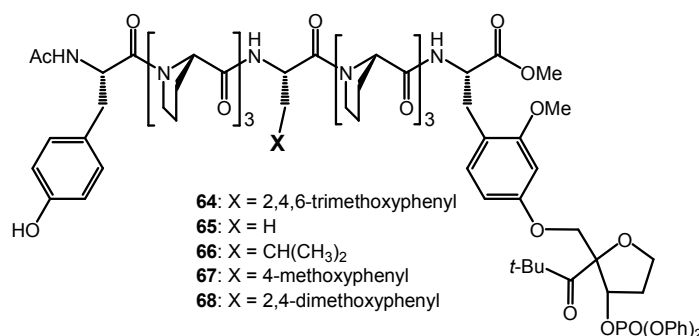


Figure 31: Transient absorption spectrum of **64**, 40 ns after laser irradiation.

Moreover, the absorption detected at 550 nm results from 2,4,6-trimethoxyphenylalanine radical cation, and thus indicates the occurrence of oxidized relay amino acid. Therefore, the distances in peptide **64** render it suitable as a sensor for *intramolecular* ET between all three aromatic side chains. In addition, several hints were available, that triproline spacers guarantee a defined structure. First, in peptide **39**, containing the ester-linked C-terminal injector, the distance between electron acceptor and electron donor was too large to allow the intramolecular reaction, leading to the conclusion that no conformers with short through-space distances are present. Second, it can be derived from the literature, that the onset of secondary structure in oligoproline can be expected starting from three consecutive prolines.^[79] Moreover, the preferred conformation of oligoproline in polar solvents, the polyproline II helix, has a repeat unit of three prolines,^[96] so that an alignment of residues in a proline matrix using triproline spacers, can be assumed to result in a regular pattern.

Peptide **64** thus seemed to be the ideal starting point for the investigation of side-chain relevance for ET through oligopeptides. To this end, several peptides were synthesized, in which the hexaproline matrix was parted into two triproline sequences by the introduction of a central amino acid, with a side chain **X**. This side chain was varied with respect to its electronic properties, i.e. its ability to serve as a relay in sequential ET (Scheme 27). The relevance of **X** for efficient ET can then be estimated by comparison of the signal intensities of acceptor radical cation and donor radical in different peptides at a fixed delay after charge injection.



Scheme 27: Peptides used to estimate side-chain participation in sequential ET.

For this comparison, three conditions have to be met: Structural unity among the different peptides has to be achieved, *intramolecular* ET between all three redox sites has to be observable in the reference system, containing the spectroscopic sensor, and ET has to be of medium efficiency in this system, so that deviations in both directions (increased or reduced efficiency) can be resolved in the measurements.

Peptides with sequences analogous to **64** seem to fulfill this conditions and were therefore chosen as model for the investigation of the influence of specific amino acid side chains on long-distance ET in peptides. The syntheses of these peptides follow the syntheses described in chapter 6.2, with SPPS synthesis (Fmoc-strategy), followed by coupling to the free amine of the electron acceptor precursor in solution phase, used for all peptides containing commercially available amino acids in the N-terminal part, **65-67** (cf. Scheme 23 and Scheme 24, page 61) and solution phase synthesis (Boc-strategy) for the peptides containing our non-natural methoxysubstituted phenylalanines, **64** and **68** (cf. Scheme 22, page 60).

7.2 Structure

To gain more information about the structure of peptides **64** - **68**, circular dichroism (CD) spectra of these peptides were recorded (Figure 32). The solvent system needed for LFP experiments, a 3:1 mixture of acetonitrile and water, was used for CD spectroscopy. Due to the high sensitivity of this analytical method, the peptides had to be dissolved in low concentrations of approximately $20 \mu\text{g mL}^{-1}$.

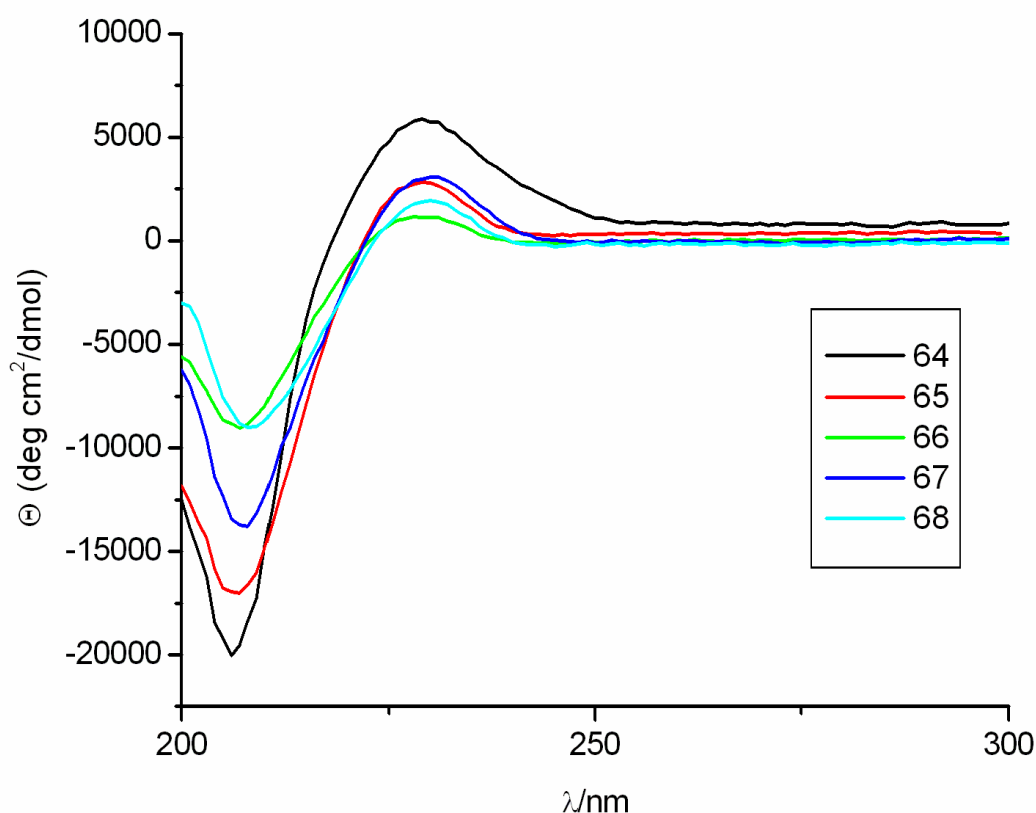


Figure 32: CD spectra of peptides **64** - **68** in acetonitrile/water (3:1) at 25 °C, with concentrations of approximately $20 \mu\text{g mL}^{-1}$.

The spectra show the characteristic shape expected for a polyproline II (PPII) helix, with a strong negative band around 206 nm and a weaker positive band at 229 nm.^[96]

The PPII helix is the typical structure adopted by proline oligomers in polar solvents, especially water,^[97, 98] and an important secondary structure in natural enzymes.^[99, 100] All peptide bonds are *trans*-configured, with Ramachandran angles (cf. Figure 7, page 13) of -78° (Φ) and $+146^\circ$ (Ψ), respectively.^[101] The repeat unit of the left-handed helix consists of three prolines, with a lateral transition given with 3.12 \AA per residue.^[96, 102]

Results from Förster resonance energy (FRET) measurements have been used to estimate end-to-end distances in proline oligomers. While long peptides, containing 20-40 residues have been shown to exhibit unexpectedly fast and efficient fluorescence quenching, pointing towards significant bending of the molecule and thus shortened end-to-end distances,^[103] proline oligomers of up to 12 residues can be approximated by a rigid rod structure^[104] and are thus suited to serve as spectroscopic rulers, providing spacers of defined length.

The stability of the helix conformation of peptides **64** - **68** in the solvent system was checked by a melting experiment, in which the peptide solution was heated up to 80 °C and the absorption at the maximum of the CD spectrum was monitored. Just a modest linear decrease, no phase transition, could be observed within a temperature range from 10 °C to 80 °C. This points to a high stability of the helix conformation and it can thus be concluded, that a large majority of the peptides in the LFP experiments is present in PPII conformation.^[105] Since only a small fraction of the peptides undergoes photocleavage, resulting in electron acceptor formation, the observed signals in the transient absorption spectra with very high probability stem from the major conformer, exhibiting a uniform structure throughout the series of varying side chains X.

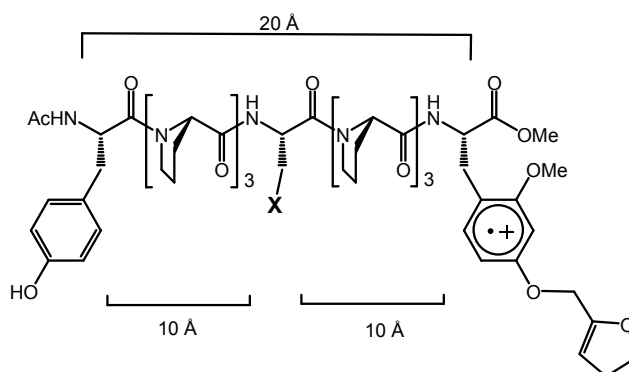


Figure 33: Distances between the relay sites arranged with triproline spacers.

Thus, the peptide series **64** - **68** is suited to serve as a model for the influence of the side chain on ET, with the properties of the side chain representing the significant factor controlling differences in this series. The distances between the relay sites can be estimated from the known properties of the PPII helix, resulting in an overall donor to acceptor distance of approx. 20 Å, i.e. a distance of approx. 10 Å between the relay and both, electron donor and acceptor (Figure 33). The aromatic residues can be assumed to be aligned in 120° angles to each other.

7.3 Results and Discussion

7.3.1 Mechanism of Electron Transfer

As a starting point for the investigation of side-chain participation in ET through peptides, peptide **64** has been chosen. In this peptide, signals of oxidized electron acceptor A (2,4-dialkoxyphenylalanine radical cation, red, $\lambda_{\max} = 450$ nm), oxidized relay amino acid R^{*+} (2,4,6-trimethoxyphenylalanine radical cation, green, $\lambda_{\max} = 550$ nm) and oxidized electron donor D^* (tyrosyl radical, blue, $\lambda_{\max} = 410$ nm) could be observed simultaneously 40 ns after laser irradiation. The efficiency of ET to the acceptor during this time could be determined to 46%, with 36% of the electrons provided from the final donor tyrosine and 10% of the charge residing on the relay amino acid.

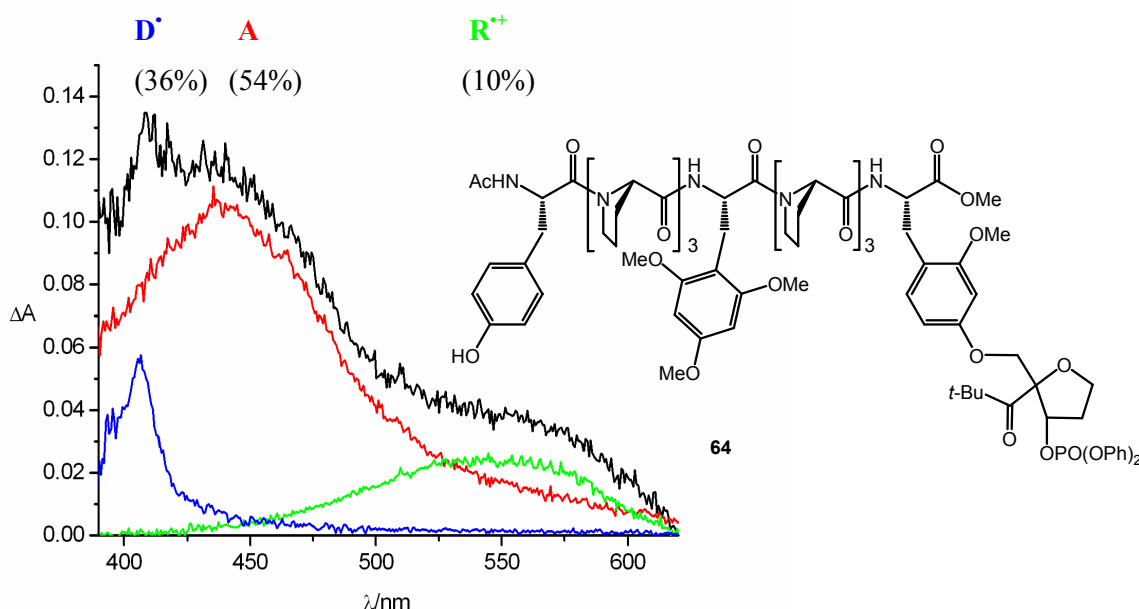


Figure 34: Graphical decomposition of the transient absorption spectrum of **64** recorded 40 ns after laser irradiation.

The simultaneous occurrence of the three transients proves, that the formation of oxidized relays is in principle possible in our peptides. Now, the question should be answered, whether the possibility to form chemical intermediates during the ET process is of relevance for donor to acceptor ET. Therefore, a peptide was synthesized, which resembles **64** in overall structure as well as electron donor and acceptor properties, yet does not feature oxidized intermediates. To this end, the aromatic side chain occupying the central position in **64** was replaced by an aliphatic residue, placing alanine at the position of the relay amino acid. The transient absorption spectrum recorded 40 ns after laser irradiation of the resulting peptide **65** is shown in Figure 35.

Obviously, no absorption is visible around 550 nm. The main part of the charge is located at the electron acceptor, leading to a strong 450 nm absorption. A small shoulder is visible at lower wavelength, indicating the formation of a small amount of tyrosyl radical. The graphical decomposition yielded a distribution of 93% oxidized electron acceptor to 7% oxidized donor. Since donor to acceptor distance in peptide **65** amounts to approximately 20 Å (see 7.2), the occurrence of *intramolecular* ET seemed highly improbable within the short time delay of the measurement. This led to the question, whether the small amount of tyrosyl radical formed can be attributed to *intermolecular* reactions.

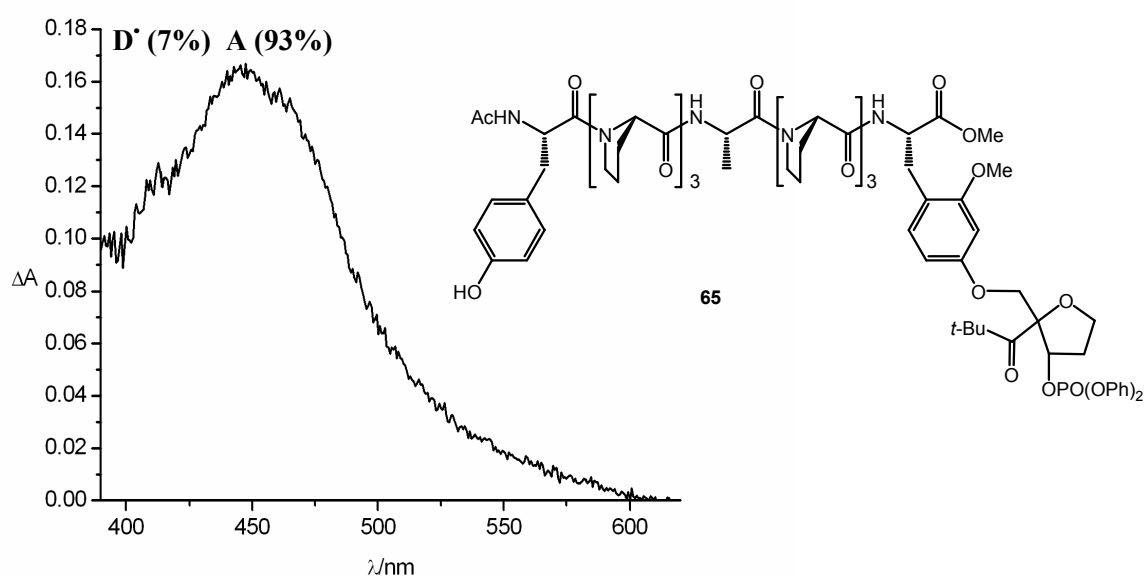
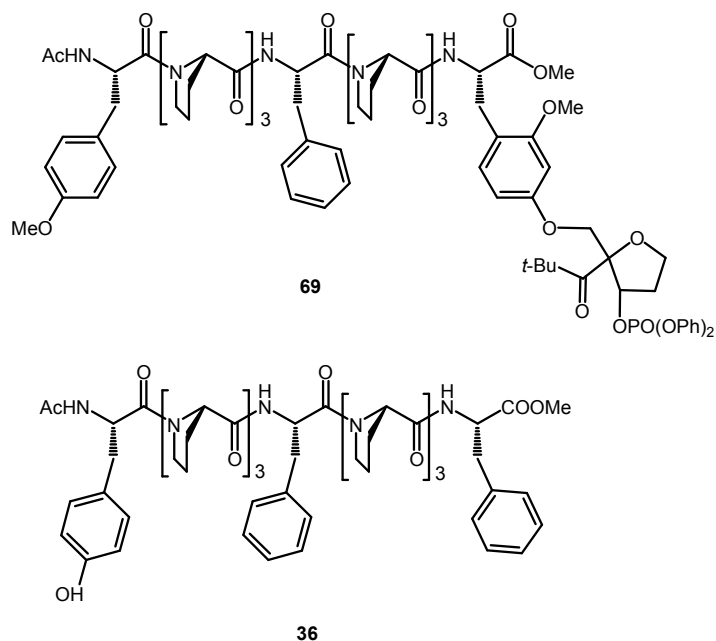


Figure 35: Transient absorption spectrum recorded 40 ns after laser irradiation of **65**.

A control experiment was carried out, using two different peptides **69** and **36**, each containing only one of the redox active aromatic side chains (Scheme 28).



Scheme 28: Peptides used in a control experiment to investigate the contribution of intermolecular ET.

Irradiation of **69** led to formation of the electron acceptor ($\lambda_{\text{max}} = 450$ nm). When equimolar amounts of **36** were added, a very weak signal at 410 nm could be observed (Figure 36). Graphical decomposition of the obtained curve resulted in a distribution of 94% acceptor radical cation (**A**) and 6% tyrosyl radical (**D**[•]). This means, that the observed donor to acceptor ET in peptide **65** can be explained by *intermolecular* ET.

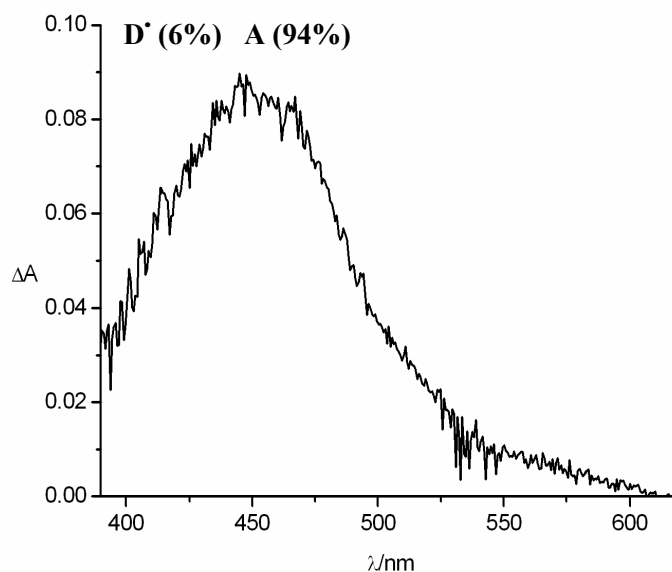


Figure 36; Transient absorption spectrum recorded 40 ns after the irradiation of an equimolar solution of peptides **36** and **69**.

Thus, the replacement of the redox active aromatic relay 2,4,6-trimethoxyphenylalanine by a non-redox active, aliphatic central amino acid results in a severe drop in *intramolecular* ET efficiency from 46% in peptide **64** to <1% in peptide **65**. This effect can be rationalized by the shutdown of a possible sequential ET pathway, consisting of two 10 Å steps, upon exchanging the aromatic side chain in peptide **64** by an aliphatic side chain in peptide **65**. While in peptide **64**, the overall distance of 20 Å can be overcome in an intramolecular reaction within less than 40 ns, using the relay as a stepping stone; in peptide **65**, in contrast, tunneling of the electron over a 20 Å spacer is required to occur in a single step. Yet superexchange ET across that distance does not take place efficiently within 40 ns. A second example for the effect an aliphatic side chain exhibits, was provided by peptide **66**, containing a leucine as central residue. The transient spectrum clearly shows the main absorption at 450 nm (94%), the wavelength of acceptor radical cation absorption. Only a minor fraction (6%) of electrons has already been transferred from tyrosine (Figure 37). This amount can be explained by *intermolecular* ET, as discussed above.

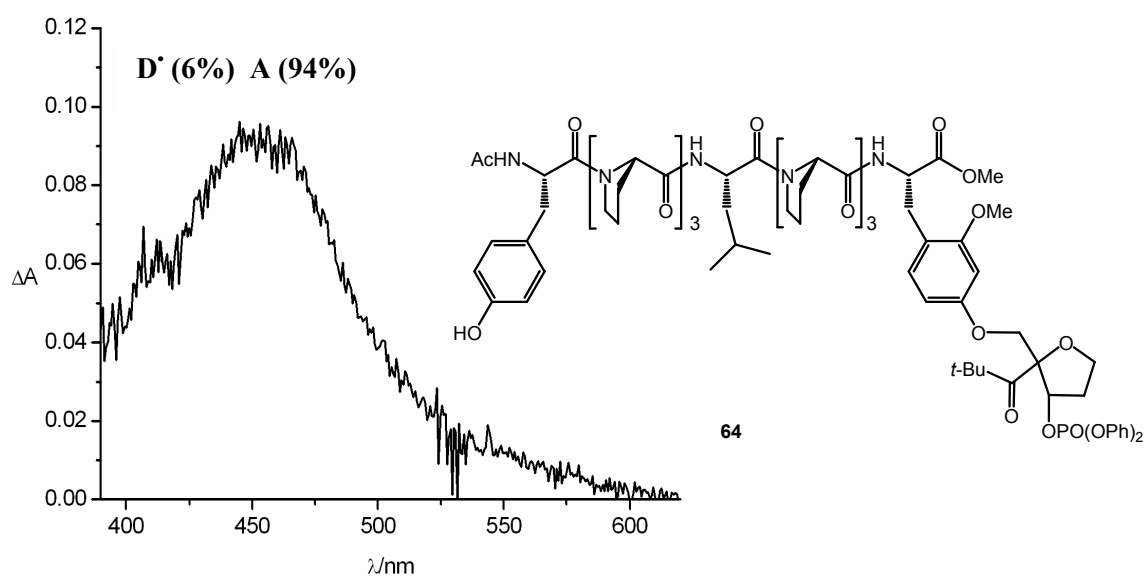


Figure 37: Transient absorption spectrum of peptide **66**, 40 ns after laser irradiation.

Thus, it was proven in two cases, that 20 Å ET across a hexaproline matrix, separated in half by an aliphatic amino acid, is not possible *intramolecularly* with fast rates. For a quantification of the observed effects, see below in paragraph 7.3.2.

To investigate, whether the efficient ET observed in peptide **64** can be traced back to the π -system provided by the central aromatic side chain, peptide **67** was constructed. In this peptide, the central position is occupied by an aromatic amino acid, that can not function as a relay in stepwise ET. The anisol ring has an oxidation potential of 1.52 V vs. NHE,^[83] exceeding the oxidizing force of the laser generated injector radical cation (**4**, $E^0 = 1.44$ V vs. NHE^[71]).

LFP of peptide **67** and observation after 40 ns led to the curve depicted in Figure 38. It shows a distinct maximum at 450 nm, the wavelength of electron acceptor absorbance. A very minor part of the charge (10%) has reached the electron donor within the delay. It can be concluded, that *intramolecular* ET is not efficiently mediated by an anisol moiety situated at the relay position. The existence of an aromatic side chain at the relay position is therefore no sufficient explanation for the ET properties of peptide **64**, as compared to **65** and **66**. Peptides of high structural similarity, such as **64** and **67**, having a similar secondary structure, as proven by CD spectroscopy, and differing only in the number of methoxy substituents at the central aromatic side chain, differ significantly in their ET properties.

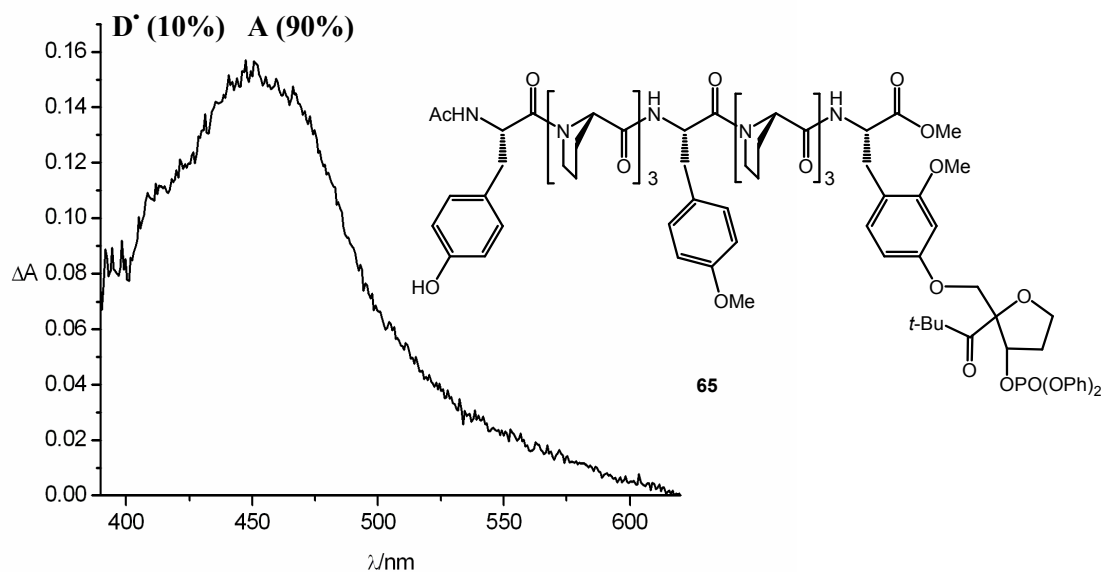


Figure 38: Transient absorption sepctrum of peptide **67**, 40 ns after laser irradiation.

The hypothesis, that the redox potential of the central amino acid, i.e. its suitability to function as an electron relay, is the main factor controlling ET efficiency, should be confirmed by investigation of the ET properties of an additional peptide **68**. This peptide contains 2,4-dimethoxyphenylalanine as central amino acid. The oxidation potential of this residue can be assumed to be similar to that of the electron acceptor, since both feature a dialkoxy substitution of the same pattern. In this respect, the design of peptide **68** accords to the situation in DNA, where electrons are transferred over large distances, using stepping stones of similar redox properties - the DNA bases.

In contrast to peptide **64**, containing three orthogonal spectroscopic sensors, ET through system **68** does only lead to two different absorption maxima. The transient absorption spectrum of the oxidized relay cannot be distinguished from the spectrum of the electron acceptor, and the absorption band around 450 nm represents the sum of oxidized electron acceptor and relay (Figure 39). It amounts to 63%. This means, that 27% of the charge has already migrated to the final donor tyrosine, causing an additional observable absorption maximum at 410 nm.

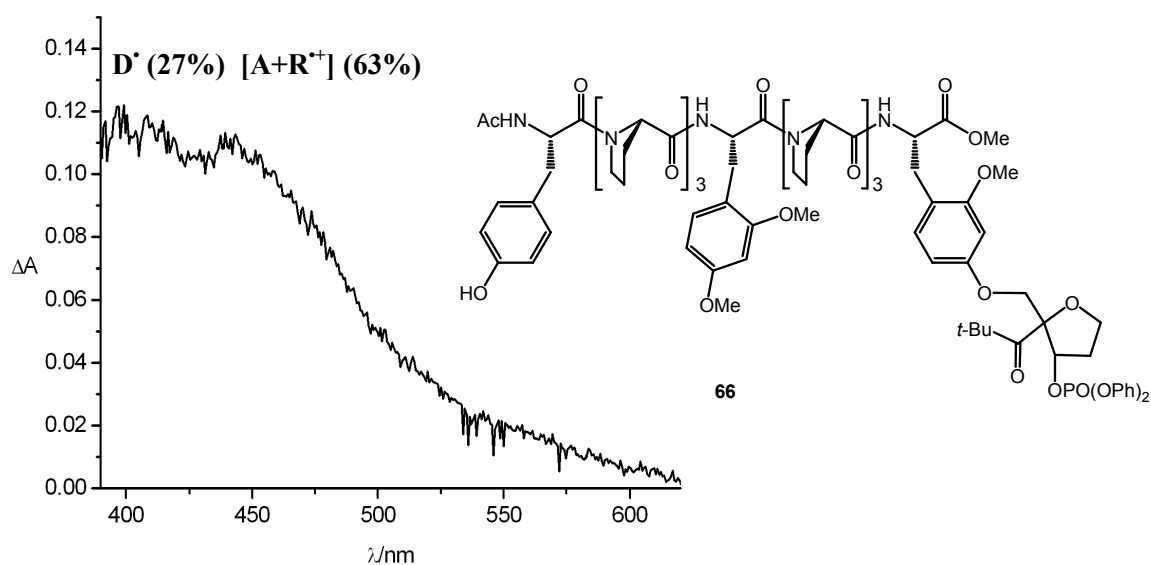
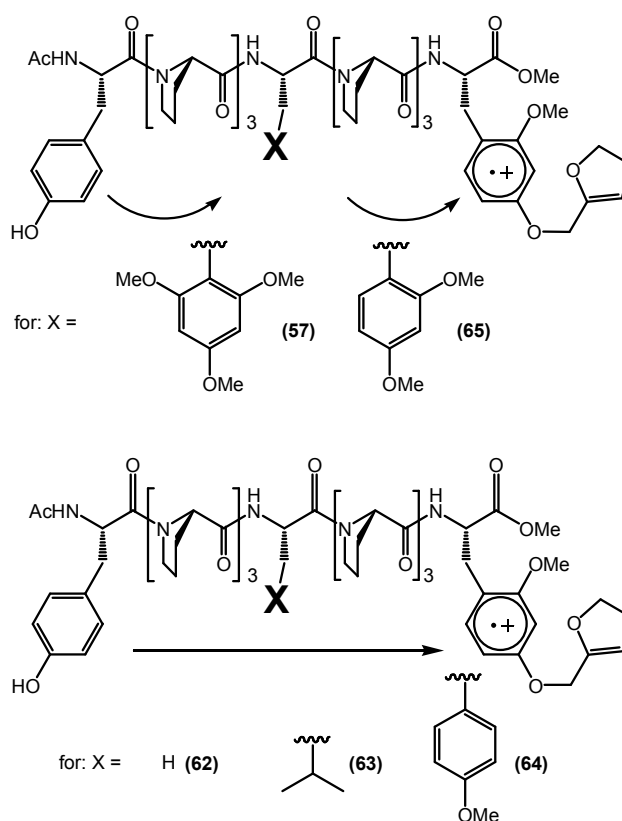


Figure 39: Transient absorption spectrum of peptide **68**, 40 ns after laser irradiation.

In summary, with peptides **64** and **68**, two examples are available for efficient ET across a 20 Å distance through a peptide matrix. Both peptides contain an oxidizable aromatic amino acid at the central position, cutting the 20 Å spacer in half. In peptide **64**, the oxidized relay generates a characteristic absorbance, different from the absorption of electron acceptor and electron donor. Using this peptide, the simultaneous detection of the oxidized forms of three redox sites involved in ET, was possible. In three peptides **65**, **66** and **67**, non-oxidizable aliphatic or aromatic side chains are present at the central position. In these peptides, no efficient *intramolecular* ET was observed. This leads to

the conclusion that efficient *intramolecular* long range ET is made possible by the presence of redox relays. These relays function as stepping stones in the ET process, with the charge possessing a lifetime at this position, generating a chemical intermediate. It can be concluded, that aromatic amino acid side chains can assist in carrying a charge over large distances, featuring electron hopping. Sequential ET pathways, using naturally occurring aromatic amino acids, have been proposed in several enzymes, e.g. ribonucleotide reductase or DNA photolyase. The importance of the respective residues has been proven by molecular biology studies, yet so far no spectroscopic evidence for the course of a consecutive reaction is available in these systems. We have now developed a peptide model, which allows the determination of sequential ET. An oxidizable relay in the matrix renders efficient donor to acceptor ET across 20 Å (or rather 2 x 10 Å) possible within short reaction times. Without this relay, ET has to occur via a single-step superexchange mechanism, which cannot be observed with high efficiency during the time frame of our experiment (Scheme 29). Thus our system allows the investigation of individual amino acids with respect to their ability to serve as stepping stones in electron hopping.



Scheme 29: The deciding factor controlling ET mechanism (and efficiency) in the oligopeptide models is the character of the side chain X. Electron transfer by hopping (on top) occurs, when oxidizable aromatic side chains are present in the peptide matrix. ET by single step superexchange (at the bottom) does not take place within the time frame of the experiment.

7.3.2 Electron Transfer Rates

To gain information about the ET rates achieved in peptides **64** - **68**, an interpretation of the quantitative data obtained from the graphical analysis was done. The data is summarized in the second column of Table 1. As a key to the interpretation, the competition between *intramolecular* and *intermolecular* ET in the respective peptides was utilized. From a control experiment, the amount of tyrosyl radical formed *intermolecularly* under the conditions of the LFP experiments was estimated to 6%. Subtraction of this value from the observed tyrosyl radical absorption leads to the values given in the last column of Table 1, representing the contribution of the *intramolecular* reaction.

Table 1: Tyrosyl radicals yielded within 40 ns after laser flash photolysis of 64 - 68 (relative error for all values: 15%), without and with correction for the contribution of intermolecular ET. The sum of oxidized aromatic side chains is set to 100%. The amount of tyrosyl radical formed by intermolecular reaction of 69 and 36 is given for comparison.

	Tyrosyl-Radical (detected)	Tyrosyl-Radical (corrected)
69+36	6.1%	=
65	6.9%	≤ 1%
66	6.1%	≤ 1%
67	10%	3%
68	27%	21%
64	36%	30%

Intermolecular reaction rates have been determined by dilution experiments carried out by Napp on peptides of type **1** (Scheme 3, page 19), in which the ET rates were determined as a function of peptide concentration.^[65, 66] Since only a small fraction of the peptides (approx. 0.1%) is cleaved by the laser flash, the peptide concentration remains constant during the experiment (pseudo first order reaction), and the rate of the bimolecular quenching reaction depends linearly on the peptide concentration employed in the experiment.

When peptide concentrations are varied and the observed ET rates are depicted as a function of concentration, the slope of the resulting line therefore represents the rate of *intermolecular* ET (Figure 40).

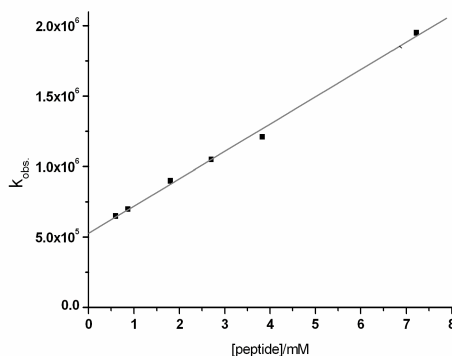


Figure 40: Dilution experiment used for the estimation of intermolecular ET.

The resulting rate constants for penta- and heptapeptide **1** amounted to approx. $3 \cdot 10^8 \text{ M}^{-1} \text{ s}^{-1}$. From this result, the rates of *intermolecular* reaction in the measurements of peptides **64** - **68**, using 5 mM peptide concentrations, can be estimated to approximately $1.5 \cdot 10^6 \text{ s}^{-1}$. Any increase in ET efficiency can be concluded to result from a rate increase of the *intramolecular* reaction, as discussed extensively above. Therefore, the ET efficiency in peptides **64** and **68**, correspond to *intramolecular* rates for donor to acceptor ET, which are 3-5 times faster than the *intermolecular* reaction rate, i.e. approximately $5-7 \cdot 10^6$.

In a next step, information about the relative rates of the two consecutive ET steps in the hopping process should be deduced. To this end, the kinetic expression for a consecutive reaction was used. In a reaction $A \rightarrow B \rightarrow C$, with k_1 determining the rate of $A \rightarrow B$ conversion and k_2 as the rate constant for the reaction of the intermediate B to the product C, the time-dependent concentrations of A, B and C are given by equations 6-8.^[106]

$$A = A_0 e^{-k_1 t} \quad (6)$$

$$B = \frac{A_0 k_1}{(k_1 - k_2)} (e^{-k_2 t} - e^{-k_1 t}) \quad (7)..$$

$$C = A_0 \left[1 + \frac{k_2}{(k_1 - k_2)} e^{-k_2 t} - \frac{k_1}{(k_1 - k_2)} e^{-k_1 t} \right] \quad (8)$$

Equation 6-8: Time dependency of the concentrations of A, B and C in a consecutive reaction $A \rightarrow B \rightarrow C$, with k_1 as rate constant for the first step and k_2 as rate constant for the second step.

The concentrations of starting material, product and intermediate at a defined time thus are a function of the rate constants k_1 and k_2 of the reaction. From the transient absorption spectrum upon LFP of peptide **64**, the relative concentrations of electron acceptor (A), oxidized relay (B) and oxidized electron donor (C) are available. While a substantial amount of C (30%, if corrected for the *intermolecular* contribution) has already been formed, when A has been reduced to 54%, the intermediate B is present in detectable concentrations of 10%. A rate ratio of 5:1 for k_2/k_1 leads to such a distribution of A, B and C, according to equations 6-8. A graphical depiction of this case is shown in Figure 41, with the observed concentration ratio indicated by a vertical line.

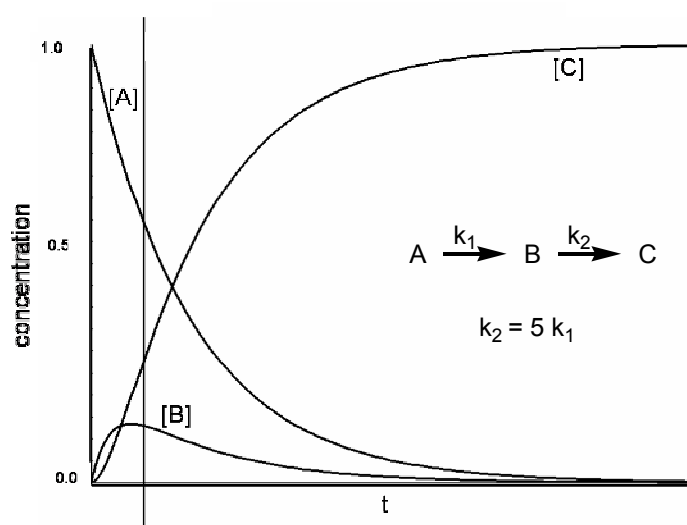
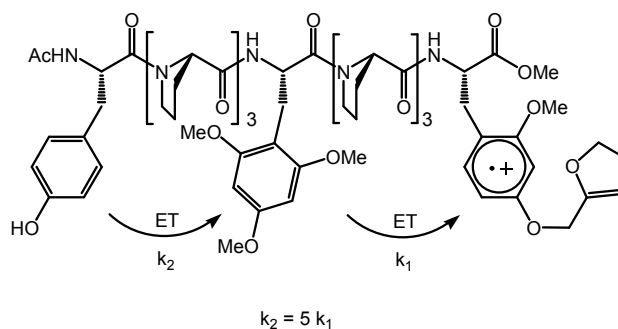


Figure 41: Time-dependent concentrations of A, B and C in a consecutive reaction $A \rightarrow B \rightarrow C$, with a 1:5 ratio of rate constants. The concentration ratio derived from LFP of peptide **64** is indicated by a vertical line.

From these considerations it can be concluded, that ET between tyrosine and the oxidized central relay amino acid 2,4,6-trimethoxyphenylalanine radical cation is five times faster than ET from the relay to the electron acceptor (Scheme 30). This result is in accordance with the oxidation potentials of the engaged redox sites. While acceptor and relay amino acid differ in oxidation potentials by only 10 mV (0.95 resp. 0.94 V vs. the ferrocene redox couple), the difference between the donor and the relay amino acid is significantly larger, with tyrosine showing a potential of 0.85 V vs. the ferrocene redox couple.



Scheme 30: relative rates for sequential ET through peptide **64**.

In summary, quantitative analysis of the data obtained from LFP experiments, yielded information about ET rates in peptides **64** and **68**. Those peptides contain central amino acids with aromatic side chains that can participate in sequential ET and thereby allow ET to occur with 20-30 times higher rates than the single-step superexchange ET in peptides **65** and **66**. *Intramolecular* electron hopping between the N-terminal electron donor tyrosine and the C-terminal electron acceptor, separated by a peptide matrix of 20 Å length, occurs with rates of approximately $5\text{-}7 \cdot 10^6$ in peptides **64** and **68**. From the relative amount of transients observed in irradiated peptide **64**, 40 ns after the flash, the rate ratio for relay to acceptor versus donor to relay ET was estimated to 1:5.

8 The Phenylalanine Effect

A surprising result was obtained, when phenylalanine was introduced as a central amino acid. The benzene ring has an oxidation potential of 2.2 V vs. NHE,^[84] which is significantly higher than the potential of the injector radical cation **4** (1.44 vs. NHE^[71]). Thus, phenylalanine cannot function as a relay in stepwiseET through our model peptides and the result of LFP was expected to resemble the case of peptide **67**, containing an anisole moiety at the central position, in which no efficient ET between donor and acceptor occurs within 40 ns (cf. Figure 38). However, the transient absorption spectrum recorded 40 ns after irradiation of **70**, shows a significant amount of tyrosyl radical, indicated by the 410 nm absorption.

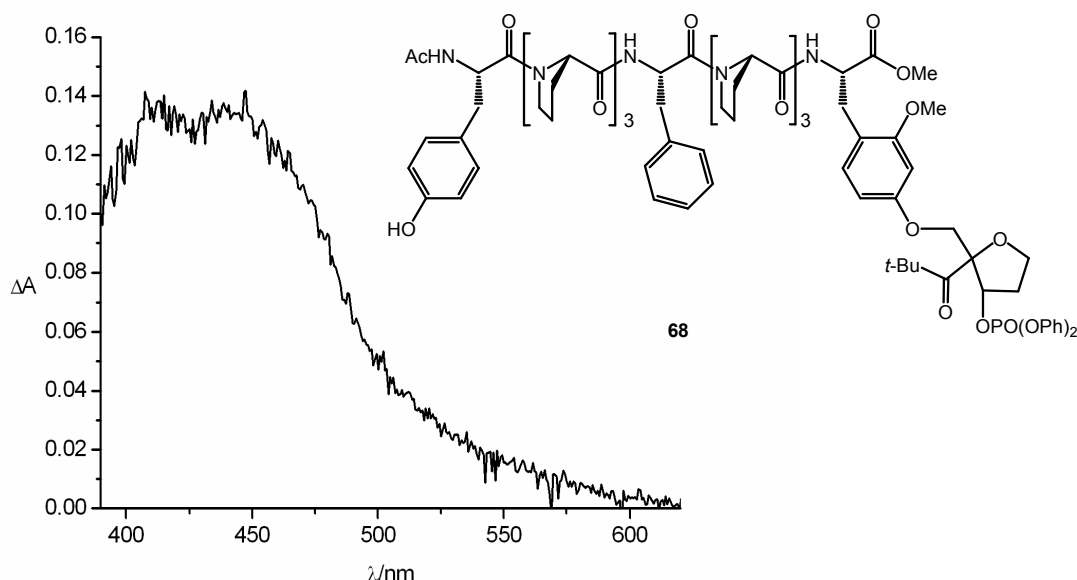
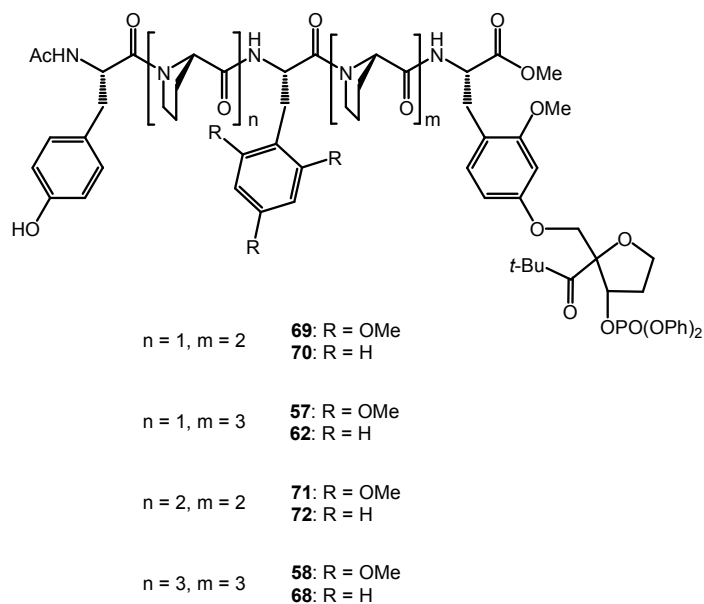


Figure 42: Transient absorption spectrum of peptide **70** 40 ns after irradiation.

The relative amount of oxidized species determined by graphical curve decomposition is 30% tyrosine and 70% electron acceptor. This amount of tyrosyl radical formed within 40 ns, can only be explained by *intramolecular* ET. The structure of peptide **70**, determined by CD-spectroscopy, is similar to the structures of peptides **64** - **68**, i.e. the peptide forms a PPII helix. The unexpectedly high ET efficiency can thus not be traced back to a different overall structure of the peptide backbone.

Comparable observations with respect to the ET properties of phenylalanine-containing peptides were made in peptides **71** and **72**, as well as **63** and **62**. ET efficiencies do not drop significantly upon replacement of the redox active trimethoxysubstituted benzene by a simple benzene moiety. In peptide **74**, containing phenylalanine as a central amino acid, ET efficiency within 40 ns even increased slightly as compared to **73**, containing the redox active methoxysubstituted relay (Scheme 31, Table 2).



Scheme 31: Peptides used to investigate the role of phenylalanine in ET.

The results of the comparison of phenylalanine-containing with 2,4,6-trimethoxyphenylalanine-containing peptides are summarized in Table 2. The relative amounts of oxidized species formed within 40 ns after the laser flash are derived by graphical decomposition of the respective transient absorption spectra (see Figure 21, page 47). All spectra not depicted in the text are reproduced in the Experimental Part.

Table 2: relative amounts of transients formed 40 ns after irradiation of peptides

	oxidized electron donor (%)	oxidized relay (%)	electron acceptor (%)
71	63	7	30
72	70	-	30
63	35	11	54
62	41	-	59
73	53	8	39
74	76	-	24
64	36	10	54
70	41	-	59

From these results, the placement of phenylalanine inside the peptide matrix seems to exhibit an influence on the donor to acceptor ET rates, which is comparable to the influence of 2,4,6-trimethoxyphenylalanine. These findings could not be rationalized so far.

9 Summary and Outlook

A peptide model was designed, which allows the investigation of amino acid side chain participation in ET through peptides. Aromatic amino acids function as oxidizable spectroscopic sensors for the direct observation of charged intermediates during the ET process. Tyrosine as electron donor, situated at the N-terminus of the peptide, provides driving force for the ET process and is irreversibly oxidized to a long-lived phenoxyl radical with a sharp absorption band. Two methoxysubstituted phenylalanine derivatives were chosen as additional spectroscopic sensors, yielding oxidized transients with different absorption spectra. They were synthesized in their enantiopure form and investigated with respect to their electrochemical and spectroscopical properties. In the peptide model, they function as C-terminal electron acceptor precursor and central relay, separated from each other and the donor by a proline matrix. The electron acceptor can be generated by laser irradiation of an injection unit, containing a *t*butyl ketone as chromophore. The half-life time of acceptor generation is estimated to 20 ns and *intermolecular* ET started to gain importance from approximately 100 ns after irradiation. Thus, transient absorption spectra recorded 40 ns after the laser flash were used for the examination of *intramolecular* ET efficiencies between the redox sites. In a first study, the injection unit was connected to the peptide C-terminus via an ester bond and peptides with a total length of 5-10 residues were synthesized. In this case, ET efficiency was observed to depend on the construction of the separating matrix. Efficient *intramolecular* ET to the electron acceptor within 40 ns after irradiation was observed in peptides, in which either donor and relay or relay and acceptor were arranged in close proximity (separated by one proline). Signals of oxidized relay were observed in all cases, proving that the occurrence of oxidized intermediates in donor to acceptor ET can be detected in this model. Efficient *intramolecular* ET through the whole chain, i.e. from the N-terminal donor to the electron acceptor, was only observed in peptides containing a total of up to four prolines in the matrix. The synthesis of a new electron acceptor precursor, in which the injection unit was connected directly, via an ether bond, to a phenoxyl function at the aromatic side chain of the C-terminal amino acid, then allowed the observation of *intramolecular* ET from the N-terminus to the C-terminus of a nonapeptide, which consisted of two triproline spacers and the three spectroscopic sensors. This peptide showed a well-defined polyproline II helical structure, leading to a donor/acceptor separation of 20 Å. The aromatic relay, functioning as spectroscopic sensor for the detection of oxidized intermediates in donor to acceptor ET, could be exchanged by a number of different amino acids, without changing the overall structure of the peptide. Thus, the peptide model allowed us to determine the influence of the central amino acid - separated from both, donor and acceptor, by 10 Å - on ET. Efficient ET was observed in those two cases, where the central amino acid was able to function as an oxidizable relay in ET. The spectrum of the peptide containing the three distinguishable spectroscopic sensors, showed the simultaneous occurrence of electron acceptor, oxidized donor and oxidized relay and thereby

proved that the charge resides on the relay site during ET. In two peptides containing aliphatic central residues, *intramolecular* donor to acceptor ET did not take place efficiently within the time frame of our experiments – a 20 to 30 fold decrease in donor oxidation was observed. A peptide containing an anisol ring as central aromatic side chain, with an oxidation potential far above the electron acceptor, did also not render efficient *intramolecular* ET possible. In conclusion, efficient ET across the 20 Å distance in our model peptides was only possible within 40 ns, if an oxidizable amino acid side chain was present inside the matrix. This side chain functioned as a stepping stone in ET, with the charge residing on it, forming a chemical intermediate. Thus, electron hopping via aromatic amino acid side chains was proven to allow distal (20 Å) ET transfer in peptides within 40 ns whereas single-step superexchange ET did not take place within 40 ns in peptides of similar structure. From considerations regarding the competition of *intermolecular* and *intramolecular* ET, the rate of *intramolecular* ET between electron acceptor and electron donor by a two-step electron hopping process, with 10 Å distance for each step, was determined to $5 - 7 \cdot 10^6 \text{ s}^{-1}$. In the peptide containing three spectroscopic sensors, the relative intensities of all signals could be used to conclude on the ratio of rate constants in the consecutive ET reaction, leading to a five times faster rate constant for donor to relay, than for relay to acceptor ET. This is consistent with the differences in driving force for the two reactions. Our model provides an experimental approach to determine the suitability of individual amino acids to function as relays in electron hopping. Future experiments could be carried out with the naturally occurring aromatic amino acids tryptophane and histidine, as well as with cysteine, as an additional oxidizable amino acid. The introduction of protection groups, to avoid deprotonation upon oxidation, which renders the ET irreversible (as in the case of tyrosine) might be necessary. First experiments lead to the assumption, that phenylalanine plays an unexpected role in the mediation of long-range ET. Whether this is due to unknown local structural features, not visible in the CD spectrum, or to electronic effects is not yet clear. This might be further investigated by the introduction of electron-donating or electron-withdrawing groups to the benzene ring.

10 Experimental Part

10.1 Conditions of Measurements

NMR-Spectrometry

Nuclear magnetic resonance (NMR) spectra were recorded on Bruker spectrometers (Avance400: 400 MHz for ^1H and 101 MHz for ^{13}C ; Avance DRX500: 500 MHz for ^1H and 125 MHz for ^{13}C) at ambient temperature in the solvents indicated, and referenced to trimethylsilate (TMS). Chemical shifts δ are given in ppm. Multiplets are assigned with s (singlett), s,br (broad singlet), d (doublet), t (triplet), q (quartet) and m (multiplet). Assignements of the signals are given in italics.

Melting Points (M.p.)

Melting points were measured on a Büchi 530 and are not corrected.

Mass Spectrometry (MS)

Electron ionization (EI) and fast atom bombardment (FAB) mass spectra were recorded by Dr. H. Nadig (University of Basel) on a VG70-250 (EI) and a MAT 312, using 3-nitrobenzyl alcohol as a matrix (FAB). Electron Spray Ionisation (ESI) spectra were recorded in methanol on a Finnigan MAT LCQ spectrometer. High Resolution Mass Spectrometry (HR-MS) were performed by the mass service at the university of Fribourg (CH) (Fredy Nydegger, "Département de Chimie Université de Fribourg"). Mass signals are given in mass units per charge. The fragments and intensities are given in brackets.

Elemental Analysis (EA)

Elemental analyses were carried out on a Leco CHN-900 device by W. Kirsch (University of Basel). The values are given in mass percent.

Enantiomeric Purity

Enantiomeric excess (*ee*) was determined by chiral HPLC (Chiracel columns from Daicel, heptane/*i*PrOH 70:30, 0.7 mL/min, 20 °C). Optical rotations were measured on a Perkin Elmer polarimeter 241. The concentrations are given in g/100 mL.

UV-Vis Spectroscopy

UV-Vis spectra were recorded on a Perkin Elmer spectrometer (Lambda Bio 40) in MeCN or MeCN/water 3:1. The extinction coefficients at 308 nm (ϵ_{308}) of peptides were determined using 5-8 mM concentrations.

High Performance Liquid Chromatography (HPLC)

HPLC chromatograms were recorded on a Water Alliance 2690 Separation Module with a 2680 Dual Mode Detector adjusted to 260 nm and 308 nm. Columns for reversed-phase HPLC were *Merck* LiChroSpher 100 (RP-18e, 5 μ m, 125 \times 4mm). Eluents were acetonitrile and nanopure water, using a gradient program reaching from 0% water to 100% in 40 min at a flow rate of 1.0 mL \cdot min $^{-1}$. Retention times (t_R) are given in minutes.

Circular Dichroism (CD) Spectroscopy

CD spectra were recorded using a Chirascan spectrometer with a spectral bandwidth of 1 nm at 25 $^{\circ}$ C with a time constant of 3 s and a step resolution of 1 nm. CD data are given as mean residual molar ellipticities (Θ_{MRW} in deg cm 2 dmol $^{-1}$). A Quartz cell with a path length of 1 cm was used with solutions containing approximately 70 μ gml $^{-1}$ (6×10^{-4} M per residue) peptide solutions.

Differential Pulse Cyclovoltammetry

Pulsed cyclovoltammetric measurements were performed using a BAS 100 B/W electrochemical workstation and a three-electrode cell, consisting of a silver-wire as pseudo-reference, a glassy carbon disk as working and a platinum wire as counter electrode. The amino acids were dissolved in degassed acetonitrile at 2 mM concentrations. Tetrabutylammoniumhexafluorophosphate was added as an electrolyte (100 mM) and ferrocene as an internal standard. The measurements were carried out under an argon blanket.

Laser Flash Photolysis (LFP)

The laser experiments were carried out using a COMPex 205 XeCl-Excimer Laser (Lambda Physik) with a pulse energy of 100-150 mJ and a pulse width of 20 ns for irradiation. A pulsed Xe-lamp served as a second light source for read-out. (cf. Figure 9). The peptides were dissolved in acetonitrile/water 3:1 in concentrations of 5-8 mM, degassed in three freeze/thaw cycles and stored under vacuum in a quartz cuvette (4.5 cm x 1 cm x 1 cm). Transient absorption spectra were recorded with an iStar ICCD detector (Andor). The signals of 5 laser flashes were accumulated. Time-resolved measurements were carried out using a 1P28 photomultiplier. Photosensitization experiments were carried out in oxygen-saturated acetonitrile with 1 mM concentrations of compound, 0.1 mM dicyanonaphthalene and 20 mM biphenyl. The data was processed using MacFitFlash and Origin.

10.2 Synthesis

10.2.1 Materials, Solvents and Reagents

Technical grade solvents used for extraction and column chromatography were distilled prior to use. Absolute solvents were purchased from *Fluka* or *Aldrich* in septum sealed bottles. Deuterated solvents were purchased from *Cambridge Isotope Laboratories, Inc.*. Nanopure water, used in LFP, CD spectroscopy and HPLC chromatography, was filtered over a *Barnstead* ultrapure water system.

Amino acids, coupling reagents and resins for SPPS were ordered from *Novabiochem* or *Bachem* and used without further processing. The chiral Rh-catalyst was ordered from *Strem* and stored under argon-atmosphere at r.t.. Other materials and reagents were purchased from *Fluka*, *Aldrich* and *Acros* in the highest available grade and used without further purification. Ion exchange chromatography was performed on Dowex 400 resin activated by washing with 2 M aq. sodium hydroxide and subsequently 2 M acetic acid. Silica gel 60 (*Fluka*) was used for flash chromatography. TLC plates from *Merck* were used for reaction control (silica gel 60 on aluminium sheets) and chromatographic analysis (silica gel 60 on glass). CAM-Dip (10 g cerium(IV)sulfate-tetrahydrate, 25 g ammonium-heptamolybdate-tetrahydrate, 100 mL sulfuric acid (96%), 900 mL water) was used for staining of the TLC plates.

10.2.2 Notation

Peptide sequences are noted from the N-terminus to the C-terminus. Amino acids are denoted in the three letter code, with N-terminal and C-terminal protection groups separated by hyphens and side-chain protection groups given in brackets, e.g Ac-Tyr(OBn)-OH for N-acetyl-O-benzyl-tyrosine. All non-racemic amino acids are used as L-enantiomers. The non-natural amino acids are abbreviated as follows:

DMP: 2,4,6-trimethoxyphenylalanine

TMP: 2,4-dimethoxyphenylalanine

DAP (dialkoxyphenylalanine): 3-{4-[2-(2,2-dimethylpropionyl)-3-(diphenoxyphosphoryl-oxy)tetrahydrofuran-2-ylmethoxy]-2-methoxyphenyl}propionic acid methylester (electron acceptor precursor **44**)

In peptides containing the injection unit **2**, linked to the C-terminus via an ester bond (peptides **18**), this unit will be denoted as: **Inj**. Two examples for the resulting nomenclature for peptides of type **18** resp. **54** are given in Figure 43.

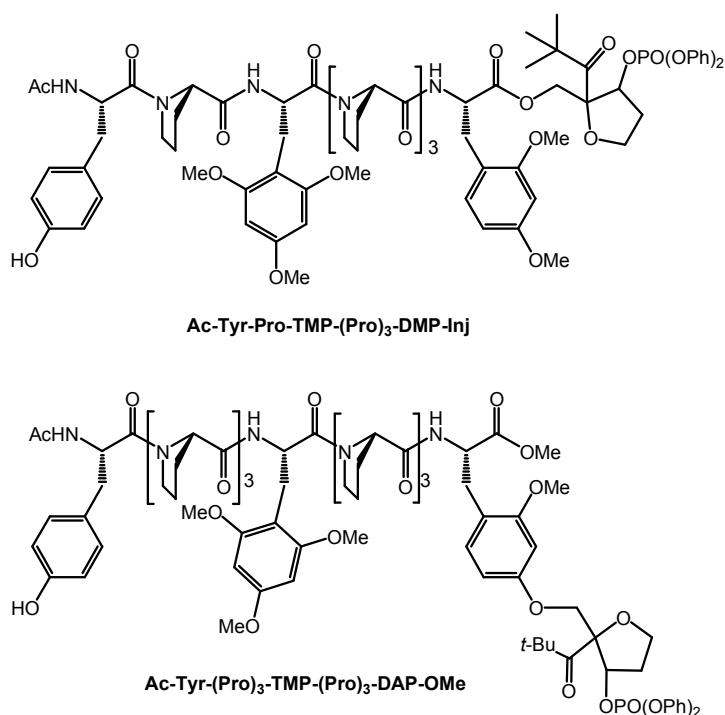


Figure 43: Nomenclature for oligopeptides.

10.2.3 General Procedures (GP)

Synthetic steps following a general procedure are indicated by roman numbering, according to the following section.

I. Deprotection of *tert*-Butylcarbamates – Boc Deprotection (GP I)

To remove the *tert*-butyloxycarbonyl (Boc) protection group from the amine function of an amino acid (or peptide), the respective compound was dissolved in a cold hydrogen chloride solution (4 M in 1,4-dioxane) and stirred at r.t. for 30 min. After coevaporation with toluene under reduced pressure, the dry, solid amine hydrochloride could be obtained as a foam by addition of small amounts of CH₂Cl₂ and evaporation of all solvent traces under high vacuum. Completeness of the deprotection reaction was checked by ESI-MS, before subjecting the amine hydrochloride to the next coupling step.

II. Deprotection of *tert*-Butylesters (GP II)

To remove the *tert*-butylester group from the carbonic acid function of an amino acid (or peptide), the respective compound was dissolved in a 1:1 (v/v) mixture of trifluoroacetic acid and CH₂Cl₂ and stirred for 45-90 minutes at r.t.. Progress of the reaction was checked by TLC (CH₂Cl₂, 4% MeOH, 1% AcOH). Evaporation of the solvents under reduced pressure and coevaporation with toluene yielded the free acid as a yellowish solid.

III. Deprotection of Aromatic Benzylethers [Tyr(OBn)] (GP III)

The benzylether protection group at the side-chain of tyrosine residues was removed by a hydrogenation procedure, using palladium on activated charcoal (10%) as a catalyst and 1 bar hydrogen pressure. The reaction was carried out in methanol and reaction progress was checked by TLC (CH₂Cl₂, 4-15% MeOH). Acetic acid was added to enhance catalytic activity, if necessary. After complete conversion of the starting material (2-8 hs), the reaction mixture was filtered over celite, the filtrate was washed thoroughly with methanol, and the solvents were removed under reduced pressure before further purification of the crude product.

IV. Deprotection of Aromatic *tert*-Butylethers [Tyr(OtBu)] (GP IV)

The benzylether protection group at the side-chain of tyrosine residues was removed by dissolving the compound in a 3:2 (v/v) mixture of CH₂Cl₂ and trifluoroacetic acid and stirring at r.t. for 15 min. After coevaporation with toluene under reduced pressure, the deprotected peptide could be obtained as a solid by addition of small amounts of CH₂Cl₂ and drying under high vacuum. Completeness of the deprotection was checked by ESI-MS, before subjecting the peptide to the purification procedure (GP VII).

V. Peptide Couplings in Solution

Peptide couplings were carried out under inert gas atmosphere. The carboxylic acid was dissolved in DMF/CH₂Cl₂ (1:3, v/v) with 2 eq. of coupling reagent (2-(1H-benzotriazole-1-yl)-1,1,3,3-tetramethyluronium tetrafluoroborate (TBTU) or 2-(6-chloro-1-H-benzotriazole-1-yl)-1,1,3,3-tetramethyluronium hexafluorophosphate (HCTU)). The amine (1 eq.) was added in CH₂Cl₂ with 4 eq. of N,N'-diisopropylethylamine (DIPEA). The reaction mixture was stirred for 3-6 hs, then poured into a separatory funnel, containing a biphasic system of sat. aq. NH₄Cl-solution and EtOAc. After washing with sat. aq. NH₄Cl-solution (2x) and sat. aq. NHCO₃-solution (2x), each followed by brine, the organic phase was dried (MgSO₄) and concentrated under reduced pressure. Crude products were filtered over silica (CH₂Cl₂, 4%-15% methanol) and submitted to the next reaction step or the purification procedure (GP VII) after ESI-MS control. Yields of peptide couplings varied between 60 and 80%.

VI. Acetylation in Solution

To acetylate the N-terminus of a peptide, the peptide was dissolved in CH₂Cl₂ and 10 eq. of acetic anhydride as well as 10 eq. of N,N'-diisopropylethylamine (DIPEA) were added, before stirring for 30 min at r.t.. Completeness of the reaction was checked by TLC (CH₂Cl₂, 4%-15% methanol) or ESI-MS. After removal of the solvents under reduced pressure, the residue was dissolved in EtOAc and washed with aq. NH₄Cl-solution and sat. aq. NHCO₃-solution, each followed by brine. The organic phase was dried (MgSO₄) and concentrated under reduced pressure, before crude products were filtered over silica (CH₂Cl₂, 4%-15% methanol) and submitted to the next reaction step or the purification procedure (GP VII).

VII. Peptide Purification

Peptides used in LFP measurements were purified by column chromatography, using a gradient of methanol in CH₂Cl₂, starting from 4% (1% for very short peptides) and reaching to 10-20%, depending on the polarity of the respective peptides. For gradients of >10% methanol, the resulting product was dissolved in CH₂Cl₂ (containing up to 4% methanol to increase solubility) and filtered, to remove silica particles. Purity of the peptides was checked by HPLC chromatography and UV-spectroscopy. The extinction coefficient at 308 nm, stemming from the pivaloyl chromophore, should be below 60 (below 100 in some larger peptides). Hydrogenation with Pd/C and subsequent column chromatography has been proven to be an efficient method to remove UV-active impurities. Therefore, some peptides without benzyl-ether protection groups were subjected to this procedure, if stirring with activated charcoal was not sufficient for the removal of yellowish impurities. Peptides were dried by addition of small amounts of CH₂Cl₂ and subsequent removal of all solvent traces at the high vacuum line, to yield white foams.

VIII. Solid Phase Peptide Synthesis (SPPS)

a) Procedure

Solid phase peptide synthesis was carried out employing a Syro I Peptide Synthesizer (MultiSynTech GmbH, Witten, Germany), with plastic syringes as reaction vessels. 2-Chlorotrityl resin, preloaded with proline (*Novabiochem*) was used as the solid matrix. Fmoc-protected amino acids and coupling reagents were purchased from *Novabiochem* and *Bachem*. 2-(6-chloro-1-H-benzotriazole-1-yl)-1,1,3,3-tetramethyluronium hexafluorophosphate (HCTU) was used as a coupling reagent. For the peptide couplings, the Fmoc-protected amino acid (4 eq., 0.5 M in DMF), HCTU (4 eq. 0.5 M in DMF) and N,N'-diisopropylethylamine (DIPEA, 12 eq., 3 M in NMP) were added to the resin. The mixture was agitated for 1 h and subsequently washed with DMF (3x). For Fmoc-deprotection, a mixture of piperidine and DMF (1:5, v/v) was added to the resin. The reaction mixture was agitated for 5 min and for another 10 min after addition of fresh piperidine solution, and then washed with DMF (5x).

b) Acetylation

After the last deprotection step, the resin was thoroughly washed. Then 30 eq. of acetic anhydride and 30 eq. of triethylamine were added in CH₂Cl₂ (3 mL total volume). After shaking for 30 min, the resin was washed with CH₂Cl₂ and subjected to the cleavage procedure.

c) Cleavage of the Peptide

The resin was covered with a 1:1:8 (v/v/v) mixture of trifluoroethanol, acetic acid and CH₂Cl₂ and shaken for 30 min, then washed with CH₂Cl₂, collecting all solvents. The procedure was repeated. The combined solutions were then concentrated under reduced pressure, cooled to 0 °C and cold Et₂O was added. The precipitated peptide was washed with cold Et₂O (3x), then dried in high vacuum.

10.2.4 Characterisation of Peptides

A complete NMR-spectroscopical analysis was carried out for the small peptides **16** and **17**, as well as for the molecules **15** to **13**, to confirm that the building blocks are stable to the reaction conditions used in peptide synthesis. Based on these peptides, a protocol for peptide characterisation was established, which consists of HPLC and ESI-MS analysis, as well as UV-spectroscopy to determine the purity of the peptide (cf. **GP VII**).

10.3 Compounds

2 (2*R*,3*S*)-2-*tert*-Butylcarbonyl-3-diphenoxyphosphoryloxy-2-hydroxymethyl-tetrahydrofuran

Alcohol **2** was synthesized according to procedures established in the Giese group, starting from pivaldehyde in 7 steps with 3% overall yield.^[65, 66]

The NMR and mass spectroscopical data are given here. For full characterisation see the indicated references.

¹H-NMR (CDCl₃, 400 MHz): δ = 7.37-7.31 (m, 4H; H_{Ar}), 7.24-7.17 (m, 6H; H_{Ar}), 5.36-5.28 (m, 1H; CH-OP), 4.17-4.07 (m, 2H; CH₂CH₂), 3.60-3.53 (m, 2H; CH₂OH), 2.72 (br, 1H OH), 2.33-2.24 (m, 2H; OCH₂CH₂), 1.16 (s, 9H; C(CH₃)₃).

¹³C-NMR (101 MHz, CDCl₃): δ = 215.7 (s, C=O, CO*t*Bu), 150.6 (d, J_{C-P} = 6.9 Hz, C_{Ar}-OP), 150.5 (d, J_{C-P} = 7.2 Hz, C_{Ar}-OP), 130.0 (d, 2 *p*-CH_{Ar}(PhOP)), 125.7 (d, 2 *m*-CH_{Ar}(PhOP)), 125.6 (d, 2 *m*-CH_{Ar}(PhOP)), 120.4 (d, J_{C-P} = 4.9 Hz, 2 *o*-CH_{Ar}(PhOP)), 120.3 (d, J_{C-P} = 5.3 Hz, 2 *o*-CH_{Ar}(PhOP)), 94.5 (d, J_{C-P} = 9.1 Hz, CCH-OP), 83.7 (d, J_{C-P} = 5.0 Hz, CHCH₂), 68.2, 67.2 (2t, OCH₂CH₂, CH₂OH), 45.5 (s, C(CH₃)₃), 33.1 (t, OCH₂CH₂), 25.9 (q, C(CH₃)₃).

MS (ESI, MeOH, *m/z*): 891 ([2*M*+Na]⁺, 100), 457 ([*M*+Na]⁺, 40).

8 3-(2,4-dimethoxy-phenyl)-2-nitro-propionic acid methyl ester

1,2-Dimethoxybenzaldehyde (3.0 g, 18 mmol), methylnitroacetate (2.0 mL, 22 mmol), dimethylamine hydrochloride (3.0 g, 57 mmol) and KF (157 mg, 2.71 mmol) were refluxed in toluene (110 mL) for 12 h, using a Dean-Stark water trap. The solvent was removed under reduced pressure and the remaining orange solid was dissolved in CH₂Cl₂ and washed three times with water. The organic phase was dried (MgSO₄) and concentrated under vacuum to give α -nitro-acrylic acid-methylester **7** as an orange oil, which was used in the following reaction without further purification. The raw product of **7** was dissolved in chloroform (226 mL) and isopropanol (67 mL) and Merck Silica gel (36 g) was added. NaBH₄ (3.4 g, 90 mmol) was added portionwise to the vigorously stirred suspension during 5 min. After additional 2h of stirring, acetic acid (10 mL) was added carefully and the solid components were removed by filtration. The remaining solution was concentrated under reduced pressure and the crude product was dissolved in CH₂Cl₂/water (5:1). After extraction of the aq. phase with CH₂Cl₂, the

combined organic phases were dried (MgSO₄) and concentrated under vacuum. The residue was purified by column chromatography (EtOAc/hexane 1:9) to give **8** as a yellow solid; yield: 3.2 g (60%).

¹H-NMR (400 MHz, CDCl₃, 25°C, TMS): δ = 7.00 (d, *J* = 8.1 Hz, 1H; *o*-H_{Ar}), 6.44-6.38 (m, 2H; *2m*-H_{Ar}), 5.51 (dd, *J* = 9.3, 5.8 Hz, 1H; CH-(CH₂C_{Ar})), 3.82, 3.80, (2s, 6H; 2 C_{Ar}-OCH₃), 3.78 (s, 3H; CO₂CH₃), 3.46 (dd, *J* = 14.1, 5.8 Hz, 1H; CH_aH_b-C_{Ar}), 3.38 (dd, *J* = 14.1, 9.3 Hz, 1H; CH_aH_b-C_{Ar}).

¹³C-NMR (101 MHz, CDCl₃, 25°C): δ = 165.2 (s, C=O, CO₂CH₃), 161.0 (s, *o*-C_{Ar}-OCH₃), 158.6 (s, *p*-C_{Ar}-OCH₃), 131.9 (d, *o*-CH_{Ar}), 114.5 (s, C_{Ar}-CH₂), 104.4, 98.8 (d, 2 *m*-CH_{Ar}), 87.4 (d, CH-(CH₂C_{Ar})), 55.58, 55.57 (q, 2 C_{Ar}-OCH₃), 53.7 (q, CO₂CH₃), 31.9 (t, CH₂-C_{Ar}).

MS (ESI, MeOH, *m/z*): 292 ([M+Na]⁺, 100).

EA: calc. for C₁₂H₁₅NO₆: C: 53.53, H: 5.62, N: 5.20; found C: 53.44, H: 5.57, N: 5.18.

9 (rac)-2,4-dimethoxyphenylalanine-methylester [(rac)-DMP-OMe]

Arylpropionate **8** (3 g, 11 mmol) was stirred in dry methanol (50 mL) with palladium on activated charcoal (300 mg, 10%). Ammoniumformiate (3.5 g, 56 mmol) was added in a single portion. After stirring for 72 hs, the reaction mixture was filtered over celite and the filtrate was washed thoroughly with methanol. After concentration of the solution under reduced pressure, water and CH₂Cl₂ was added to the crude product. The aqueous phase was acidified with acetic acid and extracted with CH₂Cl₂ (3x). The combined organic phases were dried (MgSO₄), concentrated under vacuum and the resulting crude product was purified by column chromatography (CH₂Cl₂ → 4% MeOH in CH₂Cl₂) to yield **9** as a white foam (1.5 g, 56%).

¹H-NMR (400 MHz, CDCl₃/MeOH (30:1), 25°C, TMS): δ = 7.00 (d, *J* = 8.1 Hz, 1H; *o*-H_{Ar}), 6.43-6.39 (m, 2H; *2m*-H_{Ar}), 3.77 (s, 6H, 2 C_{Ar}-COCH₃), 3.68 (s, 3H, CO₂CH₃), 3.74 (dd, *J* = 8.1, 5.6 Hz, 1H; CH-(CH₂C_{Ar})), 3.03 (dd, *J* = 13.5, 5.6 Hz, 1H; CH_aH_b-C_{Ar}), 2.76 (dd, *J* = 13.4, 8.1 Hz, 1H; CH_aH_b-C_{Ar}).

^{13}C -NMR (101 MHz, CDCl_3 , 25°C): δ = 175.9 (s, C=O, CO_2CH_3), 160.1 (s, o - $\text{C}_{\text{Ar}}\text{-OCH}_3$), 158.7 (s, p - $\text{C}_{\text{Ar}}\text{-OCH}_3$), 131.7 (d, o - CH_{Ar}), 117.9 (s, $\text{C}_{\text{Ar}}\text{-CH}_2$), 104.1, 98.7 (d, 2 m - CH_{Ar}), 55.5 (d, $\text{CH}(\text{CH}_2\text{C}_{\text{Ar}})$), 54.6, 52.1 (q, 2 $\text{C}_{\text{Ar}}\text{-OCH}_3$), 35.6 (t, $\text{CH}_2\text{-C}_{\text{Ar}}$).

MS (ESI, MeOH m/z): 240 ($[\text{M}+\text{H}]^+$, 100).

10 *N*-acetyl-(*rac*)-2,4-dimethoxyphenylalanine-methylester [(*rac*)-Ac-DMP-OMe]

(*rac*)-2,4-Dimethoxyphenylalanine-methylester **9** (200 mg, 1.25 mmol) was stirred in a 1:1 mixture of sat. aq. Na_2CO_3 -solution and dioxane (6 mL) with acetic anhydride (0.53 mL, 5.6 mmol) for 2 h at r.t.. Extraction with CH_2Cl_2 , concentration of the dried (MgSO_4) organic phases under reduced pressure and purification of the resulting crude product by column chromatography (1% MeOH in CH_2Cl_2 → 2% MeOH in CH_2Cl_2) yielded **10** as a white foam (285 mg, 81%).

M.p. = 103-105 °C.

^1H -NMR (400 MHz, MeOD, 25°C, TMS): δ = 6.96 (d, J = 8.1 Hz, 2H; $\text{H}_{\text{Ar}}\text{-6}$), 6.44-6.41 (m, 2H; $\text{H}_{\text{Ar}}\text{-3, 5}$), 4.69 (dd, J = 13.6, 6.3 Hz, 1H; $\text{C}_{\alpha}\text{H}$), 3.81, 3.79, 3.71 (s, 9H; 3 $\text{CH}_3\text{-O}$), 3.03 (d, J = 6.3 Hz, 2H; $\text{C}_{\alpha}\text{HCH}_2$), 1.93 (CH_3CO).

^{13}C -NMR (101 MHz, MeOH): δ = 172.9 (s, C=O, CO_2Me), 170.1 (s, C=O, COCH_3), 160.6 (s, o - $\text{C}_{\text{Ar}}\text{-OCH}_3$), 158.8 (s, p - $\text{C}_{\text{Ar}}\text{-OCH}_3$), 131.9 (d, CH_{Ar}), 131.6 (d, CH_{Ar}), 117.2 (s, C_{Ar}), 104.8 (d, CH_{Ar}), 99.0 (d, CH_{Ar}), 55.8, 55.7, 52.5 (q, 3 $\text{CH}_3\text{-O}$), 53.7 (d, $\text{C}_{\alpha}\text{H}$), 32.1 (t, CH_2), 23.5 (s, COCH_3).

MS (FAB, NBA, m/z): 151 (86), 180 (24), 222 (62), 282 (100, $[\text{M}]^+$).

MS (ESI, MeOH m/z): 585 (100, $[2\text{M}+\text{Na}]^+$), 304 (40, $[\text{M}+\text{Na}]^+$).

EA: calc. for $\text{C}_{14}\text{H}_{18}\text{NO}_5$: C: 59.99, H: 6.47, N: 5.00; found C: 60.03, H: 6.59, N: 5.11.

11 *N*-acetyl-(*rac*)-2,4,6-trimethoxyphenylalanine-methylester [(*rac*)-Ac-TMP-OMe]

(*rac*)-2,4,6-Trimethoxyphenylalanine-methylester^[88] (337 mg, 1.25 mmol) was stirred in a 1:1 mixture of sat. aq. Na_2CO_3 -solution and dioxane (6 mL) with acetic anhydride (0.53 mL, 5.6 mmol) for 2 h at r.t.. Extraction with CH_2Cl_2 , concentration of the dried (MgSO_4) organic phases under reduced

pressure and purification of the resulting crude product by column chromatography (1% MeOH in CH₂Cl₂ → 2% MeOH in CH₂Cl₂) yielded **11** as a white foam (311 mg, 81%).

M.p. = 131-132 °C.

¹H-NMR (400 MHz, MeOD, 25°C, TMS): δ = 6.18 (s, 2H; H_{Ar}), 4.44 (t, *J* = 7.6 Hz, 1H; C_αH), 3.78, 3.77, 3.63 (s, 12H; 4 x CH₃-O), 3.05 (dd, *J* = 13.2, 7.6 Hz, 1H; C_αHCHH), 2.93 (dd, *J* = 13.2, 7.6 Hz, 1H; C_αHCHH), 1.89 (CH₃CO).

¹³C-NMR (101 MHz, MeOH): δ = 174.3 (s, C=O, CO₂Me), 173.0 (s, C=O, COCH₃), 162.0 (s, *o*C_{Ar}-OCH₃), 160.5 (s, *p*C_{Ar}-OCH₃), 106.0 (s, C_{Ar}), 91.4 (d, 2CH_{Ar}), 56.1, 55.7, 52.4(q, 4CH₃-O), 54.0 (d, C_αH), 25.8 (t, CH₂), 22.3 (s, COCH₃).

MS (ESI, MeOH *m/z*): 645.0 (100, [2*M*+Na]⁺), 334.3 (24, [*M*+Na]⁺).

EA: calc. for C₁₅H₂₁NO₆: C: 57.87, H: 6.80, N: 4.50; found C: 57.76, H: 6.64, N: 4.32.

12 2-*tert*-butoxycarbonyl-(*rac*)-3-(2,4-dimethoxy-phenyl)-propionic acid 2-(2,2-dimethyl-propionyl)-3-(diphenoxy-phosphoryloxy)-tetrahydro-furan-2-ylmethyl ester [(*rac*)-Boc-DMP-Inj]

2,4-Dimethoxyphenylalanine-methylester **9** (400 mg, 1.67 mmol) was suspended in sat. aq. Na₂CO₃-solution (54 mL) using sonication and stirred at 40 °C for 18 h. After cooling to r.t., di-*tert*-butyldicarbonate (730 mg, 3.34 mmol) was added in dioxane (18 mL). The mixture was stirred another 60 min, then cooled to 0 °C and acidified to pH 2 by careful addition of HCl (37%). Extraction with EtOAc, followed by extraction of the organic phase with 1 M NaOH, washing of the resulting aq. phase with EtOAc and subsequent addition of 1 M HCl at 0 °C, led to precipitation of pure Boc-2,4-dimethoxyphenylalanine as a white solid in 80% yield, which was filtered and dried under high vacuum (for analytical data see **30**).

Boc-2,4-dimethoxyphenylalanine (107 mg, 330 μmol), TBTU (212 mg, 660 μmol) and DMAP (81 mg, 660 μmol) was dissolved in DMF (3 mL) and CH₂Cl₂ (6 mL) under an argon-atmosphere. Alcohol **2** (143 mg, 330 μmol) was added, dissolved in CH₂Cl₂ with DIPEA (226 μL, 1.32 mmol). The solution was stirred for 3 h at r.t.. The reaction was quenched by pouring it onto sat. aq. NH₄CO₃-solution (15 mL) covered with a layer of EtOAc. After washing with brine, then sat. aq. NaHCO₃-solution and again brine, the organic phase was dried (MgSO₄), concentrated under reduced pressure

and the residue was purified by column chromatography (hexane/EtOAc 4:1 → 1:1) and dried under high vacuum to yield **12** as a white foam; yield 220 mg (90%).

¹H-NMR (400 MHz, CDCl₃, 25°C, TMS): δ = 7.37-7.31 (m, 4H; H_{Ar}(PhOP)), 7.24-7.18 (m, 6H; H_{Ar}(PhOP)), 6.97-6.92 (m, 1H; *o*-H_{Ar}-(Phe-(OCH₃)₂)), 6.44-6.40 (m, 2H; *m*-H_{Ar}-(Phe-(OCH₃)₂)), 5.18-5.12 (m, 2H; NH, CH-OP), 4.47-4.37 (m, 1H; C_αHCH₂), 4.29-4.09 (m, 4H; COOCH₂, OCH₂CH₂), 3.79, 3.78 (2s, 6H; 2C_{Ar}-OCH₃), 3.04-2.87 (m, 2H; C_αHCH₂), 2.30-2.17 (m, 2H; OCH₂CH₂), 1.37 (s, 9H, CO₂C(CH₃)₃), 1.18, 1.16 (2s, 9H, C(CH₃)₃).

¹³C-NMR (125 MHz, CDCl₃): δ = 212.6 (s, C=O; CO_tBu), 172.0 (s, C=O, CH_αCO₂), 160.2 (s, *p*-C_{Ar}OCH₃), 158.5 (s, *o*-C_{Ar}-OCH₃), 150.4 (s, *J*_{C-P} = 7.1 Hz, C_{Ar}-OP), 150.3 (s, *J*_{C-P} = 7.3 Hz, C_{Ar}-OP), 131.5 (d, *o*-CH_{Ar}(Ph(OCH₃)₂)), 129.8 (d, 4 *m*-CH_{Ar}(PhOP)), 125.6, 125.4 (2s, 2 *p*-CH_{Ar}(PhOP)), 120.2 (d, *J*_{C-P} = 4.9 Hz, 2 *o*-CH_{Ar}(PhOP)), 120.1 (d, *J*_{C-P} = 4.9 Hz, 2 *o*-CH_{Ar}(PhOP)), 116.6 (s, C_{Ar}CH₂CH_α), 104.3 (d, *m*-CH_{Ar}(Ph(OCH₃)₂)), 98.6 (d, *m*-CH_{Ar}(Ph(OCH₃)₂)), 95.0 (s, OCCHCH₂), 84.0 (d, *J*_{C-P} = 5.5 Hz, CHOP), 79.6 (s, CO₂C(CH₃)₃), 68.1, 68.2 (2t, OCH₂CH₂, COOCH₂), 55.3, 55.4 (2q, 2 C_{Ar}OCH₃), 54.3, 54.1 (d, CH_α), 45.3 (s, C(CH₃)₃), 33.2 (t, CH₂CH₂), 32.2 (t, C_{Ar}CH₂CH_α), 28.3 (q, CO₂C(CH₃)₃), 25.8 (q, C(CH₃)₃).

MS (ESI, MeOH *m/z*): 764 ([*M*+Na]⁺, (100)), 1505 ([2*M*+Na]⁺, (15)).

EA: calc. for C₃₈H₄₈NO₁₂P: C: 61.53, H: 6.52, N: 1.89; found C: 61.47, H: 6.60, N: 1.80.

13 2-Acetylamino-3-(4-hydroxy-phenyl)-propionic acid 2-(2,2-dimethyl-propionyl)-3-(diphenoxy-phosphoryloxy)-tetrahydro-furan-2-ylmethyl ester [Ac-Tyr-Inj]

Boc-tyrosinebenzylether (112 mg, 300 μmol), TBTU (192 mg, 600 μmol) and DMAP (74 mg, 600 μmol) were dissolved in DMF (3 mL) and CH₂Cl₂ (6 mL) under an Ar-atmosphere. Alcohol **2** (130 mg, 300 μmol) was added in CH₂Cl₂ (2 mL) with DIPEA (0.20 mL, 1.2 mmol). The solution was stirred for 2.5 h at r.t.. The reaction was quenched by pouring it onto sat. aq. NH₄CO₃-solution (15 mL) covered with a layer of EtOAc. After washing with brine, then sat. aq. NaHCO₃-solution and again brine, the organic phase was dried (MgSO₄), concentrated under reduced pressure and the residue was filtered over silica (hexane/EtOAc 1:1) and dried under high vacuum to yield a white foam. Boc-deprotection was achieved according to **GP I** then CH₂Cl₂ (6 mL), DIPEA (308 μL, 1.8 mmol) and acetic anhydride (84 μL, 0.90 mmol) were added and the solution was stirred for 60 min at r.t.. Evaporation of CH₂Cl₂ was followed by an aq. workup procedure, using EtOAc as organic phase and washing with sat. aq. NH₄Cl-solution and sat. aq. NaHCO₃-solution (1x) each followed by brine.

Deprotection of the benzyl-group was achieved according to **GP III**. Purification of the crude product by column chromatography (hexane/EtOAc 1:1) yielded **13**; yield: 167 mg (87%).

$^1\text{H-NMR}$ (400 MHz, CDCl_3 , 25°C , TMS): δ = 7.40-7.33 (m, 4H; $\text{H}_{\text{Ar}}(\text{PhOP})$), 7.25-7.18 (m, 6H; $\text{H}_{\text{Ar}}(\text{PhOP})$), 6.97, 6.90 (2d, J = 8.56, 8.34 Hz, 2H, $o\text{-H}_{\text{Ar}}(\text{Tyr})$), 6.81, 6.74 (2d, J = 8.34, 8.56 Hz, 2H, $m\text{-H}_{\text{Ar}}(\text{Tyr})$), 6.10-5.89 (m, 1H; NH), 5.04-4.81 (m, 1H; CH-OP), 4.72-4.57 (m, 1H; $\text{C}_\alpha\text{HCH}_2$), 4.27-3.85 (m, 4H; COOCH_2 , OCH_2CH_2), 3.13-2.73 (m, 2H; $\text{C}_\alpha\text{HCH}_2$), 2.11-1.75 (m, 2H; OCH_2CH_2), 1.61 (s, 3H, COCH_3), 1.57, 1.11 (2s, 9H, $\text{C}(\text{CH}_3)_3$).

$^{13}\text{C-NMR}$ (100 MHz, CDCl_3): δ = 212.8 (s, C=O; $\text{CO}t\text{Bu}$), 171.8 (s, C=O, CO_2), 170.4 (s, C=O, COCH_3), 156.1 (s, $p\text{-C}_{\text{Ar}}\text{-OH}$), 150.4 (s, $J_{\text{C-P}}$ = 7.3 Hz, $\text{C}_{\text{Ar}}\text{-OP}$), 150.2 (s, $J_{\text{C-P}}$ = 6.9 Hz, $\text{C}_{\text{Ar}}\text{-OP}$), 130.4, 130.1 (d, $o\text{-CH}_{\text{Ar}}(\text{Tyr})$, $m\text{-CH}_{\text{Ar}}(\text{PhOP})$), 127.3 (s, $\text{C}_{\text{Ar}}\text{CH}_2$), 126.0 (d, $p\text{-CH}_{\text{Ar}}(\text{PhOP})$), 120.4, 120.3 (d, $J_{\text{C-P}}$ = 5.0 Hz, 2 $o\text{-CH}_{\text{Ar}}(\text{PhOP})$), 116.8 (d, $m\text{-CH}_{\text{Ar}}(\text{Tyr})$), 94.7 (s, OCCHCH_2), 84.8, 84.0 (d, $J_{\text{C-P}}$ = 5.0 Hz, CHOP), 68.8, 68.5, 68.2, 68.1 (t, OCH_2CH_2 , COOCH_2), 54.5 (d, CH_α), 45.6 (s, $\text{C}(\text{CH}_3)_3$), 38.1 (t, $\text{CH}_2\text{CH}_\alpha$), 33.2 (t, CH_2CH_2), 25.9 (q, $\text{C}(\text{CH}_3)_3$), 23.1 (q, COCH_3).

MS (ESI, MeOH m/z): 662 ($[\text{M}+\text{Na}]^+$, (100)), 1300 ($[\text{2M}+\text{Na}]^+$, (30)).

$\epsilon_{308} = 35 \text{ M}^{-1}\text{cm}^{-1}$.

HPLC (Merck LiChroSpher 100-5, RP-18e; acetonitrile/water 0% to 100% in 40 min): t_{R} 29.9'.

14 2-Acetylamino-(*rac*)-3-(2,4,6-trimethoxy-phenyl)-propionic acid 2-(2,2-dimethyl-propionyl)-3-(diphenoxy-phosphoryloxy)-tetrahydro-furan-2-ylmethyl ester [(*rac*)-Ac-TMP-Inj]

Boc-2,4,6-dimethoxyphenylalanine^[66, 88] (cf. also **31**) (117 mg, 330 μmol), TBTU (212 mg, 660 μmol) and DMAP (81 mg, 660 μmol) were dissolved in DMF (3 mL) and CH_2Cl_2 (6 mL) under an Ar-atmosphere. Alcohol **2** (143 mg, 330 μmol) was added in CH_2Cl_2 (2 mL) with DIPEA (226 μL , 1.32 mmol). The solution was stirred for 3.5 h at r.t.. The reaction was quenched by pouring it onto sat. aq. NH_4CO_3 -solution (15 mL) covered with a layer of EtOAc. After washing with brine, then sat. aq. NaHCO_3 -solution and again brine, the organic phase was dried (MgSO_4), concentrated under reduced pressure and the residue was filtered over silica (hexane/EtOAc 1:1) and dried under high vacuum to yield a yellowish foam. Boc-deprotection was achieved according to **GPI** then acetylation was carried

out (**GP VI**). Yellow impurities were removed by stirring in methanol with Pd/C, filtration and column chromatography (hexane/EtOAc 1:1) to give pure **14**; yield: 173 mg (68%).

$^1\text{H-NMR}$ (400 MHz, CDCl_3 , 25°C, TMS): δ = 7.37-7.31 (m, 4H; $\text{H}_{\text{Ar}}(\text{PhOP})$), 7.25-7.16 (m, 6H; $\text{H}_{\text{Ar}}(\text{PhOP})$), 6.35-6.30 (m, 1H; NH), 6.12 (s, 2H; $m\text{-H}_{\text{Ar}}(\text{Phe}(\text{OCH}_3)_3)$), 5.26-5.19 (m, 1H; CH-OP), 4.53-4.43 (m, 1H; $\text{C}_{\alpha}\text{HCH}_2$), 4.35-4.04 (m, 4H; COOCH_2 , OCH_2CH_2), 3.80, 3.79, 3.78 (3s, 9H; $3\text{C}_{\text{Ar}}\text{-OCH}_3$), 3.13-3.04 (m, 1H; $\text{C}_{\alpha}\text{HCH}_a\text{H}_b$), 2.95-2.88 (m, 1H; $\text{C}_{\alpha}\text{HCH}_a\text{H}_b$), 2.40-2.15 (m, 2H; OCH_2CH_2), 1.87 (s, 3H, COCH_3), 1.19, 1.17 (2s, 9H, $\text{C}(\text{CH}_3)_3$).

$^{13}\text{C-NMR}$ (100 MHz, CDCl_3): δ = 213.1 (s, C=O; COtBu), 172.3 (s, C=O, CO_2), 170.3 (s, C=O, COCH_3), 160.9 (s, $p\text{-C}_{\text{Ar}}\text{OH}_3$), 159.3 (s, $o\text{-C}_{\text{Ar}}\text{-OCH}_3$), 150.8, 150.7 (2s, $J_{\text{C-P}} = 7.2$ Hz, $\text{C}_{\text{Ar}}\text{-OP}$), 130.2 (d, $m\text{-CH}_{\text{Ar}}(\text{PhOP})$), 125.9, 125.8 (s, $2 p\text{-CH}_{\text{Ar}}(\text{PhOP})$), 120.5 (d, $J_{\text{C-P}} = 5.0$ Hz, $o\text{-CH}_{\text{Ar}}(\text{PhOP})$), 105.2 (s, $\text{C}_{\text{Ar}}\text{CH}_2\text{CH}_{\alpha}$), 95.6, 95.5 (s, OCCHCH_2), 91.0 (d, $m\text{-CH}_{\text{Ar}}(\text{Ph}(\text{OCH}_3)_2)$), 84.9, 84.6 (d, $J_{\text{C-P}} = 5.3$ Hz, CHOP), 68.7, 68.5 (2t, OCH_2CH_2 , COOCH_2), 56.0, 55.7 (2q, $3 \text{C}_{\text{Ar}}\text{OCH}_3$), 53.8, 53.6 (d, CH_{α}), 45.7 (s, $\text{C}(\text{CH}_3)_3$), 33.7, 33.5 (2t, CH_2CH_2 , $\text{C}_{\text{Ar}}\text{CH}_2\text{CH}_{\alpha}$), 26.1 (q, $\text{C}(\text{CH}_3)_3$), 23.3 (q, COCH_3).

MS (ESI, MeOH m/z): 736 ($[\text{M}+\text{Na}]^+$, (100)), 1449 ($[\text{2M}+\text{Na}]^+$, (75)).

$\epsilon_{308} = 39 \text{ M}^{-1}\text{cm}^{-1}$.

HPLC (Merck LiChroSpher 100-5, RP-18e; acetonitrile/water 0% to 100% in 40 min): t_{R} 34.6'.

15 2-Acetylamino-(rac)-3-(2,4-dimethoxy-phenyl)-propionic acid 2-(2,2-dimethyl-propionyl)-3-(diphenoxy-phosphoryloxy)-tetrahydro-furan-2-ylmethyl ester [(rac)-Ac-DMP-Inj]

Boc-deprotection of **12** (220 mg, 297 μmol) was carried out according to **GP I** then CH_2Cl_2 (6 mL), DIPEA (305 μL , 1.78 mmol) and acetic anhydride (84 μL , 0.89 mmol) were added and the solution was stirred for 30 min at r.t.. Evaporation of CH_2Cl_2 was followed by an aqueous workup procedure, using EtOAc as organic phase and washing with sat. aq. NH_4Cl -solution and sat. aq. NaHCO_3 -solution (1x) each followed by brine. The crude product obtained after drying of the organic phase and removal of the solvent under reduced pressure was purified by column chromatography (hexane/EtOAc 1:1) to give **15** (yield: 163 mg, 80%).

$^1\text{H-NMR}$ (400 MHz, CDCl_3 , 25°C , TMS): $\delta = 7.37\text{-}7.32$ (m, 4H; $\text{H}_{\text{Ar}}(\text{PhOP})$), $7.24\text{-}7.18$ (m, 6H; $\text{H}_{\text{Ar}}(\text{PhOP})$), $6.97\text{-}6.90$ (m, 1H; *o*- $\text{H}_{\text{Ar}}(\text{Phe}(\text{OCH}_3)_2)$), $6.45\text{-}6.40$ (m, 2H; *m*- $\text{H}_{\text{Ar}}(\text{Phe}(\text{OCH}_3)_2)$), 6.21 (br, 1H; NH), $5.21\text{-}5.15$ (m, 1H; CH-OP), $4.71\text{-}4.60$ (m, 1H; $\text{C}_\alpha\text{HCH}_2$), $4.31\text{-}4.05$ (m, 4H; COOCH_2 , OCH_2CH_2), 3.79 , 3.78 (2s, 6H; $2\text{C}_{\text{Ar}}\text{-OCH}_3$), $3.07\text{-}2.88$ (m, 2H; $\text{C}_\alpha\text{HCH}_2$), $2.29\text{-}2.15$ (m, 2H; OCH_2CH_2), 1.91 (s, 3H, COCH_3), 1.18 , 1.16 , 1.15 (3s, 9H, $\text{C}(\text{CH}_3)_3$).

$^{13}\text{C-NMR}$ (125 MHz, CDCl_3): $\delta = 212.6$ (s, C=O; COtBu), 171.5 (s, C=O, CO_2), 169.7 (s, C=O, COCH_3), 160.3 (s, *p*- $\text{C}_{\text{Ar}}\text{OCH}_3$), 158.4 (s, *o*- $\text{C}_{\text{Ar}}\text{OCH}_3$), 150.4 (s, $J_{\text{C-P}} = 7.3$ Hz, $\text{C}_{\text{Ar}}\text{-OP}$), 150.2 (s, $J_{\text{C-P}} = 7.3$ Hz, $\text{C}_{\text{Ar}}\text{-OP}$), 131.6 (d, *o*- $\text{CH}_{\text{Ar}}(\text{Ph}(\text{OCH}_3)_2)$), 129.8 (d, 2 *m*- $\text{CH}_{\text{Ar}}(\text{PhOP})$), 129.7 (d, 2 *m*- $\text{CH}_{\text{Ar}}(\text{PhOP})$), 125.5 (s, 2 *p*- $\text{CH}_{\text{Ar}}(\text{PhOP})$), 120.2 (d, $J_{\text{C-P}} = 5.0$ Hz, 2 *o*- $\text{CH}_{\text{Ar}}(\text{PhOP})$), 120.1 (d, $J_{\text{C-P}} = 5.0$ Hz, 2 *o*- $\text{CH}_{\text{Ar}}(\text{PhOP})$), 116.4 (s, $\text{C}_{\text{Ar}}\text{CH}_2\text{CH}_\alpha$), 104.5 (d, *m*- $\text{CH}_{\text{Ar}}(\text{Ph}(\text{OCH}_3)_2)$), 98.7 (d, *m*- $\text{CH}_{\text{Ar}}(\text{Ph}(\text{OCH}_3)_2)$), 95.0 , 94.8 (s, OCCHCH_2), 84.2 , 83.8 (d, $J_{\text{C-P}} = 5.4$ Hz, CHOP), 68.2 (2t, OCH_2CH_2 , COOCH_2), 55.4 (2q, 2 $\text{C}_{\text{Ar}}\text{OCH}_3$), 53.4 (d, CH_α), 45.3 (s, $\text{C}(\text{CH}_3)_3$), 33.2 (t, CH_2CH_2), 31.8 (t, $\text{C}_{\text{Ar}}\text{CH}_2\text{CH}_\alpha$), 25.9 (q, $\text{C}(\text{CH}_3)_3$), 23.0 (q, COCH_3).

MS (ESI, MeOH m/z): 706 ($[\text{M}+\text{Na}]^+$, (100)), 1390 ($[\text{2M}+\text{Na}]^+$, (45)).

EA: calc. for $\text{C}_{35}\text{H}_{42}\text{NO}_{11}\text{P}$: C: 61.49, H: 6.19, N: 2.05; found C: 60.02, H: 6.09, N: 2.03.

$\varepsilon_{308} = 55 \text{ M}^{-1}\text{cm}^{-1}$.

HPLC (Merck LiChroSpher 100-5, RP-18e; acetonitrile/water 0% to 100% in 40 min): $t_{\text{R}} 33.7'$.

16 Ac-(*rac*)TMP-Pro-(*rac*)DMP-Inj

Boc-TMP-OH (Boc-2,4,6-dimethoxyphenylalanine^[66, 88] (cf. also **31**)) was coupled to H-Pro-OtBu according to **GP V**, then deprotected (**GP I**) and acetylated (**GP VI**). Deprotection of the C-terminus (**GP II**) yielded the free acid (Ac-(*rac*)TMP-Pro-OH), which was coupled to deprotected **12** (**GP I**) using **GP V**. Purification by column chromatography (**GP VII**) yielded **16**.

$^1\text{H-NMR}$ (400 MHz, CDCl_3 , 25°C , TMS): $\delta = 7.35\text{-}7.29$ (m, 4H; $\text{H}_{\text{Ar}}(\text{PhOP})$), $7.23\text{-}7.17$ (m, 6H; $\text{H}_{\text{Ar}}(\text{PhOP})$), $7.09\text{-}6.84$ (m, 1H; $o\text{-H}_{\text{Ar}}\text{-(Phe-(OCH}_3)_2)$), $6.83\text{-}6.46$ (m, 2H; $m\text{-H}_{\text{Ar}}\text{-(Tyr)}$), $6.42\text{-}6.32$, $6.14\text{-}5.99$ (2 m, 4H; $m\text{-H}_{\text{Ar}}\text{-(Phe-(OCH}_3)_x)$), $5.32\text{-}5.07$ (m, 1H; CH-OP), $4.89\text{-}4.48$ (m, 2H; $2\text{C}_\alpha\text{H(Phe(OCH}_3)_x)$), $4.29\text{-}3.91$ (m, 5H; COOCH_2 , OCH_2CH_2 , $\text{CH}_\alpha(\text{Pro})$), $3.38\text{-}3.69$ (m, 15H; $5\text{C}_{\text{Ar}}\text{-OCH}_3$), $3.60\text{-}2.76$ (m, 6H; H-5 (Pro), $\text{C}_\alpha\text{HCH}_2$), $2.48\text{-}1.64$ (m, 9H; OCH_2CH_2 , H-3 (Pro), H-4 (Pro), COCH_3), $1.15\text{-}1.13$ (m, 9H, $\text{C(CH}_3)_3$).

$^{13}\text{C-NMR}$ (100 MHz, CDCl_3): (to abstract from the diastereoisomers present in the solution, only signal which differ by more than 1 ppm are given) $\delta = 213$ (s, C=O; COtBu), 172, 171, 170 (s, 4 C=O, CO_2 , 2 CO-NH , CO-N), 160 (s, 2 $p\text{-C}_{\text{Ar}}\text{OCH}_3$), 159 (s, 3 $o\text{-C}_{\text{Ar}}\text{-OCH}_3$), 150 (s, $\text{C}_{\text{Ar}}\text{-OP}$), 132 (d, $o\text{-CH}_{\text{Ar}}(\text{Ph(OCH}_3)_2)$), 129 (d, $m\text{-CH}_{\text{Ar}}(\text{PhOP})$), 126 (d, $p\text{-CH}_{\text{Ar}}(\text{PhOP})$), 120 (d, 2 $o\text{-CH}_{\text{Ar}}(\text{PhOP})$), 118, 117 (s, $\text{C}_{\text{Ar}}\text{CH}_2\text{CH}_\alpha$), 105, 104, 98, 91 (d, $m\text{-CH}_{\text{Ar}}(\text{Ph(OCH}_3)_x)$), 95 (s, OCCHCH_2), 84 (d, CHOP), 68 (t, OCH_2CH_2 , COOCH_2), 60 (d, $\text{CH}_\alpha(\text{Pro})$), 56, 55 (q, $\text{C}_{\text{Ar}}\text{OCH}_3$), 53, 52 (d, $\text{CH}_\alpha(\text{Phe(OCH}_3)_x)$), 47, 46 (t, $\text{CH}_2(\text{Pro})$), 45 (s, $\text{C(CH}_3)_3$), 33 (t, OCH_2CH_2), 32 (t, $\text{C}_\alpha\text{HCH}_2(\text{Phe(OCH}_3)_x)$), 25 (q, $\text{C(CH}_3)_3$), 23 (q, COCH_3).

MS (ESI, MeOH m/z): 1040 ($[\text{M}+\text{Na}]^+$, (100)).

$\epsilon_{308} = 42\text{ M}^{-1}\text{cm}^{-1}$.

HPLC (Merck LiChroSpher 100-5, RP-18e; acetonitrile/water 0% to 100% in 40 min): t_{R} 36.0'.

17 Ac-Tyr-Pro-(rac)DMP-Inj

Boc-Tyr(OBn)-OH was coupled to H-Pro-OtBu according to **GP V**, then deprotected (**GP I**) and acetylated (**GP VI**). Deprotection of the C-terminus (**GP II**) yielded the free acid (Ac-(rac)DMP-Pro-OH), which was coupled to deprotected **12** (**GP I**) using **GP V**. Benzyl deprotection (**GP III**) followed by column chromatography (**GP VII**) yielded **17**.

$^1\text{H-NMR}$ (400 MHz, CDCl_3 , 25°C , TMS): $\delta = 7.35\text{-}7.31$ (m, 4H; $\text{H}_{\text{Ar}}(\text{PhOP})$), $7.23\text{-}7.16$ (m, 6H; $\text{H}_{\text{Ar}}(\text{PhOP})$), $7.01\text{-}6.90$ (m, 3H; $o\text{-H}_{\text{Ar}}\text{-(Phe-(OCH}_3)_2)$), $2\text{ }o\text{-H}_{\text{Ar}}\text{-(Tyr)}$), $6.70\text{-}6.57$ (m, 2H; $m\text{-H}_{\text{Ar}}\text{-(Tyr)}$), $6.42\text{-}6.37$ (m, 2H; $m\text{-H}_{\text{Ar}}\text{-(Phe-(OCH}_3)_2)$), $5.33\text{-}5.14$ (m, 1H; CH-OP), $4.92\text{-}4.83$ (m, 1H; $\text{C}_\alpha\text{H(Tyr)}$), $4.72\text{-}4.60$ (m, 1H; $\text{C}_\alpha\text{H(Phe(OCH}_3)_2)$), $4.46\text{-}4.00$ (m, 5H; COOCH_2 , OCH_2CH_2 , $\text{CH}_\alpha(\text{Pro})$), $3.77\text{-}3.69$ (m, 6H; $2\text{C}_{\text{Ar}}\text{-OCH}_3$), $3.58\text{-}3.46$ (m, 2H; H-5 (Pro)), $3.11\text{-}2.76$ (m, 4H, $\text{C}_\alpha\text{HCH}_2$), $2.35\text{-}1.83$ (m, 6H; OCH_2CH_2 , H-3 (Pro), H-4 (Pro)), 1.91 (s, 3H, COCH_3), 1.16 (s, 9H, $\text{C(CH}_3)_3$).

^{13}C -NMR (125 MHz, CDCl_3): (to abstract from the diastereoisomers present in the solution, only signal which differ by more than 1 ppm are given) δ = 212 (s, C=O; CO t Bu), 172, 171, 170 (s, 4 C=O, CO $_2$, 2 CO-NH, CO-N), 160 (s, *p*-C $_{Ar}$ OCH $_3$), 158 (s, *o*-C $_{Ar}$ -OCH $_3$), 156 (q, C $_{Ar}$ -OH), 150 (s, C $_{Ar}$ -OP), 132 (d, *o*-CH $_{Ar}$ (Ph(OCH $_3$) $_2$)), 130 (d, *o*-CH $_{Ar}$ (Tyr)), 129 (d, *m*-CH $_{Ar}$ (PhOP)), 127 (s, C $_{Ar}$ CH $_2$ CH $_{\alpha}$ (Tyr)), 125 (d, 2 *p*-CH $_{Ar}$ (PhOP)), 120 (d, 2 *o*-CH $_{Ar}$ (PhOP)), 116 (s, C $_{Ar}$ CH $_2$ CH $_{\alpha}$), 115 (d, *m*-CH $_{Ar}$ (Tyr)), 104 (d, *m*-CH $_{Ar}$ (Ph(OCH $_3$) $_2$)), 98 (d, *m*-CH $_{Ar}$ (Ph(OCH $_3$) $_2$)), 95 (s, OCCHCH $_2$), 84 (d, CHOP), 68 (t, OCH $_2$ CH $_2$, COOCH $_2$), 60 (d, CH $_{\alpha}$ (Pro)), 55 (q, C $_{Ar}$ OCH $_3$), 53 (d, CH $_{\alpha}$ (Phe(OCH $_3$) $_2$)), 52 (d, CH $_{\alpha}$ (Tyr)), 47, 46 (t, CH $_2$ (Pro)), 45 (s, C(CH $_3$) $_3$), 38 (t, C $_{\alpha}$ HCH $_2$ (Tyr)), 33 (t, OCH $_2$ CH $_2$), 32 (t, C $_{\alpha}$ HCH $_2$ (Phe(OCH $_3$) $_2$)), 26 (q, C(CH $_3$) $_3$), 23 (q, COCH $_3$).

MS (ESI, MeOH m/z): 966 ($[M+\text{Na}]^+$, (100+)).

$\epsilon_{308} = 42 \text{ M}^{-1}\text{cm}^{-1}$.

HPLC (Merck LiChroSpher 100-5, RP-18e; acetonitrile/water 0% to 100% in 40 min): t_R 32.3'.

19 4-[1-(2,4-Dimethoxy-phenyl)-meth-(Z)-ylidene]-2-phenyl-4H-oxazol-5-one

2,4-Dimethoxybenzaldehyde (10 g, 60 mmol), hippuric acid (11 g, 63 mmol) and NaOAc (4.9 g, 60 mmol) were stirred in acetic anhydride (30 mL) at 85°C for 3 h. The mixture was cooled to 0 °C and cold EtOH was added. The formed orange precipitate was filtered and washed with cold EtOH and hot water to yield oxazolone **19** as a yellow solid; yield: 13.3 g (72%).

M.p. = 161-163 °C.

^1H -NMR (MeOD, 400 MHz): δ = 8.90 (d, J = 8.8 Hz, 1H; H $_{Ar}$ -6), 8.17-8.14 (m, 2H; H $_{Ar}$ -2', 6'), 7.81 (s, 1H; CH), 7.61-7.47 (m, 3H; H $_{Ar}$ -3', 4', 5'), 6.66 (dd, J = 8.8, 2.3 Hz, 1H; H $_{Ar}$ -5), 6.45 (d, J = 2.3 Hz, 1H; H $_{Ar}$ -3), 3.89 (s, 6H; 2CH $_3$ -O).

^{13}C -NMR (MeOH, 101 MHz): δ = 168.7 (s, C=O), 164.5 (s, C=N), 161.5 (s, *p*C $_{Ar}$ -OCH $_3$), 161.0 (s, *o*C $_{Ar}$ -OCH $_3$), 134.1 (s, C $_{Ar}$), 133.1 (d, CH $_{Ar}$), 130.6 (d, CH $_{Ar}$), 129.2 (d, 2CH $_{Ar}$), 128.4 (d, 2CH $_{Ar}$), 126.7 (d, CH=C), 123.2 (s, CH=C), 116.6 (s, C $_{Ar}$), 106.7 (d, CH $_{Ar}$), 98.1 (d, CH $_{Ar}$), 56.0, 56.1 (q, 2CH $_3$ -O).

MS (EI, 70 eV, m/z): 309 ($[M]^+$, 30), 206 (64), 105 (100), 77 (25).

EA: calc. for C₂₀H₂₁NO₆: C: 69.89, H: 4.89, N: 4.53; found C: 69.63, H: 4.92, N: 4.40.

20 2-Phenyl-4-[1-(2,4,6-trimethoxy-phenyl)-meth-(Z)-ylidene]-4H-oxazol-5-one.

2,4,6-Trimethoxybenzaldehyde (15 g, 76 mmol), hippuric acid (14.4, 80 mmol) and sodium acetate (6.3 g, 76 mmol) were stirred in acetic anhydride (40 mL) at 85°C for 2 h. The mixture was cooled to 0 °C and cold EtOH was added. The mixture was left in the fridge for 1 h. The resulting yellow precipitate was filtered and washed with cold EtOH and hot H₂O to yield oxazolone **20** as a yellow solid; yield: 12.9 g (50%).

M.p. = 150-152 °C.

¹H-NMR (400 MHz, CDCl₃, 25°C, TMS): δ = 8.06 (d, *J* = 7.6 Hz, 2H; H_{Ar}-2', 6'), 7.57-7.43 (m, 3H; H_{Ar}-3', 4', 5'), 7.47 (s, 1H; CH), 6.15 (s, 2H; H_{Ar}-3, 5), 3.87, 3.86, 3.84 (s, 9H; 3CH₃-O).

¹³C-NMR (101 MHz, CDCl₃): δ = 168.6 (s, C=O), 164.7 (s, *p*-C_{Ar}-OCH₃), 161.2 (s *o*-2C_{Ar}-OCH₃), 161.0 (s, C=N), 132.9 (d, CH_{Ar}), 132.8 (s, C=CH), 129.1 (d, 2CH_{Ar}), 128.3 (d, 2CH_{Ar}), 126.9 (d, C=CH), 105.9 (s, C_{Ar}), 91.3 (d, 2CH_{Ar}), 56.3, 55.9 (q, 3CH₃-O).

MS (EI, 70 eV, *m/z*): 339 (36, [M]⁺), 206 (64), 105 (100), 77 (24).

HR-MS (ESI): *m/z*=362.0997, calcd. for C₁₉H₁₇NO₅ (M+Na): 362.1107.

21 (Z)-2-Benzoylamino-3-(2,4-dimethoxy-phenyl)-acrylic acid methyl ester

Oxazolone **19** (13.3 g, 43 mmol) and Na₂CO₃ (13.7 g, 129 mmol) were suspended in MeOH (150 mL) and then refluxed for 2 h. The mixture was filtered hot and the remaining solution was concentrated under reduced pressure to 10% of the original volume. Crystallisation at 4°C over night and subsequent washing with methanol/water 1:1 yielded **21** as white crystalline needles; yield: 11.1 g (76%).

M.p. = 136-138 °C.

¹H-NMR (CDCl₃, 400 MHz): δ = 8.07 (s, 1H; NH), 7.85 (d, *J* = 7.4 Hz, 2H; H_{Ar}-2', 6'), 7.57 (s, 1H; CH), 7.51 (d, *J* = 7.6 Hz, 1H; H_{Ar}-6), 7.48-7.40 (m, 3H; H_{Ar}-3', 4', 5'), 6.45-6.40 (m, 2H; H_{Ar}-3, 5), 3.87, 3.84, 3.79 (s, 9H; 3CH₃-O).

^{13}C -NMR (CDCl_3 , 101 MHz): δ = 166.5 (s, C=O, CO_2Me), 165.8 (s, C=O, COPh), 162.4 (s, $p\text{-C}_{\text{Ar}}\text{-OCH}_3$), 158.9 (s, $o\text{-C}_{\text{Ar}}\text{-OCH}_3$), 134.3 (s, C_{Ar}), 132.4 (d, CH_{Ar}), 131.5 (d, CH_{Ar}), 129.1 (d, 2CH_{Ar}), 127.8 (d, 2CH_{Ar}), 126.5 (d, $\text{CH}=\text{C}$), 123.9 (s, $\text{CH}=\text{C}$), 116.2 (s, C_{Ar}), 105.7 (d, CH_{Ar}), 99.1 (d, CH_{Ar}), 56.3, 55.8, 53.0 (q, $3\text{CH}_3\text{-O}$).

MS (ESI, m/z): 364 ($[M+\text{Na}]^+$, 100).

EA: calc. for $\text{C}_{20}\text{H}_{21}\text{NO}_6$: C: 66.85, H: 5.61, N: 4.10; found C: 66.95, H: 5.53, N: 4.03.

22 (Z)-2-Benzoylamino-3-(2,4,6-trimethoxy-phenyl)-acrylic acid methyl ester

Oxazolone **20** (14 g, 41 mmol) and sodium carbonate (11.4 g, 107 mmol) were suspended in MeOH (140 mL) and refluxed for 1 h. The mixture was filtered hot and the remaining solution was concentrated under reduced pressure to 10% of the original volume. Recrystallisation of the resulting solid from hot MeOH yielded **22** as large white crystals; yield: 12.9 g (85%).

M.p. 141-143°C.

^1H -NMR (CDCl_3 , 400 MHz): δ = 8.54 (s, 1H; NH), 7.80 (d, J = 7.6 Hz, 2H; $\text{H}_{\text{Ar}}\text{-2'}$, 6'), 7.51-7.40 (m, 3H; $\text{H}_{\text{Ar}}\text{-3'}$, 4', 5'), 7.32 (s, 1H; CH), 6.15 (s, 2H; $\text{H}_{\text{Ar}}\text{-3}$, 5), 3.86 (s, 6H; $2\text{CH}_3\text{-O}$, COOCH_3), 3.81 (s, 3H; $\text{CH}_3\text{-O}$).

^{13}C -NMR (MeOH, 101 MHz): δ = 166.1 (s, C=O, CO_2Me), 165.3 (s, C=O, COPh), 162.7 (s, $p\text{-C}_{\text{Ar}}\text{-OCH}_3$), 159.0 (s, $o\text{-2C}_{\text{Ar}}\text{-OCH}_3$), 134.6 (s, C_{Ar}), 132.1 (d, CH_{Ar}), 128.9 (d, 2CH_{Ar}), 127.7 (d, 2CH_{Ar}), 126.7 (s, $\text{C}=\text{CH}$), 121.7 (d, $\text{C}=\text{CH}$), 105.6 (s, C_{Ar}), 91.5 (d, 2CH_{Ar}), 56.6, 55.8, 52.8 (q, $4\text{CH}_3\text{-O}$).

MS (ESI, m/z): 394 ($[M+\text{Na}]^+$, 100).

EA: calc. for $\text{C}_{20}\text{H}_{21}\text{NO}_6$: C: 64.68, H: 5.70, N: 3.77; found C: 64.67, H: 5.57, N: 3.72.

23 2-(S)-Benzoylamino-3-(2,4-dimethoxy-phenyl)-propionic acid methyl ester

Acrylic acid methyl ester **21** (1.0 g, 2.9 mmol) was suspended in MeOH (15 mL). After the addition of 3R,4R-(+)-bis(diphenylphosphino)-1-benzylpyrrolidine(1,5-cyclooctadiene) rhodium(I) (11 mg, ca. 0.45 mol%), the mixture was stirred for 15 minutes at r.t. The reaction suspension was then enclosed in an autoclave and hydrogenated (50 bar H_2 , 15 h). The formed brown solution was concentrated

under reduced pressure and the residue purified by column chromatography (EtOAc/hexane 2:1) to yield **23** as a white solid; yield: 970 mg (96%, *ee* > 95%).

M.p. 97-99 °C., $[\alpha]_{\text{D}}^{20} = +17.5 \text{ cm}^3 \text{ g}^{-1} \text{ dm}^{-1}$ (*c* = 1.38 in CH₂Cl₂).

¹H-NMR (MeOD, 400 MHz): δ = 7.70 (d, *J* = 6.8 Hz, 2H; H_{Ar}-2', 6'), 7.52-7.45 (m, 1H; H_{Ar}-4'), 7.42-7.37 (m, 2H; H_{Ar}-3', 5'), 7.03 (d, *J* = 8.1 Hz, 2H; H_{Ar}-6), 6.47-6.40 (m, 2H; H_{Ar}-3, 5), 4.85 (dd, *J* = 13.1, 6.3 Hz, 1H; C_αH), 3.80, 3.78, 3.74 (s, 9H; 3CH₃-O), 3.17 (d, *J* = 6.3 Hz, 2H; C_αHCH₂).

¹³C-NMR (MeOH, 101 MHz): δ = 172.4 (s, C=O, CO₂Me), 167.0 (s, C=O, C_{OPh}), 160.2 (s, *o*C_{Ar}-OCH₃), 158.3 (s, *p*C_{Ar}-OCH₃), 134.1 (s, C_{Ar}), 131.7 (d, CH_{Ar}), 131.6 (d, CH_{Ar}), 128.5 (d, 2CH_{Ar}), 127.0 (d, 2CH_{Ar}), 116.9 (s, C_{Ar}), 104.6 (d, CH_{Ar}), 98.7 (d, CH_{Ar}), 55.5, 55.4, 52.2 (q, 3CH₃-O), 54.1 (d, C_αH), 31.6 (t, CH₂).

MS (ESI, *m/z*): 366 ([*M*+Na]⁺, 100).

EA: calc. for C₂₀H₂₁NO₆: C: 66.46, H: 6.16, N: 4.08; found C: 66.65, H: 5.95, N: 4.03.

24 2-(S)-Benzoylamino-3-(2,4,6-trimethoxy-phenyl)-propionic acid methyl ester

Acrylic acid methyl ester **22** (1.0 g, 2.7 mmol) was suspended in 15 mL of MeOH and after the addition of 3R,4R-(+)-bis(diphenylphosphino)-1-benzylpyrrolidine(1,5-cyclooctadiene) rhodium(I) (11 mg, ca. 0.5 mol%), the mixture was stirred for 15 minutes at r.t. The reaction suspension was then enclosed in an autoclave and hydrogenated (50 bar H₂, 15 h). The formed brown solution was concentrated under reduced pressure and the residue purified by column chromatography (EtOAc/hexane 2:1) to yield **24** as a white solid; yield: 955 mg (95%, *ee* > 95%).

M. p. 147-149 °C; $[\alpha]_{\text{D}}^{20} = -38.7 \text{ cm}^3 \text{ g}^{-1} \text{ dm}^{-1}$ (*c* = 0.99 in H₂O).

¹H-NMR (MeOD, 400 MHz): δ = 6.15 (d, *J* = 8.6 Hz, 2H; H_{Ar}-2', 6'), 5.99-5.87 (m, 3H; H_{Ar}-3', 4', 5'), 4.64 (s, 2H; H_{Ar}-3, 5), 3.06 (dd, *J* = 8.6 Hz, *J* = 5.8 Hz, 1H; C_αH), 2.24, 2.21, 2.15 (s, 12H; 4CH₃-O), 1.65 (dd, *J* = 13.4 Hz, *J* = 5.8 Hz, 1H; C_αHCHH), 1.54 (dd, *J* = 13.4 Hz, *J* = 8.6 Hz, 1H; C_αHCHH).

¹³C-NMR (MeOH, 101 MHz): δ = 171.7 (s, C=O, CO₂Me), 167.3 (s, C=O, C_{OPh}), 159.6 (s C_{Ar}-OCH₃), 157.9 (s, 2C_{Ar}-OCH₃), 132.6 (s, C_{Ar}), 130.4 (d, CH_{Ar}), 127.1 (d, 2CH_{Ar}), 125.6 (d, 2CH_{Ar}), 103.6 (s, C_{Ar}), 89.0 (d, 2CH_{Ar}), 53.7, 53.2, 50.1 (q, 4CH₃-O), 52.4 (d, C_αH), 22.9 (t, CH₂).

MS (ESI, m/z): 396 ($[M+Na]^+$, 100).

HR-MS (ESI): $m/z=396.1413$, calcd. for $C_{20}H_{23}NO_6$ ($M+Na$): 396.1525.

25 2-(S)-Amino-3-(2,4-dimethoxy-phenyl)-propionic acid (21) ["2,4-Dimethoxyphenyl-alanine", DMP]

Propionic acid methyl ester **23** was dissolved in H_2O (15 mL) and acetic anhydride (15 mL). HCl (32%, 30 mL) was added carefully and the solution was stirred for 2 h at $110^\circ C$. After cooling and concentration under reduced pressure, water (15 mL) was added and the mixture was extracted with CH_2Cl_2 (3 x 5 mL). The aqueous phase was concentrated under vacuum, the residue was subjected to ion exchange chromatography and amino acid **25** was obtained as a white solid; yield: 470 mg (73%).

M.p. $228-230^\circ C$. $[\alpha]_D^{20} = -36.5\text{ cm}^3\text{g}^{-1}\text{dm}^{-1}$ ($c=1.02$ in MeOH).

1H -NMR (MeOD, 400 MHz): $\delta = 5.53$ (d, $J = 8.1$ Hz, 1H; H_{Ar-6}), 4.96 (s, 1 H_{Ar-3}), 4.89 (dd, $J = 8.1$, 2.0 Hz, 1H; H_{Ar-5}), 2.26 (s, 3H; O- CH_3), 2.25-2.18 (m, 1H; $C_\alpha H$), 2.19 (s, 3H; CH_3 -O), 1.28 (dd, $J = 13.6$, 4.52 Hz, 2H; $C_\alpha HCH_2$).

^{13}C -NMR (MeOD, 101 MHz): $\delta = 171.5$ (s, C=O, CO_2H), 159.6 (s, p - C_{Ar} - OCH_3), 157.5 (s, o - C_{Ar} - OCH_3), 130.3 (d, CH_{Ar-6}), 114.9 (s, C_{Ar-CH_2}), 103.3 (d, CH_{Ar-5}), 97.0 (d, CH_{Ar-3}), 54.5 (d, $C_\alpha H$), 53.2 (q, 2 CH_3 -O), 30.2 (t, $C_\alpha HCH_2$).

MS (FAB, NBA m/z): 226 ($[M+1]^+$, 100), 209 (18), 180 (22), 151 (43).

HR-MS (ESI): $m/z=226.1074$, calcd. for $C_{11}H_{15}NO_4$ ($M+1$): 226.1001.

26 2-(S)-Amino-3-(2,4,6-trimethoxy-phenyl)-propionic acid (22). ["2,4,6-Trimethoxyphenyl-alanine", TMP]

Propionic acid methyl ester **24** was dissolved in H_2O (15 mL) and acetic anhydride (15 mL). HCl (32%, 30 mL) was added carefully and the solution was stirred for 2 h at $110^\circ C$. After cooling and concentration under reduced pressure, water (15 mL) was added and the mixture was extracted with CH_2Cl_2 (3 x 5 mL). The aqueous phase was concentrated under vacuum, the residue was subjected to ion exchange chromatography and amino acid **26** was obtained as a white solid; yield: 479 mg (70%).

M.p. 219-221 °C; $[\alpha]_D^{20} = -14.1 \text{ cm}^3 \text{ g}^{-1} \text{ dm}^{-1}$ (c=0.6 in MeOH).

$^1\text{H-NMR}$ (MeOD/D₂O, 400 MHz): $\delta = 4.86$ (s, 2H; H_{Ar}-3, 5), 2.43 (s, 9H; 3O-CH₃), 2.30 (dd, $J = 10.1$ Hz, $J = 3.8$ Hz, 1H; C_αH), 1.86 (dd, $J = 13.9$ Hz, $J = 3.8$ Hz, 1H; C_αHCHH), 1.60 (dd, $J = 13.9$ Hz, $J = 10.1$ Hz, 1H; C_αHCHH).

$^{13}\text{C-NMR}$ (MeOH, 101 MHz): $\delta = 172.4$ (s, C=O, CO₂H), 159.7 (s, C_{Ar}-OCH₃), 158.2 (s, 2C_{Ar}-OCH₃), 103.0 (s, C_{Ar}), 89.4 (d, 2CH_{Ar}), 54.7 (d, C_αH), 54.0, 53.8 (q, 3CH₃-O), 23.4 (t, CH₂).

MS (FAB, NBA): 256 ($[M]^+$, 100), 239 (21), 210 (24), 181 (52).

HR-MS (ESI): $m/z=256.1185$, calcd. for C₁₂H₁₇NO₅ (M+1): 256.1107.

29 HCl·H₂N-DMP-Inj

Boc-DMP-OH **30** (65 mg, 0.20 mmol), TBTU (64 mg, 0.20 mmol) and DMAP (24 mg, 0.20 mmol) were dissolved in DMF (3 mL) and CH₂Cl₂ (6 mL) under an Ar-atmosphere. Alcohol **2** (143 mg, 330 μmol) was added dissolved in CH₂Cl₂ with DIPEA (140 μL, 800 μmol). The solution was stirred for 2 h at r.t., then TBTU (64 mg, 0.20 mmol) was added, before stirring for another 2 h. The reaction was quenched by pouring it onto sat. aq. NH₄CO₃-solution (15 mL) covered with a layer of EtOAc. After washing with brine, then sat. aq. NaHCO₃-solution and again brine, the organic phase was dried (MgSO₄), concentrated under reduced pressure and the residue was by column chromatography (hexane/EtOAc 2:1 → 1:2) and dried under high vacuum to yield Boc-DMP-Inj as a white foam (99 mg, 67%). (Not converted **2** could be regained during column chromatography. The reaction could not be driven to complete conversion by addition of more or different (HCTU, HATU) coupling reagents.)

$^1\text{H-NMR}$ (400 MHz, CDCl₃, 25°C, TMS): $\delta = 7.37$ -7.31 (m, 4H; H_{Ar}(PhOP)), 7.24-7.18 (m, 6H; H_{Ar}(PhOP)), 6.97-6.92 (m, 1H; *o*-H_{Ar}-(Phe-(OCH₃)₂)), 6.44-6.40 (m, 2H; *m*-H_{Ar}-(Phe-(OCH₃)₂)), 5.18-5.12 (m, 2H; NH, CH-OP), 4.47-4.37 (m, 1H; C_αHCH₂), 4.29-4.09 (m, 4H; COOCH₂, OCH₂CH₂), 3.79, 3.78 (2s, 6H; 2C_{Ar}-OCH₃), 3.04-2.87 (m, 2H; C_αHCH₂), 2.30-2.17 (m, 2H; OCH₂CH₂), 1.37 (s, 9H, CO₂C(CH₃)₃), 1.18, 1.16 (2s, 9H, C(CH₃)₃).

^{13}C -NMR (125 MHz, CDCl_3): δ = 212.6 (s, C=O; $\text{CO}t\text{Bu}$), 172.0 (s, C=O, $\text{CH}_\alpha\text{CO}_2$), 160.2 (s, p - $\text{C}_{\text{Ar}}\text{OCH}_3$), 158.5 (s, o - $\text{C}_{\text{Ar}}\text{OCH}_3$), 150.4 (s, $J_{\text{C-P}} = 7.1$ Hz, $\text{C}_{\text{Ar}}\text{-OP}$), 150.3 (s, $J_{\text{C-P}} = 7.3$ Hz, $\text{C}_{\text{Ar}}\text{-OP}$), 131.5 (d, o - $\text{CH}_{\text{Ar}}(\text{Ph}(\text{OCH}_3)_2)$), 129.8 (d, 4 m - $\text{CH}_{\text{Ar}}(\text{PhOP})$), 125.6, 125.4 (2s, 2 p - $\text{CH}_{\text{Ar}}(\text{PhOP})$), 120.2 (d, $J_{\text{C-P}} = 4.9$ Hz, 2 o - $\text{CH}_{\text{Ar}}(\text{PhOP})$), 120.1 (d, $J_{\text{C-P}} = 4.9$ Hz, 2 o - $\text{CH}_{\text{Ar}}(\text{PhOP})$), 116.6 (s, $\text{C}_{\text{Ar}}\text{CH}_2\text{CH}_\alpha$), 104.3 (d, m - $\text{CH}_{\text{Ar}}(\text{Ph}(\text{OCH}_3)_2)$), 98.6 (d, m - $\text{CH}_{\text{Ar}}(\text{Ph}(\text{OCH}_3)_2)$), 95.0 (s, OCCHCH_2), 84.0 (d, $J_{\text{C-P}} = 5.5$ Hz, CHOP), 79.6 (s, $\text{CO}_2\text{C}(\text{CH}_3)_3$), 68.1, 68.2 (2t, OCH_2CH_2 , COOCH_2), 55.3, 55.4 (2q, 2 $\text{C}_{\text{Ar}}\text{OCH}_3$), 54.3, 54.1 (d, CH_α), 45.3 (s, $\text{C}(\text{CH}_3)_3$), 33.2 (t, CH_2CH_2), 32.2 (t, $\text{C}_{\text{Ar}}\text{CH}_2\text{CH}_\alpha$), 28.3 (q, $\text{CO}_2\text{C}(\text{CH}_3)_3$), 25.8 (q, $\text{C}(\text{CH}_3)_3$).

MS (ESI, MeOH m/z): 764 ($[\text{M}+\text{Na}]^+$, (100)), 1505 ($[\text{2M}+\text{Na}]^+$, (15)).

Boc-DMP-Inj was then converted to the amine hydrochloride **29** used in subsequent peptide couplings by **GP I**. Conversion of this deprotection reaction was controlled by ESI-MS spectroscopy.

30 Boc-DMP-OH

2,4-dimethoxyphenylalanine **25** (163 mg, 720 μmol) was suspended in methanol with NaHCO_3 (180 mg, 2.14 mmol) using sonication and di-*tert*-butyldicarbonate (158 mg, 720 μmol) was added. Reaction progress was followed by TLC (CH_2Cl_2 4% methanol 1% AcOH) and additional di-*tert*-butyldicarbonate was added in small portions, to drive the reaction to completion. After complete conversion of the starting material (2-4 hs), the reaction mixture was filtered and evaporated to dryness. The residue was dissolved in water and the product was precipitated as a white voluminous solid by acidification with sat. aq. KHSO_3 -solution, and dried in high vacuum (208 mg, 89%).

^1H -NMR (400 MHz, MeOD, 25°C, TMS): δ = 7.02 (d, 1H, $J = 8.34$ Hz, H_{Ar}), 6.44-6.42 (m, 2H, H_{Ar}), 5.44-5.27 (m, 1H, NH), 4.45-4.33 (m, 1H; C_αH), 3.79 (s, 6H; 3 O-CH_3), 3.11-3.01 (m, 2H, $\text{C}_\alpha\text{HCH}_2$), 1.39 (s, br $\text{C}(\text{CH}_3)_3$).

^{13}C -NMR (101 MHz, MeOH): δ = 177.7 (s, C=O, CO_2H), 160.3, 158.7 (s, $\text{C}_{\text{Ar}}\text{-OCH}_3$), 155.8 (s, CO_2tBu), 131.8 (d, o - $\text{C}_{\text{Ar}}\text{H}$), 116.8 (s, $\text{C}_{\text{Ar}}\text{CH}_2$), 104.4 (d, m - CH_{Ar}), 98.6 (d, m - CH_{Ar}), 80.0 (s, $\text{C}(\text{CH}_3)_3$), 55.5, 55.3 (q, 2 OCH_3), 54.3 (d, C_αH), 31.9 (t, $\text{CH}_\alpha\text{CH}_2$), 28.4 (q, $\text{C}(\text{CH}_3)_3$).

MS (ESI, MeOH m/z): 324 (100, $[\text{M-H}]^-$).

EA: calc. for $\text{C}_{16}\text{H}_{23}\text{NO}_6$: C: 59.07, H: 7.12, N: 4.31; found C: 59.02, H: 6.95, N: 4.27.

31 Boc-TMP-OH

2,4,6-trimethoxyphenylalanine **26** (150 mg, 590 μmol) was dissolved in a 1:1 (v/v) mixture of sat. aq. Na_2CO_3 -solution and dioxane (6 mL) using sonication and di-*tert*-butyldicarbonate (256 mg, 1.17 mmol) was added. After 2 h of stirring the reaction mixture was cooled to 0 °C and acidified to pH 2 by careful addition of HCl (37%). Extraction with EtOAc, followed by extraction of the organic phase with 1 M NaOH, washing of the resulting aq. phase with EtOAc and subsequent addition of 1 M HCl at 0 °C, led to precipitation of Boc-2,4,6-trimethoxyphenylalanine **31** as a yellowish solid. Residual water could be removed by dissolving the product in CH_2Cl_2 and coevaporating it with toluene; yield: 180 mg (86%).

$[\alpha]_{\text{D}}^{20} = -16.9^\circ$ ($c = 0.49$ in CHCl_3).

$^1\text{H-NMR}$ (400 MHz, CDCl_3 , 25 °C, TMS): $\delta = 6.12$ (s, 2H; H_{Ar}), 5.49-5.40 (m, 1H, NH), 4.39-4.26 (m, 1H; C_αH), 3.80 (s, br 9H; 3 O- CH_3), 3.15 (dd, $J = 13.6, 4.4$ Hz, 1H; $\text{C}_\alpha\text{HCHH}$), 2.99 (dd, $J = 13.6, 9.2$ Hz, 1H; $\text{C}_\alpha\text{HCHH}$), 1.38 (s, br $\text{C}(\text{CH}_3)_3$).

$^{13}\text{C-NMR}$ (101 MHz, CDCl_3): $\delta = 177.8$ (s, $\text{C}=\text{O}$, CO_2H), 160.3, 159.1 (s, $\text{C}_{\text{Ar}}\text{-OCH}_3$), 156.0 (s, CO_2tBu), 105.0 (s, $\text{C}_{\text{Ar}}\text{CH}_2$), 90.4 (d, 2CH_{Ar}), 79.7 (s, $\text{C}(\text{CH}_3)_3$), 55.5, 55.3 (q, 3OCH_3), 54.1 (d, C_αH), 28.2 (q, $\text{C}(\text{CH}_3)_3$), 24.5 (t, $\text{CH}_\alpha\text{CH}_2$).

MS (ESI, MeOH m/z): 354 (100, $[\text{M-H}]^-$).

35 Ac-Phe-(Pro)₃-Phe-(Pro)₃-DMP-Inj

Boc-Phe-OH was coupled to HCl·HN-(Pro)₃-OtBu according to **GP V**, then deprotected with HCl in dioxane (**GP I**). A part of the resulting amine hydrochloride was acetylated (**GP VI**) and the C-terminal protection group was removed (**GP II**) to yield the free acid Ac-Phe-(Pro)₃-OH, which was coupled to the remaining amine hydrochloride using **GP V**. Deprotection of the resulting octapeptide Ac-Phe-(Pro)₃-Phe-(Pro)₃-OtBu was then followed by coupling to **29** (**GP V**). Purification by column chromatography (**GP VII**) yielded **35**.

MS (ESI, MeOH m/z): 1583 ($[\text{M}+\text{Na}]^+$, (100)), 803 ($[\text{M}+2\text{Na}]^{2+}$, (15)).

$\epsilon_{308} = 100 \text{ M}^{-1}\text{cm}^{-1}$.

HPLC (Merck LiChroSpher 100-5, RP-18e; acetonitrile/water 0% to 100% in 40 min): t_R 32.4'.

36 Ac-Tyr-(Pro)₃-Phe-(Pro)₃-Phe-OMe

Ac-Tyr(*O*tBu)-(Pro)₃-Phe-(Pro)₃-OH was prepared by SPPS on proline-preloaded chlorotriyl resin (0.67 mmol/g) on a 400 μ mol scale, following **GP VIII**. The cleaved peptide (0.12 mmol) was coupled to H-Phe-OMe in solution phase according to **GP V**, then deprotected (**GP IV**) and purified (**GP VII**) to give **36**; yield: 64 mg (48%).

MS (ESI, MeOH *m/z*): 1136 ($[M+Na]^+$, (100)).

$$\epsilon_{308} = 10 \text{ M}^{-1}\text{cm}^{-1}.$$

HPLC (Merck LiChroSpher 100-5, RP-18e; acetonitrile/water 0% to 100% in 40 min): t_R 20.6'.

37 Ac-Tyr-Pro-TMP-Pro-DMP-Inj

Boc-Tyr(OBn)-OH was coupled to HN-Pro-*O*tBu according to **GP V**, then deprotected with HCl in dioxane (**GP I**), acetylated (**GP VI**) deprotected (**GP II**) to yield the free acid Ac-Tyr(OBn)-Pro-OH, which was coupled to HCl·H₂N-TMP-Pro-*O*tBu [synthesized by coupling of **31** to H-Pro-*O*tBu (**GP V**) and Boc-deprotection (**GP I**)] using **GP V**. Deprotection of the resulting tetrapeptide Ac-Tyr(OBn)-Pro-TMP-Pro-*O*tBu was then followed by coupling to **29** (**GP V**). Reductive cleavage of the benzyl ether and subsequent purification of the peptide by column chromatography (**GP VII**) yielded **37**.

MS (ESI, MeOH *m/z*): 1300 ($[M+Na]^+$, (100)).

$$\epsilon_{308} = 43 \text{ M}^{-1}\text{cm}^{-1}.$$

HPLC (Merck LiChroSpher 100-5, RP-18e; acetonitrile/water 0% to 100% in 40 min): t_R 34.3'.

38 Ac-Tyr-(Pro)₃-DMP-Inj

Boc-Tyr(OBn)-OH was coupled to H-(Pro)₃-OtBu according to **GP V**, then deprotected (**GP I**) and acetylated (**GP VI**). Deprotection of the C-terminus (**GP II**) yielded the free acid (Ac-Tyr(OBn)-(Pro)₃-OH), which was coupled to deprotected **12** (**GP I**, cf. also **14**) using **GP V**. Purification by column chromatography (**GP VII**) yielded **38**.

MS (ESI, MeOH m/z): 1160 ($[M+Na]^+$, (100)).

$\epsilon_{308} = 41 \text{ M}^{-1}\text{cm}^{-1}$.

HPLC (Merck LiChroSpher 100-5, RP-18e; acetonitrile/water 0% to 100% in 40 min): t_R 30.5'.

39 Ac-Tyr-(Pro)₃-TMP-(Pro)₃-DMP-Inj

Boc-Tyr(OBn)-OH was coupled to HCl·HN-(Pro)₃-OtBu according to **GP V**, then deprotected with HCl in dioxane (**GP I**), acetylated (**GP VI**) and deprotected (**GP II**) to yield the free acid Ac-Tyr(OBn)-(Pro)₃-OH. Boc-TMP-OH **31** was coupled to HCl·HN-(Pro)₃-OtBu (**GP V**) and deprotected to the amine hydrochloride (**GP I**) HCl·H₂N-TMP-(Pro)₃-OtBu. Coupling of the free acid to the amine gave the octapeptide Ac-Tyr(OBn)-(Pro)₃-TMP-(Pro)₃-OtBu, which was deprotected (**GP II**) and coupled to **29** (**GP V**). Reductive cleavage of the benzyl ether and subsequent purification of the peptide by column chromatography (**GP VII**) yielded **39**.

MS (ESI, MeOH m/z): 1689 ($[M+Na]^+$, (100)).

$\epsilon_{308} = 65 \text{ M}^{-1}\text{cm}^{-1}$.

HPLC (Merck LiChroSpher 100-5, RP-18e; acetonitrile/water 0% to 100% in 40 min): t_R 30.6'.

40 Ac-Phe-(Pro)₃-TMP-(Pro)₃-Phe-OMe

Boc-Phe-OH was coupled to HCl·HN-(Pro)₃-OtBu according to **GP V**, then deprotected with HCl in dioxane (**GP I**). The resulting amine hydrochloride was acetylated (**GP VI**) and the C-terminal protection group was removed (**GP II**) to yield the free acid Ac-Phe-(Pro)₃-OH. Boc-TMP-OH **31** was coupled to HCl·HN-(Pro)₃-OtBu (**GP V**) and deprotected to the amine hydrochloride (**GP I**) HCl·H₂N-TMP-(Pro)₃-OtBu. Coupling of the free acid to the amine gave the octapeptide Ac-Phe-(Pro)₃-TMP-(Pro)₃-OtBu, which was deprotected (**GP II**) and coupled to H-Phe-OMe. Purification of the resulting peptide **40** by carrying out a hydrogenation procedure (Pd/C) and subsequent column chromatography (**GP VII**) yielded **40**.

MS (ESI, MeOH m/z): 1211 ([M+Na]⁺, (100)).

$$\epsilon_{308} = 7 \text{ M}^{-1}\text{cm}^{-1}.$$

HPLC (Merck LiChroSpher 100-5, RP-18e; acetonitrile/water 0% to 100% in 40 min): t_R 23.0'.

41 Ac-Tyr-(Pro)₃-TMP-Pro-DMP-Inj

Boc-Tyr(OBn)-OH was coupled to HCl·HN-(Pro)₃-OtBu according to **GP V**, then deprotected with HCl in dioxane (**GP I**), acetylated (**GP VI**) and deprotected (**GP II**) to yield the free acid Ac-Tyr(OBn)-(Pro)₃-OH. Boc-TMP-OH **31** was coupled to HCl·HN-Pro-OtBu (**GP V**) and deprotected to the amine hydrochloride (**GP I**) HCl·H₂N-TMP-Pro-OtBu. Coupling of the free acid to the amine gave the hexapeptide Ac-Tyr(OBn)-(Pro)₃-TMP-Pro-OtBu, which was deprotected (**GP II**) and coupled to **29** (**GP V**). Reductive cleavage of the benzyl ether and subsequent purification of the peptide by column chromatography (**GP VII**) yielded **41**.

MS (ESI, MeOH m/z): 1495 ([M+Na]⁺, (100)).

$$\epsilon_{308} = 58 \text{ M}^{-1}\text{cm}^{-1}.$$

HPLC (Merck LiChroSpher 100-5, RP-18e; acetonitrile/water 0% to 100% in 40 min): t_R 33.0'.

42 Ac-Tyr-Pro-TMP-(Pro)₃-DMP-Inj

Boc-Tyr(OBn)-OH was coupled to HN-Pro-OtBu according to **GP V**, then deprotected with HCl in dioxane (**GP I**), acetylated (**GP VI**) and deprotected (**GP II**) to yield the free acid Ac-Tyr(OBn)-Pro-OH. Boc-TMP-OH **31** was coupled to HCl·HN-(Pro)₃-OtBu (**GP V**) and deprotected (**GP I**) to the amine hydrochloride HCl·H₂N-TMP-(Pro)₃-OtBu. Coupling of the free acid to the amine gave the hexapeptide Ac-Tyr(OBn)-Pro-TMP-(Pro)₃-OtBu, which was deprotected (**GP II**) and coupled to **29** (**GP V**). Reductive cleavage of the benzyl ether and subsequent purification of the peptide by column chromatography (**GP VII**) yielded **42**.

MS (ESI, MeOH *m/z*): 1495 ($[M+Na]^+$, (100)).

$\epsilon_{308} = 45 \text{ M}^{-1}\text{cm}^{-1}$.

HPLC (Merck LiChroSpher 100-5, RP-18e; acetonitrile/water 0% to 100% in 40 min): t_R 32.2'.

43 Ac-Tyr-(Pro)₆-TMP-Pro-DMP-Inj

Boc-Tyr(OBn)-OH was coupled to HCl·HN-(Pro)₃-OtBu according to **GP V**, then deprotected with HCl in dioxane (**GP I**), acetylated (**GP VI**) and deprotected (**GP II**) to yield the free acid Ac-Tyr(OBn)-(Pro)₃-OH, which was coupled to the triproline fragment HCl·HN-(Pro)₃-OtBu (**GP V**) and deprotected (**GP II**) to yield the free acid Ac-Tyr(OBn)-(Pro)₆-OH. Boc-TMP-OH **31** was coupled to HN-Pro-OtBu (**GP V**) and deprotected to the amine hydrochloride (**GP I**) HCl·H₂N-TMP-Pro-OtBu. Coupling of the free acid to the amine gave the nonapeptide Ac-Tyr(OBn)-(Pro)₆-TMP-Pro-OtBu, which was deprotected (**GP II**) and coupled to **29** (**GP V**). Reductive cleavage of the benzyl ether and subsequent purification of the peptide by column chromatography (**GP VII**) yielded **43**.

MS (ESI, MeOH *m/z*): 1786 ($[M+Na]^+$, (100)), 905 ($[M+2Na]^{2+}$, (30)).

$\epsilon_{308} = 76 \text{ M}^{-1}\text{cm}^{-1}$.

HPLC (Merck LiChroSpher 100-5, RP-18e; acetonitrile/water 0% to 100% in 40 min): t_R 31.3'.

47 4-(2'-Methoxy-4'-acetoxybenzylidene)-2-phenyloxazol-5(4H)-one

4-Hydroxy-2-methoxybenzaldehyd (4.04 g, 26.6 mmol), hippuric acid (4.80 g, 26.8 mmol), sodium acetate (2.24 g, 27.3 mmol) and acetic anhydride (6.0 mL, 6.5 g, 64 mmol) were placed in a 100 mL round bottom flask, liquefied with a heat gun and then heated in an oil bath at 100°C for 2 h. The resulting solid mixture was cooled to r.t. before H₂O (30 mL) was added. The resulting suspension was filtrated, washed with aqueous Na₂CO₃ and dried in vacuo. The desired azlactone **47** was then obtained after recrystallization from acetone/H₂O (2:1) as a yellow solid; yield: 6.89 g (77%).

M.p. 188-189°C.

¹H-NMR (CDCl₃, 400 MHz): δ = 8.90 (d, J = 8.6 Hz, 1H; H_{Ar-6} (Tyr-OCH₃)), 8.19-8.12 (m, 2H; $H_{Ar-2'}$, 6'), 7.77 (s, 1H; CH), 7.62-7.56 (m, 1H; $H_{Ar-4'}$), 7.55-7.48 (m, 2H; $H_{Ar-3'}$, 5'), 6.85 (dd, J = 8.6, 2.0 Hz, 1H; H_{Ar-5} (Tyr-OCH₃)), 6.70 (d, J = 2.0 Hz, 1H; H_{Ar-3} (Tyr-OCH₃)), 3.89 (s, 3H; CH₃CO₂), 2.33 (s, 3H; C_{Ar}-OCH₃).

¹³C-NMR (CDCl₃, 101 MHz): δ = 168.9 (s, C=O, COCN), 167.8 (s, C=O, CH₃CO₂), 163.0 (s, C=N), 160.1 (s, *o*-C_{Ar}-OCH₃), 154.2 (s, *p*-C_{Ar}-OAc), 133.8 (d, CH=C), 133.1 (d, *p*-CH_{Ar}), 132.3 (s, C_{Ar}), 128.9 (d, 2*o*-CH_{Ar}), 128.2 (d, 2*m*-CH_{Ar}), 125.7 (s, CH=C), 124.9 (d, CH_{Ar-6}(Tyr-OCH₃)), 120.3 (s, C_{Ar}-CH), 114.2 (d, CH_{Ar-5}(Tyr-OCH₃)), 104.7 (d, CH_{Ar-3}(Tyr-OCH₃)), 55.8 (q, CH₃-O), 21.2 (q, CH₃CO₂).

MS (EI, 70 eV, 200 °C): m/z (%) = 337 (13), 295 (35), 105 (100), 77 (26).

EA: calc. for C₁₉H₁₅NO₅·¹/₃ H₂O: C: 66.47, H: 4.60, N: 4.08; found C: 66.54, H: 4.50, N: 4.12.

48 2-Benzoylamino-3-(4-hydroxy-2-methoxyphenyl)-acrylic acid methyl ester

A 100 mL round bottom flask was charged with 4-acetoxy-2-methoxyazlactone **47** (6.71 g, 19.9 mmol), a 1:1 mixture of CH₂Cl₂ and MeOH (80 mL) and Na₂CO₃ (1.0 g, 9.4 mmol). The mixture was stirred for 16 h at r.t., filtrated over celite and the resulting solution was concentrated under reduced until **48** precipitated as a white solid. yield: 5.53 g (85%).

M.p. 207-208°C.

¹H-NMR (CDCl₃/DMSO = 30:1, 400 MHz): δ = 8.82 (s, 1H; NH), 7.97-7.89 (m, 2H; 2*o*- H_{Ar} (CONHPh)), 7.67 (s, 1H; CH=C), 7.57-7.51 (m, 1H; *p*- H_{Ar} (CONHPh)), 7.50-7.42 (m, 3H; 2*m*- H_{Ar} (CONHPh), H_{Ar-6} (Tyr-OCH₃)), 6.43 (d, J = 2.3 Hz, 1H; H_{Ar-3} (Tyr-OCH₃)), 6.39 (dd, J = 8.6, 2.3 Hz, 1H; H_{Ar-5} (Tyr-OCH₃)), 3.84 (s, 3H; CO₂CH₃), 3.81 (s, 3H; C_{Ar}-OCH₃).

^{13}C -NMR ($\text{CDCl}_3/\text{DMSO} = 30:1$, 101 MHz): $\delta = 165.9$ (s, C=O, CO_2CH_3), 165.7 (s, C=O, CONHPh), 160.1 (s, $\text{C}_{\text{Ar}}\text{-OCH}_3$), 158.6 (s, $\text{C}_{\text{Ar}}\text{-OH}$), 133.4 (s, $\text{C}_{\text{Ar}}\text{-CONHPh}$), 131.3, 130.5 (d, $\text{CH}_{\text{Ar}}\text{-6(Tyr-OCH}_3)$, $p\text{-CH}_{\text{Ar}}(\text{CONHPh})$), 128.0 (d, $2m\text{-CH}_{\text{Ar}}(\text{CONHPh})$), 127.6 (d, C=CH), 127.2 (d, $2o\text{-CH}_{\text{Ar}}(\text{CONHPh})$), 122.4 (s, C=CH), 113.4 (s, $\text{C}_{\text{Ar}}\text{-CH}$), 107.7 (d, $\text{CH}_{\text{Ar}}\text{-5(Tyr-OCH}_3)$), 98.7 (d, $\text{CH}_{\text{Ar}}\text{-3(Tyr-OCH}_3)$), 55.2 (q, $\text{C}_{\text{Ar}}\text{-OCH}_3$), 51.8 (q, CO_2CH_3).

MS (EI, 70 eV, 250 °C): m/z (%) = 327 (47), 190 (21), 163 (8), 148 (8), 105 (100), 77 (33).

EA: calc. for $\text{C}_{18}\text{H}_{17}\text{NO}_5$: C: 66.05, H: 5.23, N: 4.28; found C: 65.86, H: 5.23, N: 4.30.

49 2-(S)-Benzoylamino-3-(4-hydroxy-2-methoxyphenyl)-propionic acid methyl ester

Acrylic acid methyl ester **48** (411 mg, 1.26 mmol) was suspended in 15 mL of MeOH and after the addition of 3R,4R-(+)-bis(diphenylphosphino)-1-benzylpyrrolidine(1,5-cyclooctadiene) rhodium(I) (4.0 mg, ca. 0.5 mol%), the mixture was stirred for 15 minutes at r.t. The reaction suspension was then enclosed in an autoclave and hydrogenated (50 bar H_2 , 24 h). The formed brown solution was concentrated under reduced pressure and the residue purified by column chromatography (EtOAc/hexane 3:1) to yield **49** as a white solid; yield: 400 mg, (96%, $ee > 95\%$).

M.p. 206-208°C. $[\alpha]_{\text{D}}^{20} = +21.2 \text{ cm}^3 \text{g}^{-1} \text{dm}^{-1}$ ($c = 0.73$ in CHCl_3).

^1H -NMR (CDCl_3 , 400 MHz): $\delta = 7.74\text{-}7.67$ (m, 2H; $2o\text{-H}_{\text{Ar}}(\text{CONHPh})$), 7.52-7.45 (m, 1H; $p\text{-H}_{\text{Ar}}(\text{CONHPh})$), 7.43-7.36 (m, 2H; $2m\text{-H}_{\text{Ar}}(\text{CONHPh})$), 7.12 (d, $J = 7.1$ Hz, 1H; NH), 6.90 (d, $J = 8.1$ Hz, 1H; $\text{H}_{\text{Ar}}\text{-6(Tyr-OCH}_3)$), 6.36 (d, $J = 2.3$ Hz, 1H; $\text{H}_{\text{Ar}}\text{-3(Tyr-OCH}_3)$), 6.32 (dd, $J = 8.1, 2.3$ Hz, 1H; $\text{H}_{\text{Ar}}\text{-5(Tyr-OCH}_3)$), 4.87 (dd, $J = 7.0, 6.2$ Hz, 1H; $\text{C}_{\alpha}\text{H}$), 3.74 (s, 3H; CO_2CH_3), 3.72 (s, 3H; $\text{C}_{\text{Ar}}\text{-OCH}_3$), 3.16-3.11 (m, 2H; $\text{C}_{\alpha}\text{HCH}_2$).

^{13}C -NMR (CDCl_3 , 101 MHz): $\delta = 172.5$ (s, C=O, CO_2CH_3), 167.4 (s, C=O, CONHPh), 158.3 (s, $\text{C}_{\text{Ar}}\text{-OCH}_3$), 156.8 (s, $\text{C}_{\text{Ar}}\text{-OH}$), 133.8 (s, $\text{C}_{\text{Ar}}\text{-CONHPh}$), 131.73, 131.66 (d, $\text{CH}_{\text{Ar}}\text{-6(Tyr-OCH}_3)$, $p\text{-CH}_{\text{Ar}}(\text{CONHPh})$), 128.5 (d, $2m\text{-CH}_{\text{Ar}}(\text{CONHPh})$), 127.0 (d, $2o\text{-CH}_{\text{Ar}}(\text{CONHPh})$), 115.9 (s, $\text{C}_{\text{Ar}}\text{-CH}$), 107.5 (d, $\text{CH}_{\text{Ar}}\text{-5(Tyr-OCH}_3)$), 99.2 (d, $\text{CH}_{\text{Ar}}\text{-3(Tyr-OCH}_3)$), 55.4 (q, $\text{C}_{\text{Ar}}\text{-OCH}_3$), 54.2 (d, $\text{C}_{\alpha}\text{H}$), 52.3 (q, CO_2CH_3), 31.7 (t, CH_2).

MS (FAB, NBA): m/z (%): 330 ($[M+1]^+$, 100), 270 (24), 208 (30), 105 (37).

EA: calc. for $\text{C}_{18}\text{H}_{19}\text{NO}_5$: C: 65.64, H: 5.81, N: 4.25; found C: 65.33, H: 5.93, N: 4.27.

50 2-(S)-Amino-3-(4-hydroxy-2-methoxyphenyl)-propionic acid (13). ["4-Hydroxy-2-phenylalanine"]

Propionic acid methyl ester **49** (400 mg, 1.21 mmol) was dissolved in HCl (32%)/H₂O (10 mL, 3:2 v/v) and stirred for 5 h at 110°C. After cooling and concentration under reduced pressure, H₂O was added (15 mL) and the mixture was extracted with CH₂Cl₂ (3 x 5 mL). The aqueous phase was concentrated under vacuum, the residue was subjected to ion exchange chromatography and amino acid **50** was obtained as a white solid; yield: 200 mg (78%).

M.p. 166-168°C. $[\alpha]_D^{20} = -32.4 \text{ cm}^3 \text{ g}^{-1} \text{ dm}^{-1}$ (c = 0.11 in H₂O).

¹H-NMR (D₂O, 400 MHz): $\delta = 7.04$ (d, $J = 8.2$ Hz, 1H; $H_{\text{Ar-6}}$ (Tyr-OCH₃)), 6.53 (d, $J = 2.3$ Hz, 1H; $H_{\text{Ar-3}}$ (Tyr-OCH₃)), 6.45 (dd, $J = 8.2, 2.3$ Hz, 1H; $H_{\text{Ar-5}}$ (Tyr-OCH₃)), 3.92 (dd, $J = 8.0, 4.7$ Hz, 1H; C $_{\alpha}$ H), 3.80 (s, 3H; OCH₃), 3.23 (dd, $J = 14.5, 4.7$ Hz, 1H; C $_{\alpha}$ HCHH), 2.92 (dd, $J = 14.5, 8.0$ Hz, 1H; C $_{\alpha}$ HCHH).

¹³C-NMR (D₂O/MeOH_{trace}, 101 MHz): $\delta = 174.8$ (s, C=O, CO₂H), 159.2 (s C_{Ar}-OCH₃), 157.1 (s, C_{Ar}-OH), 132.8 (d, CH_{Ar-6}(Tyr-OCH₃)), 115.7 (s, C_{Ar}-CH₂), 108.0 (d, CH_{Ar-5}(Tyr-OCH₃)), 99.9 (d, CH_{Ar-3}(Tyr-OCH₃)), 56.1 (d, C $_{\alpha}$ H), 55.9 (q, OCH₃), 31.4 (t, CH₂); MS (FAB, NBA): m/z (%): 365 ([M+NBA+H]⁺, 5), 212 ([M+H]⁺, 100), 166 (22), 137 (43).

MS (EI, 70 eV, 200 °C): m/z (%): 211 ([M]⁺, 1), 137 ([2-OMe,4-OH-PhCH₂]⁺, 100), 107 (34), 77 (9).

EA: calc. for C₁₀H₁₃NO₄^{1/3} H₂O: C: 55.29, H: 6.34, N: 6.45; found C: 55.21, H: 6.64, N: 6.39.

51 2-tert-Butoxycarbonylamino-3-(4-hydroxy-2-methoxy-phenyl)-propionic acid methyl ester

1.) To a suspension of amino acid **50** (30 mg, 0.14 mmol) in MeOH (30 mL), SOCl₂ (0.36 mL, 0.71 mmol) was added dropwise. After 2 days of stirring at r.t., the mixture was concentrated under vacuum to give 2-amino-3-(4-hydroxy-2-methoxy-phenyl)-propionic acid methyl ester as a yellow solid in quantitative yield.

2.) To a suspension of 2-amino-3-(4-hydroxy-2-methoxy-phenyl)-propionic acid methyl ester (70 mg, 0.31 mmol) in CH₂Cl₂ (3 mL) was added Et₃N (60 μ L, 0.47 mmol) at r.t.. After 10 minutes of stirring, Boc₂O (75 mg, 0.34 mmol) in CH₂Cl₂ (2 mL) was added dropwise. 30 minutes later, sat. aq. NH₄Cl-solution (5 mL) was added and the mixture was extracted with CH₂Cl₂ (3 x 3 mL). The combined organic phases were dried, concentrated under vacuum and the residue was purified by column

chromatography (EtOAc/hexane 3:1, quick, the product slowly decomposes on SiO₂!) to give **51** as a white solid; yield: 40 mg (35%).

1. 2-Amino-3-(4-hydroxy-2-methoxy-phenyl)-propionic acid methyl ester

M.p. 128-130°C.

¹H-NMR (MeOD, 400 MHz): δ = 6.92 (d, J = 8.4 Hz, 1H; H_{Ar-6} (Tyr-OCH₃)), 6.46 (d, J = 2.3 Hz, 1H; H_{Ar-3} (Tyr-OCH₃)), 6.36 (dd, J = 8.4, 2.3 Hz, 1H; H_{Ar-5} (Tyr-OCH₃)), 4.21 (dd, J = 7.3, 5.6 Hz, 1H; $C_{\alpha}H$), 3.81 (s, 3H; CO₂CH₃), 3.78 (s, 3H; C_{Ar} -OCH₃), 3.21 (dd, J = 14.4, 5.6 Hz, 1H; $C_{\alpha}HCHH$), 2.99 (dd, J = 14.4, 7.3 Hz, 1H; $C_{\alpha}HCHH$).

¹³C-NMR (101 MHz, MeOD, 25°C): δ = 168.1 (s, C=O, CO₂CH₃), 157.7, 157.3 (2s, C_{Ar} -OCH₃, C_{Ar} -OH), 130.3 (d, CH_{Ar-6} (Tyr-OCH₃)), 111.8 (s, C_{Ar} -CH₂), 105.7 (d, CH_{Ar-5} (Tyr-OCH₃)), 97.5 (d, CH_{Ar-3} (Tyr-OCH₃)), 53.2 (q, C_{Ar} -OCH₃), 51.9 (d, $C_{\alpha}H$), 50.9 (q, CO₂CH₃), 29.6 (t, $C_{\alpha}HCH_2$).

MS (FAB, NBA): m/z (%): 226 ($[M]^+$, 100), 212 (62), 137 (32).

2.

M.p. 103-105°C.

¹H-NMR (CDCl₃, 400 MHz): δ = 6.90 (d, J = 7.8 Hz, 1H; H_{Ar-6} (Tyr-OCH₃)), 6.37 (d, J = 2.3 Hz, 1H; H_{Ar-3} (Tyr-OCH₃)), 6.33 (dd, J = 7.8, 2.3 Hz, 1H; H_{Ar-5} (Tyr-OCH₃)), 5.18 (d, J = 11.4, 1H; NH), 4.44 (m, 1H; $C_{\alpha}H$), 3.77 (s, 3H; CO₂CH₃), 3.70 (s, 3H; C_{Ar} -OCH₃), 2.97 (m, 2H; $C_{\alpha}HCH_2$), 1.39 (s, 9H; CO₂C(CH₃)₃).

¹³C-NMR (101 MHz, CDCl₃, 25°C): δ = 172.1 (s, C=O, CO₂CH₃), 159.8 (s, C_{Ar} -OCH₃), 155.5 (s, C_{Ar} -OH), 151.7 (s, C=O, CO₂C(CH₃)₃), 131.6 (d, CH_{Ar-6} (Tyr-OCH₃)), 120.5 (s, C_{Ar} -CH₂), 112.5 (d, CH_{Ar-5} (Tyr-OCH₃)), 108.4 (d, CH_{Ar-3} (Tyr-OCH₃)), 84.1 (s, C(CH₃)₃), 55.8 (q, C_{Ar} -OCH₃), 54.0 (d, $C_{\alpha}H$), 52.7 (q, CO₂CH₃), 32.2 (t, $C_{\alpha}HCH_2$), 28.6 (q, C(CH₃)₃).

MS (ESI, MeOH): m/z (%): 348 ($[M+Na]^+$, 24), 673 ($[2M+Na]^+$, 9), 683 (30), 741 (100).

52 Trifluoro-methanesulfonic acid 2-(2,2-dimethylpropionyl)-3-(diphenoxyphosphoryloxy) tetrahydrofuran-2-yl methyl ester

To a solution of alcohol **2** (188 mg, 0.433 mmol) in CH₂Cl₂ (2 mL), pyridine (0.11 mL, 1.4 mmol) was added at 0 °C. After 10 min of stirring, Tf₂O (0.14 mL, 0.82 mmol) was added dropwise and the reaction mixture was warmed to r.t.. After the addition of sat. aq. NH₄Cl-solution (2 mL) and phase separation, the aq. phase was extracted with CH₂Cl₂ (3 x 2 mL). The combined organic phases were dried (MgSO₄) and concentrated under vacuum to give triflate **52** as a white solid; yield: 251 mg (82%).

M.p. 96-97°C.

¹H-NMR (CDCl₃, 400 MHz): δ = 7.39-7.32 (m, 4H; H_{Ar}), 7.27-7.17 (m, 6H; H_{Ar}), 5.17-5.12 (m, 1H; CHCH₂), 4.71 (d, J = 11.4 Hz, 1H; CHHOTf), 4.32 (d, J = 11.4 Hz, 1H; CHHOTf), 4.28-4.15 (m, 2H; OCH₂CH₂), 2.30-2.20 (m, 2H; OCH₂CH₂), 1.18 (s, 9H; C(CH₃)₃).

¹³C-NMR (101 MHz, CDCl₃): δ = 212.3 (s, C=O, CO_tBu), 150.6 (d, J_{C-P} = 6.9 Hz, C_{Ar}-OP), 150.5 (d, J_{C-P} = 7.3 Hz, C_{Ar}-OP), 130.3 (d, 2 *p*-CH_{Ar}(PhOP)), 126.2 (d, 2 *m*-CH_{Ar}(PhOP)), 126.0 (d, 2 *m*-CH_{Ar}(PhOP)), 120.5 (d, J_{C-P} = 5.0 Hz, 2 *o*-CH_{Ar}(PhOP)), 120.4 (d, J_{C-P} = 5.0 Hz, 2 *o*-CH_{Ar}(PhOP)), 118.9 (q, J = 320 Hz, CF₃), 94.5 (d, J_{C-P} = 10.0 Hz, CCH-OP), 83.5 (dd, J_{C-P} = 5.0 Hz, CHCH₂), 78.3 (t, CH₂OSO₂CF₃), 69.1 (t, OCH₂CH₂), 45.6 (s, C(CH₃)₃), 33.7 (t, OCH₂CH₂), 26.0 (q, C(CH₃)₃).

MS (FAB, NBA): m/z (%): 367 ([*M*+1]⁺, 52), 251 (100), 77 (18), 57 (70).

53 2-tert-Butoxycarbonylamino-3-{4-[2-(2,2-dimethylpropionyl)-3-(diphenoxyphosphoryloxy)tetrahydrofuran-2-ylmethoxy]-2-methoxyphenyl}propionic acid methyl ester [Boc-DAP-OMe]

To a solution of **51** (70 mg, 0.22 mmol) in DMF (3 mL) was added Cs₂CO₃ (101 mg, 0.236 mmol) at r.t.. After 10 min of stirring, a solution of triflate **52** (218 mg, 0.215 mmol) in DMF (2 mL) was added dropwise and stirring was continued for 3 h. Then, sat. aq. NH₄Cl-solution (2 mL) was added and the mixture was extracted with EtOAc (3 x 3 mL). The combined organic phases were washed with water (3 x 3 mL), dried (MgSO₄) and concentrated under vacuum. Column chromatography (hexane/EtOAc 2:1) gave **9** as a white solid; yield: 83 mg (52%).

M.p. 47-49°C.

$^1\text{H-NMR}$ (CDCl_3 , 400 MHz): $\delta = 7.39\text{-}7.31$ (m, 4H; $\text{H}_{\text{Ar}}(\text{PhOP})$), $7.27\text{-}7.16$ (m, 6H; $\text{H}_{\text{Ar}}(\text{PhOP})$), 6.95 (d, $J = 7.8$ Hz, 1H; $\text{H}_{\text{Ar}}\text{-}6(\text{Tyr-OCH}_3)$), $6.36\text{-}6.31$ (m, 2H; $\text{H}_{\text{Ar}}\text{-}3(\text{Tyr-OCH}_3)$, $\text{H}_{\text{Ar}}\text{-}5(\text{Tyr-OCH}_3)$), $5.35\text{-}5.31$ (m, 1H; CH-OP), $5.19\text{-}5.11$ (br, 1H; NH), $4.49\text{-}4.38$ (m, 1H; $\text{C}_\alpha\text{HCH}_2$), $4.31\text{-}4.09$ (m, 4H; OCH_2CO , OCH_2CH_2), 3.78 , (s, 3H; $\text{C}_{\text{Ar}}\text{-OCH}_3$), 3.68 (s, 3H; CO_2CH_3), $3.03\text{-}2.84$ (m, 2H; $\text{C}_\alpha\text{HCH}_2$), $2.50\text{-}2.38$ (m, 1H; OCH_2CHH), $2.28\text{-}2.20$ (m, 1H; OCH_2CHH), 1.39 , 1.22 (2s, $2 \times 9\text{H}$, $2\text{C}(\text{CH}_3)_3$).

$^{13}\text{C-NMR}$ (101 MHz, CDCl_3): $\delta = 213.0$ (s, C=O; CO_tBu), 172.1 (s, C=O, CO_2CH_3), 159.2 (s, $\text{C}_{\text{Ar}}\text{-OCH}_3$), 158.9 (s, C=O, NHCO_2tBu), 155.6 (s, $\text{C}_{\text{Ar}}\text{-OCH}_2$), 150.8 (d, $J_{\text{C-P}} = 7.3$ Hz, $\text{C}_{\text{Ar}}\text{-OP}$), 150.7 (d, $J_{\text{C-P}} = 7.3$ Hz, $\text{C}_{\text{Ar}}\text{-OP}$), 131.9 (d, $\text{CH}_{\text{Ar}}\text{-}6(\text{Tyr-OCH}_3)$), 130.2 (d, $2 p\text{-CH}_{\text{Ar}}(\text{PhOP})$), 126.2 (d, $2 m\text{-CH}_{\text{Ar}}(\text{PhOP})$), 126.0 (d, $2 m\text{-CH}_{\text{Ar}}(\text{PhOP})$), 120.6 (d, $J_{\text{C-P}} = 5.0$ Hz, $2 o\text{-CH}_{\text{Ar}}(\text{PhOP})$), 120.5 (d, $J_{\text{C-P}} = 5.0$ Hz, $2 o\text{-CH}_{\text{Ar}}(\text{PhOP})$), 118.1 (s, $\text{C}_{\text{Ar}}\text{-CH}_2$), 105.3 (d, $\text{CH}_{\text{Ar}}\text{-}6(\text{Tyr-OCH}_3)$), 99.2 (s, $\text{CH}_{\text{Ar}}\text{-}3(\text{Tyr-OCH}_3)$), 96.8 , 96.7 (s, OCCHCH_2), 84.8 (dd, $J_{\text{C-P}} = 5.7$ Hz, CCHCH_2), 79.9 (s, $\text{OC}(\text{CH}_3)_3$), 73.4 (t, OCH_2CH_2), 68.4 (t, $\text{CH}_2\text{OC}_{\text{Ar}}$), 55.8 (q, $\text{C}_{\text{Ar}}\text{-OCH}_3$), 54.5 (d, $\text{C}_{\square}\text{H}$), 52.4 (q, CO_2CH_3), 45.8 (s, $\text{C}(\text{CH}_3)_3$), 34.2 (t, $\text{C}_\alpha\text{HCH}_2$), 32.6 (t, OCH_2CH_2), 28.7 (q, $\text{C}(\text{CH}_3)_3$), 26.0 (q, $\text{C}(\text{CH}_3)_3$).

MS (ESI, MeOH m/z): 764 ($[\text{M}+\text{Na}]^+$, 100); MS (FAB, NBA): m/z (%): 780 ($[\text{M-H}+\text{K}]^+$, 11), 642 (23), 553 (15), 251 (23), 167 (19), 57 (100).

EA: calc. for $\text{C}_{38}\text{H}_{48}\text{NO}_{12}\text{P}$: C: 61.53, H: 6.52, N: 1.89; found C: 61.37, H: 6.51, N: 1.60.

59 Ac-Tyr-Pro-Phe-Pro-DMP-Inj

Boc-Tyr(OBn)-OH was coupled to HN-Pro-OtBu according to **GP V**, then deprotected with HCl in dioxane (**GP I**), acetylated (**GP VI**) and deprotected (**GP II**) to yield the free acid Ac-Tyr(OBn)-(Pro-OH). Boc-Phe-OH was coupled to HN-Pro-OtBu (**GP V**) and deprotected to the amine hydrochloride (**GP I**) $\text{HCl}\cdot\text{H}_2\text{N-Phe-Pro-OtBu}$. Coupling of the free acid to the amine gave the tetrapeptide Ac-Tyr(OBn)-Pro-Phe-Pro-OtBu, which was deprotected (**GP II**) and coupled to **29**, according to (**GP V**). Reductive cleavage of the benzyl ether and subsequent purification of the peptide by column chromatography (**GP VII**) yielded **59**.

MS (ESI, MeOH m/z): 1211 ($[\text{M}+\text{Na}]^+$, (100)).

$\epsilon_{308} = 40 \text{ M}^{-1}\text{cm}^{-1}$.

HPLC (Merck LiChroSpher 100-5, RP-18e; acetonitrile/water 0% to 100% in 40 min): t_{R} 33.3'.

60 Ac-Tyr-Pro-Phe-(Pro)₃-DMP-Inj

Ac-Tyr(*Ot*Bu)-Pro-Phe-(Pro)₃-OH was prepared by SPPS on proline-preloaded chlorotriyl resin (0.67 mmol/g) on a 670 μ mol scale, following **GP VIII**. The cleaved peptide (117 mg, 0.143 mmol) was coupled to **29** (0.11 mmol) in solution phase according to **GP V**, then deprotected (**GP IV**) and purified (**GP VII**), including a hydrogenation procedure (Pd/C), to give **60**; yield: 95 mg (62% rel. to **29**).

MS (ESI, MeOH *m/z*): 1404 ($[M+Na]^+$, (100)).

$$\varepsilon_{308} = 42 \text{ M}^{-1}\text{cm}^{-1}.$$

HPLC (Merck LiChroSpher 100-5, RP-18e; acetonitrile/water 0% to 100% in 40 min): t_R 31.7'.

61 Ac-Tyr-Pro-Phe-Pro-DAP

Ac-Tyr(*Ot*Bu)-Pro-Phe-Pro-OH was prepared by SPPS on proline-preloaded chlorotriyl resin (0.67 mmol/g) on a 400 μ mol scale, following **GP VIII**. The cleaved peptide (126 mg, 200 μ mol) was coupled to deprotected **53** (190 μ mol, **GP I**), according to (**GP V**). Cleavage of the *t*butyl ether (**GP IV**) and subsequent purification of the peptide by applying a hydrogenation procedure (**GP III**, 2 hs) and subsequent column chromatography (**GP VII**) yielded **61** (190 mg, 85%).

MS (ESI, MeOH *m/z*): 1211 ($[M+Na]^+$, (100)).

$$\varepsilon_{308} = 66 \text{ M}^{-1}\text{cm}^{-1}.$$

HPLC (Merck LiChroSpher 100-5, RP-18e; acetonitrile/water 0% to 100% in 40 min): t_R 33.1'.

62 Ac-Tyr-Pro-Phe-(Pro)₃-DAP

Ac-Tyr(*Ot*Bu)-Pro-Phe-(Pro)₃-OH was prepared by SPPS on proline-preloaded chlorotriyl resin (0.67 mmol/g) on a 670 μ mol scale, following **GP VIII**. The cleaved peptide (106 mg, 130 μ mol) was coupled to deprotected **53** (100 μ mol, **GP I**), according to (**GP V**). Cleavage of the *t*butyl ether (**GP IV**) and subsequent purification of the peptide by applying a hydrogenation procedure (**GP III**, 1 h) and subsequent column chromatography (**GP VII**) yielded **62** (86 mg, 62%).

MS (ESI, MeOH m/z): 1404 ($[M+Na]^+$, (100)).

$\epsilon_{308} = 47 \text{ M}^{-1}\text{cm}^{-1}$.

HPLC (Merck LiChroSpher 100-5, RP-18e; acetonitrile/water 0% to 100% in 40 min): t_R 30.9'.

63 Ac-Tyr-Pro-TMP-(Pro)₃-DAP

Boc-Tyr(OBn)-OH was coupled to HN-Pro-OtBu according to **GP V**, then deprotected with HCl in dioxane (**GP I**), acetylated (**GP VI**) and deprotected (**GP II**) to yield the free acid Ac-Tyr(OBn)-Pro-OH. Boc-TMP-OH **31** was coupled to HCl·HN-(Pro)₃-OtBu (**GP V**) and deprotected (**GP I**) to the amine hydrochloride HCl·H₂N-TMP-(Pro)₃-OtBu. Coupling of the free acid to the amine gave the hexapeptide Ac-Tyr(OBn)-Pro-TMP-(Pro)₃-OtBu, which was deprotected (**GP II**) and coupled to deprotected **53** (**GP I**), according to **GP V**. Reductive cleavage of the benzyl ether and subsequent purification of the peptide by column chromatography (**GP VII**) yielded **63**.

MS (ESI, MeOH m/z): 1495 ($[M+Na]^+$, (100)).

$\epsilon_{308} = 60 \text{ M}^{-1}\text{cm}^{-1}$.

HPLC (Merck LiChroSpher 100-5, RP-18e; acetonitrile/water 0% to 100% in 40 min): t_R 31.0'.

64 Ac-Tyr-(Pro)₃-TMP-(Pro)₃-DAP

Boc-Tyr(OBn)-OH was coupled to HCl·HN-(Pro)₃-OtBu according to **GP V**, then deprotected with HCl in dioxane (**GP I**), acetylated (**GP VI**) and deprotected (**GP II**) to yield the free acid Ac-Tyr(OBn)-(Pro)₃-OH. Boc-TMP-OH **31** was coupled to HCl·HN-(Pro)₃-OtBu (**GP V**) and deprotected to the amine hydrochloride (**GP I**) HCl·H₂N-TMP-(Pro)₃-OtBu. Coupling of the free acid to the amine gave the octapeptide Ac-Tyr(OBn)-(Pro)₃-TMP-(Pro)₃-OtBu, which was deprotected (**GP II**) and coupled to deprotected **53** (**GP I**), according to **GP V**. Reductive cleavage of the benzyl ether and subsequent purification of the peptide by column chromatography (**GP VII**) yielded **64**.

MS (ESI, MeOH m/z): 1689 ($[M+Na]^+$, (100)).

$\epsilon_{308} = 58 \text{ M}^{-1}\text{cm}^{-1}$.

HPLC (Merck LiChroSpher 100-5, RP-18e; acetonitrile/water 0% to 100% in 40 min): t_R 30.6'.

65 Ac-Tyr-(Pro)₃-Ala-(Pro)₃-DAP

Ac-Tyr(*Ot*Bu)-(Pro)₃-Ala-(Pro)₃-OH was prepared by SPPS on proline-preloaded chlorotriyl resin (0.67 mmol/g) on a 400 μ mol scale, following **GP VIII**. The cleaved peptide (93 mg, 0.10 mmol) was coupled to deprotected **53** (90 μ mol, **GP I**), according to **GP V**. Cleavage of the *t*butyl ether (**GP IV**) and subsequent purification of the peptide by column chromatography (**GP VII**) yielded **65** (93 mg, 69%).

MS (ESI, MeOH m/z): 1523 ($[M+Na]^+$, (100)).

$$\epsilon_{308} = 74 \text{ M}^{-1}\text{cm}^{-1}.$$

HPLC (Merck LiChroSpher 100-5, RP-18e; acetonitrile/water 0% to 100% in 40 min): t_R 27.9'.

66 Ac-Tyr-(Pro)₃-Leu-(Pro)₃-DAP

Ac-Tyr(*Ot*Bu)-(Pro)₃-Leu-(Pro)₃-OH was prepared by SPPS on proline-preloaded chlorotriyl resin (0.69 mmol/g) on a 414 μ mol scale, following **GP VIII**. The cleaved peptide (98 mg, 0.10 mmol) was coupled to deprotected **53** (100 μ mol, **GP I**), according to (**GP V**), but without aq. workup, instead the reaction mixture was evaporated to dryness, by coevaporation with toluene and filtered over silica. Cleavage of the *t*butyl ether (**GP IV**) and subsequent purification of the peptide by column chromatography (**GP VII**) yielded **66** (56 mg, 36%).

MS (ESI, MeOH m/z): 1565 ($[M+Na]^+$, (100)), 794 ($[M+2Na]^{2+}$, (20)).

$$\epsilon_{308} = 81 \text{ M}^{-1}\text{cm}^{-1}.$$

HPLC (Merck LiChroSpher 100-5, RP-18e; acetonitrile/water 0% to 100% in 40 min): t_R 29.4'.

67 Ac-Tyr-(Pro)₃-Tyr(OMe)-(Pro)₃-DAP

Ac-Tyr(O*t*Bu)-(Pro)₃-Tyr(OMe)-(Pro)₃-OH was prepared by SPPS on proline-preloaded chlorotriyl resin (0.69 mmol/g) on a 414 μmol scale, following **GP VIII**. The cleaved peptide (214 mg, 220 μmol) was coupled to deprotected **53** (212 μmol, **GP I**), according to **GP V**. Cleavage of the *tert*-butylether (**GP IV**) and subsequent purification of the peptide by column chromatography (**GP VII**) yielded **62** (80 mg, 23%).

MS (ESI, MeOH *m/z*): 1629 ($[M+Na]^+$, (100)), 826 ($[M+2Na]^{2+}$, (20)).

ϵ_{308} (MeCN/water 3:1) = 86 M⁻¹cm⁻¹.

HPLC (Merck LiChroSpher 100-5, RP-18e; acetonitrile/water 0% to 100% in 40 min): t_R 30.2'.

68 Ac-Tyr-(Pro)₃-DMP-(Pro)₃-DAP

Boc-Tyr(OBn)-OH was coupled to HCl·HN-(Pro)₃-O*t*Bu according to **GP V**, then deprotected with HCl in dioxane (**GP I**), acetylated (**GP VI**) and deprotected (**GP II**) to yield the free acid Ac-Tyr(OBn)-(Pro)₃-OH. Boc-DMP-OH **30** was coupled to HCl·HN-(Pro)₃-O*t*Bu (**GP V**) and deprotected (**GP I**) to the amine hydrochloride HCl·H₂N-DMP-(Pro)₃-O*t*Bu. Coupling of the free acid to the amine gave the octapeptide Ac-Tyr(OBn)-(Pro)₃-DMP-(Pro)₃-O*t*Bu, which was deprotected (**GP II**) and coupled to deprotected **53** (**GP I**), according to **GP V**. Reductive cleavage of the benzyl ether and subsequent purification of the peptide by column chromatography (**GP VII**) yielded **64**.

MS (ESI, MeOH *m/z*): 1659 ($[M+Na]^+$, (100)).

ϵ_{308} = 100 M⁻¹cm⁻¹

HPLC (Merck LiChroSpher 100-5, RP-18e; acetonitrile/water 0% to 100% in 40 min): t_R 30.1'.

69 Ac-Tyr(OMe)-(Pro)₃-Phe-(Pro)₃-DAP

Ac-Tyr(OMe)-(Pro)₃-Phe-(Pro)₃-OH was prepared by SPPS on proline-preloaded chlorotriyl resin (0.67 mmol/g) on a 400 μmol scale, following **GP VIII**. The cleaved peptide (106 mg, 110 μmol) was coupled to deprotected **53** (100 μmol, **GP I**), according to **GP V**. The resulting peptide **69** was

purified by stirring with activated charcoal in methanol and subsequent column chromatography (**GP VII**) (yield: 105 mg, 66%).

MS (ESI, MeOH m/z): 1612 ($[M+Na]^+$, (100)).

$\epsilon_{308} = 90 \text{ M}^{-1}\text{cm}^{-1}$.

HPLC (Merck LiChroSpher 100-5, RP-18e; acetonitrile/water 0% to 100% in 40 min): t_R 31.2'.

70 Ac-Tyr-(Pro)₃-Phe-(Pro)₃-DAP

Ac-Tyr(*O*tBu)-(Pro)₃-Phe-(Pro)₃-OH was prepared by SPPS on proline-preloaded chlorotriyl resin (0.67 mmol/g) on a 400 μmol scale, following **GP VIII**. The cleaved peptide (156 mg, 155 μmol) was coupled to deprotected **53** (150 μmol , **GP I**), according to **GP V**, but without aq. workup, instead the reaction mixture was evaporated to dryness by coevaporation with toluene and filtered over silica. Cleavage of the *t*butyl ether (**GP IV**) and subsequent purification of the peptide by column chromatography (**GP VII**) yielded **70** (131 mg, 55%).

MS (ESI, MeOH m/z): 1599 ($[M+Na]^+$, (100)).

$\epsilon_{308} = 69 \text{ M}^{-1}\text{cm}^{-1}$.

HPLC (Merck LiChroSpher 100-5, RP-18e; acetonitrile/water 0% to 100% in 40 min): t_R 29.4'.

71 Ac-Tyr-(Pro)-TMP-(Pro)₂-DAP

Boc-Tyr(OBn)-OH was coupled to HN-Pro-*O*tBu according to **GP V**, then deprotected with HCl in dioxane (**GP I**), acetylated (**GP VI**) and deprotected (**GP II**) to yield the free acid Ac-Tyr(OBn)-Pro-OH. Boc-TMP-OH **31** was coupled to HCl·HN-(Pro)₂-*O*tBu (**GP V**) and deprotected (**GP I**) to the amine hydrochloride HCl·H₂N-TMP-(Pro)₂-*O*tBu. Coupling of the free acid to the amine gave the pentapeptide Ac-Tyr(OBn)-Pro-TMP-(Pro)₂-*O*tBu, which was deprotected (**GP II**) and coupled to deprotected **53** (**GP I**), according to **GP V**. Reductive cleavage of the benzyl ether and subsequent purification of the peptide by column chromatography (**GP VII**) yielded **71**.

MS (ESI, MeOH m/z): 1398 ($[M+Na]^+$, (100)).

$$\varepsilon_{308} = 74 \text{ M}^{-1}\text{cm}^{-1}$$

HPLC (Merck LiChroSpher 100-5, RP-18e; acetonitrile/water 0% to 100% in 40 min): t_R 32.5'.

72 Ac-Tyr-Pro-Phe-(Pro)₂-DAP

Ac-Tyr(*Ot*Bu)-Pro-Phe-(Pro)₂-OH was prepared by SPPS on proline-preloaded chlorotriyl resin (0.67 mmol/g) on a 400 μmol scale, following **GP VIII**. The cleaved peptide (122 mg, 170 μmol) was coupled to deprotected **53** (150 μmol , **GP I**), according to **GP V**. Cleavage of the *t*butyl ether (**GP IV**) and subsequent purification of the peptide by column chromatography (**GP VII**) yielded **72** (144 mg, 75%).

MS (ESI, MeOH m/z): 1307 ($[M+Na]^+$, (100)).

$$\varepsilon_{308} = 61 \text{ M}^{-1}\text{cm}^{-1}$$

HPLC (Merck LiChroSpher 100-5, RP-18e; acetonitrile/water 0% to 100% in 40 min): t_R 32.4'.

73 Ac-Tyr-(Pro)₂-TMP-(Pro)₂-DAP

Boc-Tyr(OBn)-OH was coupled to HCl·HN-(Pro)₂-*Ot*Bu according to **GP V**, then deprotected with HCl in dioxane (**GP I**), acetylated (**GP VI**) and deprotected (**GP II**) to yield the free acid Ac-Tyr(OBn)-(Pro)₂-OH. Boc-TMP-OH **31** was coupled to HCl·HN-(Pro)₂-*Ot*Bu (**GP V**) and deprotected to the amine hydrochloride (**GP I**) HCl·H₂N-TMP-(Pro)₂-*Ot*Bu. Coupling of the free acid to the amine gave the hexapeptide Ac-Tyr(OBn)-(Pro)₂-TMP-(Pro)₂-*Ot*Bu, which was deprotected (**GP II**) and coupled to deprotected **53** (**GP I**), according to (**GP V**). Reductive cleavage of the benzyl ether and subsequent purification of the peptide by column chromatography (**GP VII**) yielded **73**.

MS (ESI, MeOH m/z): 1495 ($[M+Na]^+$, (100)), 759 ($[M+2Na]^{2+}$, (7)).

$$\varepsilon_{308} = 100 \text{ M}^{-1}\text{cm}^{-1}$$

HPLC (Merck LiChroSpher 100-5, RP-18e; acetonitrile/water 0% to 100% in 40 min): t_R 32.0'.

74 Ac-Tyr-(Pro)₂-Phe-(Pro)₂-DAP

Ac-Tyr(*Ot*Bu)-(Pro)₂-Phe-(Pro)₂-OH was prepared by SPPS on proline-preloaded chlorotriyl resin (0.67 mmol/g) on a 400 μ mol scale, following **GP VIII**. The cleaved peptide (138 mg, 170 μ mol) was coupled to deprotected **53** (150 μ mol, **GP I**), according to **GP V**. Cleavage of the *t*butyl ether (**GP IV**) and subsequent purification of the peptide by column chromatography (**GP VII**) yielded **74** (126 mg, 52%).

MS (ESI, MeOH m/z): 1404 ($[M+Na]^+$, (100)).

$\epsilon_{308} = 69 \text{ M}^{-1}\text{cm}^{-1}$.

HPLC (Merck LiChroSpher 100-5, RP-18e; acetonitrile/water 0% to 100% in 40 min): t_R 31.4'.

10.4 List of LFP Experiments

2-Acetylamino-3-(4-hydroxy-phenyl)-propionic acid 2-(2,2-dimethyl-propionyl)-3-(diphenoxy-phosphoryloxy)-tetrahydro-furan-2-ylmethyl ester [Ac-Tyr-Inj] (13)

Figure 15, page 29.

2-Acetylamino-(rac)-3-(2,4,6-trimethoxy-phenyl)-propionic acid 2-(2,2-dimethyl-propionyl)-3-(diphenoxy-phosphoryloxy)-tetrahydro-furan-2-ylmethyl ester [(rac)-Ac-TMP-Inj] (14)

Figure 15, page 29.

2-Acetylamino-(rac)-3-(2,4-dimethoxy-phenyl)-propionic acid 2-(2,2-dimethyl-propionyl)-3-(diphenoxy-phosphoryloxy)-tetrahydro-furan-2-ylmethyl ester [(rac)-Ac-DMP-Inj] (15)

Figure 15, page 29.

Ac-(rac)TMP-Pro-(rac)DMP-Inj (16)

Figure 17, page 32.

Ac-Tyr-Pro-(rac)DMP-Inj (17)

Figure 18, page 33.

Ac-Phe-(Pro)3-Phe-(Pro)3-DMP-Inj (35)

Figure 20, page 45; Figure 25, page 52.

Ac-Tyr-(Pro)3-Phe-(Pro)3-Phe-OMe (36)

Figure 20, page 45; Figure 25, page 52; Figure 36, page 74.

Ac-Tyr-Pro-TMP-Pro-DMP-Inj (37)

Figure 22, page 48.

Ac-Tyr-(Pro)3-DMP-Inj (38)

Figure 23, page 49.

Ac-Tyr-(Pro)3-TMP-(Pro)3-DMP-Inj (39)

Figure 24, page 50.

Ac-Phe-(Pro)3-TMP-(Pro)3-Phe-OMe (40)

Figure 25, page 52.

Ac-Tyr-(Pro)3-TMP-Pro-DMP-Inj (41)

Figure 26, page 53.

Ac-Tyr-Pro-TMP-(Pro)3-DMP-Inj (42)

Figure 27, page 54.

Ac-Tyr-(Pro)6-TMP-Pro-DMP-Inj (43)

Figure 28, page 55.

Ac-Tyr-Pro-Phe-Pro-DMP-Inj (59)

Figure 30 (upper left), page 64

Ac-Tyr-Pro-Phe-(Pro)3-DMP-Inj (60)

Figure 30 (lower left), page 64

Ac-Tyr-Pro-Phe-Pro-DAP (61)

Figure 30 (upper right), page 64

Ac-Tyr-Pro-Phe-(Pro)3-DAP (62)

Figure 30 (lower right), page 64

Ac-Tyr-Pro-TMP-(Pro)3-DAP (63)

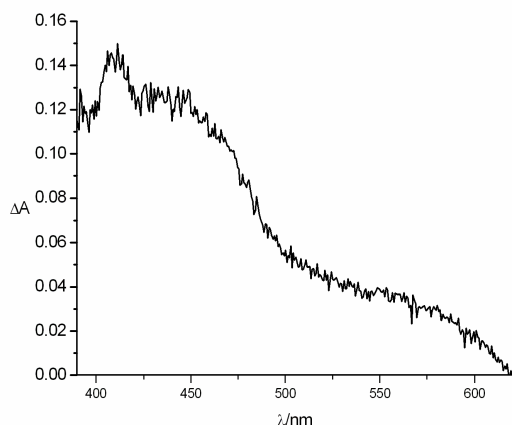


Figure 44: Transient absorption spectrum of peptide 63, 40 ns after laser irradiation.

Ac-Tyr-(Pro)3-TMP-(Pro)3-DAP (64)

Figure 31, page 68; Figure 34, page 72.

Ac-Tyr-(Pro)3-Ala-(Pro)3-DAP (65)

Figure 35, page 73.

Ac-Tyr-(Pro)3-Leu-(Pro)3-DAP (66)

Figure 37, page 75.

Ac-Tyr-(Pro)3-Tyr(OMe)-(Pro)3-DAP (67)

Figure 38, page 76.

Ac-Tyr-(Pro)3-DMP-(Pro)3-DAP (68)

Figure 39, page 77.

Ac-Tyr(OMe)-(Pro)3-Phe-(Pro)3-DAP (69)

Figure 36, page 74.

Ac-Tyr-(Pro)3-Phe-(Pro)3-DAP (70)

Figure 42, page 83.

Ac-Tyr-(Pro)-TMP-(Pro)₂-DAP (71)

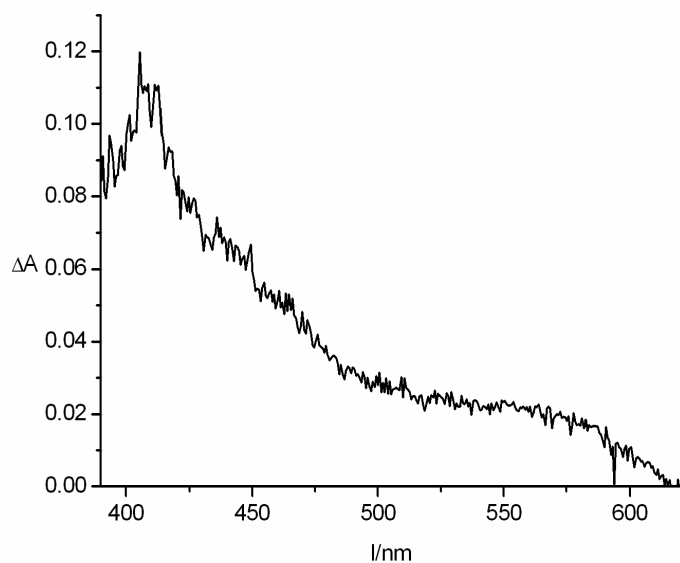


Figure 45: Transient absorption spectrum of peptide 71, 40 ns after irradiation.

Ac-Tyr-Pro-Phe-(Pro)₂-DAP (72)

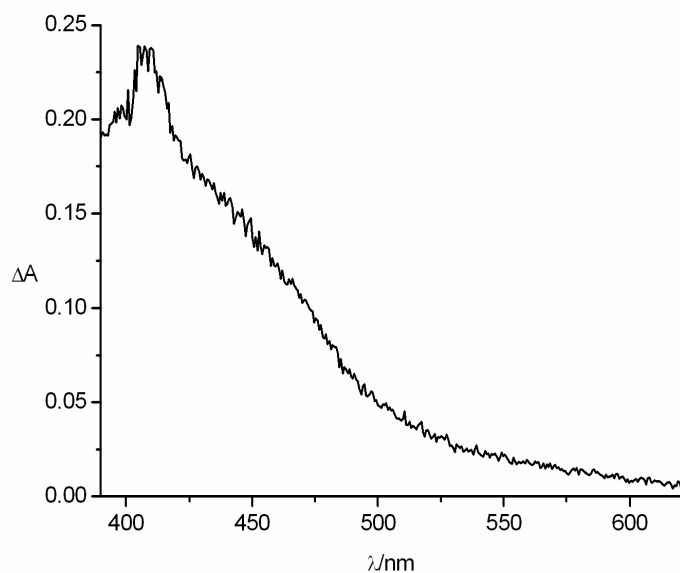


Figure 46: Transient absorption spectrum of peptide 72, 40 ns after irradiation.

Ac-Tyr-(Pro)₂-TMP-(Pro)₂-DAP (73)

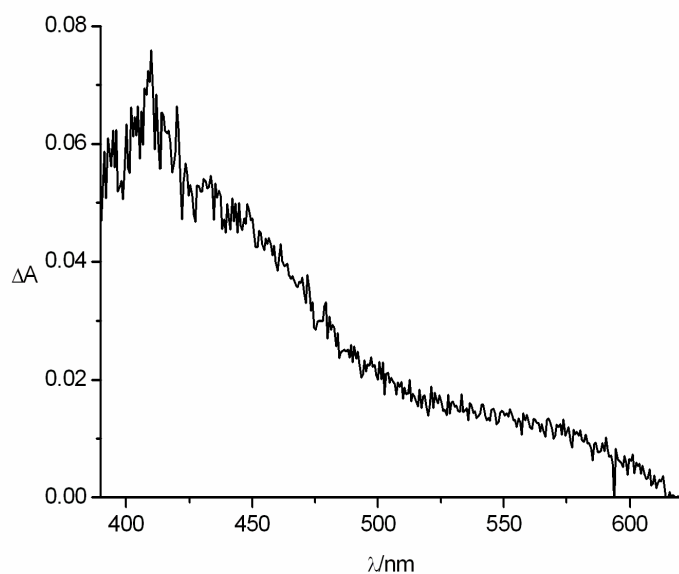


Figure 47: Transient absorption spectrum of peptide 59, 40 ns after irradiation.

Ac-Tyr-(Pro)₂-Phe-(Pro)₂-DAP (74)

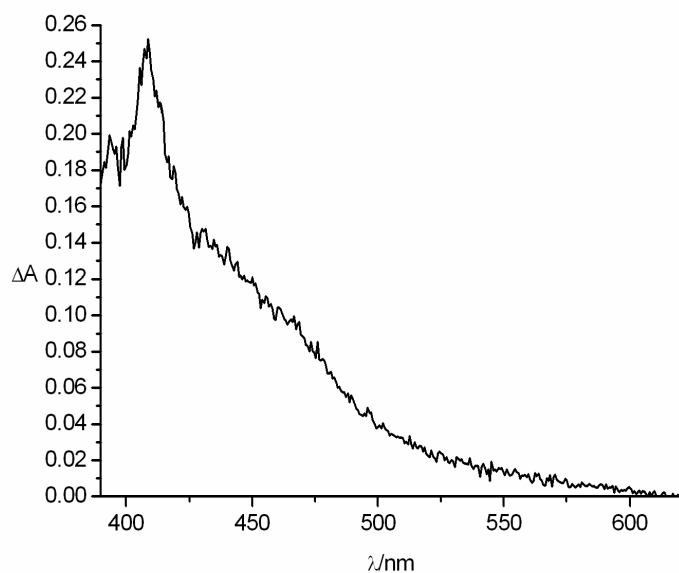


Figure 48: Transient absorption spectrum of peptide 74, 40 ns after irradiation.

11 Abbreviations

A	acceptor (electron acceptor)
Å	Ångström
abs.	absolute
Ac	acetyl
Ac ₂ O	acetic anhydride
approx.	approximately
aq.	aqueous
Ar	aromatic (aryl)
Asp	aspartate
Bn	benzyl
Boc	<i>tert</i> -butyloxycarbonyl
Boc ₂ O	di- <i>tert</i> -butyldicarbonate
BP	biphenyl
br	broad
C	activated charcoal
°C	Celsius degree
calc.	calculated
CCD	charge coupled device
CD	circular dichroism
cf.	confer
cm	centimetre
Cys	cysteine
D	donor (electron donor)
δ	chemical shift (NMR)
ΔA	transient absorption
DAP	3-{4-[2-(2,2-dimethylpropionyl)-3-(diphenoxyphosphoryl-oxy)tetrahydrofuran-2-ylmethoxy]-2-methoxyphenyl}propionic acid methylester
DCN	dicyanonaphtalene
DIPEA	N,N'-diisopropylethylamine
DMAP	4-(dimethylamino)-pyridine
DMF	dimethylformamide
DMP	2,4-dimethoxyphenylalanine
DMSO	dimethylsulfoxide

DNA	2'-deoxyribonucleic acid
ϵ	extinction coefficient
EA	elemental analysis
<i>ee</i>	enantiomeric excess
e.g.	for example
e.i.	that is
EI	electron ionization
eq.	equivalent
ESI-MS	electron spray ionisation mass spectrometry
ET	electron transfer
Et	ethyl
EtOAc	ethylacetate
FAB	fast atom bombardement
Fmoc	9H-fluoren-9-ylmethoxycarbonyl
g	gram
GP	general procedure
h	hour(s)
HCTU	2-(6-chloro-1-H-benzotriazole-1-yl)-1,1,3,3-tetramethyl-uronium hexafluoro-phosphate
His	histidine
h ν	light
HOAc	acetic acid
HPLC	high performance liquid chromatography
HRMS	high resolution mass spectrometry
i.e.	that is
<i>J</i>	coupling constant
k	rate constant
λ	wavelength
LFP	laser flash photolysis
M	molar (mol/L)
μ	micro
M.p.	melting point
max	maximum
Me	methyl
MeOH	methanol
mg	milligram

Abbreviations

MHz	megahertz
min	minute
mL	milliliter
mM	millimolar
MS	mass spectrometry
NBA	3-nitrobenzyl alcohol
NHE	normal hydrogen electrode
nm	nanometre
NMR	nuclear magnetic resonance
ns	nanosecond
OD	optical density
Ph	phenyl
Phe	phenylalanine
PPII	polyproline II
ppm	parts per million
Pro	Proline
PSII	photosystem II
Py	pyridine
R	relay
r.t.	room temperature
rac	racemic
resp.	respectively
RNR	ribonucleotide reductase
RP	reverse phase
s	second
sat.	saturated
SCE	standard calomel electrode
SPPS	solid phase peptide synthesis
<i>t</i> or <i>tert</i>	tertiary
TBAPF ₆	tetrabutylammonium hexafluorophosphate
TBTU	2-(1H-benzotriazole-1-yl)-1,1,3,3-tetramethyluronium tetrafluoroborate
<i>t</i> -Bu	<i>tert</i> -butyl
Tf	triflate (trifluoromethanesulfonate)
Tf ₂ O	triflic anhydride
TFA	trifluoroacetic acid
TLC	thin layer chromatography

Abbreviations

TMP	2,4,6-trimethoxyphenylalanine
TMS	tetramethylsilate
t_R	retention time
Trp	tryptophane
Tyr	tyrosine
UV	ultraviolet
UV-Vis	ultraviolet and visible
V	volt
v	volume
vs.	versus

12 References

- [1] A. Szent-Györgyi, *Science* **1941**, *93*, 609.
- [2] M. G. Evans, J. Gergely, *Biochim. Biophys. Acta.* **1949**, *3*, 188.
- [3] P. Mitchell, *Nature* **1961**, 144.
- [4] A. L. Lehninger, D. L. Nelson, M. M. Cox, *Principles of Biochemistry*, Worth Publishers, New York, **1998**.
- [5] J. H. A. Nugent, *Eur. J. Biochem* **1996**, *237*, 519.
- [6] J. M. Hudson, K. Heffron, V. Kotlyar, Y. Sher, E. Maklashina, G. Cecchini, F. A. Armstrong, *J. Am. Chem. Soc.* **2005**, *127*, 6977.
- [7] W. L. Smith, T. E. Eling, R. J. Kulmacz, L. J. Marnett, A.-L. Tsai, *Biochemistry* **1992**, *31*, 3.
- [8] J. Stubbe, *Curr. Opin. Chem. Biol.* **2003**, *7*, 183.
- [9] Y.-T. Long, E. Abu-Irhayem, H.-B. Kraatz, *Chem. Eur. J.* **2005**, *11*, 5186.
- [10] R. A. Marcus, *Angew. Chem. Int. Ed. Engl.* **1993**, *32*, 1111.
- [11] R. A. Marcus, N. Sutin, *Biochim. Biophys. Acta* **1985**, *811*, 265.
- [12] V. G. Levich, *Adv. Electrochem. Sci. Eng.* **1966**, *4*, 249.
- [13] H. B. Gray, J. R. Winkler, *Q. Rev. Biophys.* **2003**, *36*, 341.
- [14] J. R. Winkler, H. B. Gray, T. R. Prytkova, I. V. Kurnikov, D. N. Beratan, in *Bioelectronics* (Eds.: I. Willner, E. Katz), Wiley-VCH, Weinheim, **2005**, pp. 15.
- [15] B. P. Paulson, J. R. Miller, W.-X. Gan, G. Closs, *J. Am. Chem. Soc.* **2005**, *127*, 4860.
- [16] D. DeVault, B. Chance, *Biophys. J.* **1966**, *6*, 825.
- [17] J. J. Hopfield, *Proc. Natl. Acad. Sci. U. S. A.* **1974**, *71*, 3640.
- [18] H. M. McConnell, *J. Chem. Phys.* **1961**, *35*, 508.
- [19] C. C. Moser, J. M. Keske, K. Warncke, R. S. Farid, P. L. Dutton, *Nature* **1992**, *355*, 796.
- [20] C. C. Page, C. C. Moser, X. X. Chen, P. L. Dutton, *Nature* **1999**, *402*, 47.
- [21] C. C. Page, C. C. Moser, P. L. Dutton, *Curr. Opin. Chem. Biol.* **2003**, *7*, 551.
- [22] C. C. Moser, C. C. Page, P. L. Dutton, *Phil. Trans. R. Soc. B* **2006**, *361*, 1295.
- [23] R. Langen, J. L. Colón, D. R. Casimiro, T. B. Karpishin, J. R. Winkler, H. B. Gray, *J. Biol. Inorg. Chem.* **1996**, *1*, 221.
- [24] N. M. Kostic, R. Margalit, C.-M. Che, H. B. Gray, *J. Am. Chem. Soc.* **1983**, *105*, 7765.
- [25] I.-J. Chang, H. B. Gray, J. R. Winkler, *J. Am. Chem. Soc.* **1991**, *113*, 7056.
- [26] H. B. Gray, J. R. Winkler, *Proc. Natl. Acad. Sci. U. S. A.* **2005**, *102*, 3534.
- [27] D. N. Beratan, J. N. Onuchic, *Photosynth. Res.* **1989**, *22*, 173.
- [28] D. N. Beratan, J. N. Onuchic, *Photosynth. Res.* **1992**, *22*, 173.
- [29] D. N. Beratan, J. N. Onuchic, J. J. Hopfield, *J. Phys. Chem.* **1987**, *86*, 4488.
- [30] J. N. Onuchic, D. N. Beratan, J. R. Winkler, H. B. Gray, *Science* **1992**, *258*, 1740.
- [31] T. R. Prytkova, I. V. Kurnikov, D. N. Beratan, *Science* **2007**, *315*, 622.
- [32] S. S. Skourtis, I. A. Balabin, T. Kawatsu, D. N. Beratan, *Proc. Natl. Acad. Sci. U. S. A.* **2005**, *102*, 3552.
- [33] A. A. Stuchebrukhov, *Theor. Chem. Acc.* **2003**, *110*, 291.
- [34] F. Polo, S. Antonello, F. Formaggio, C. Tonioli, F. Maran, *J. Am. Chem. Soc.* **2005**, *127*, 492.
- [35] S. Antonello, F. Formaggio, A. Moretto, C. Tonioli, F. Maran, *J. Am. Chem. Soc.* **2003**, *125*, 2874.
- [36] J. K. Barton, M. E. Nunez, *Curr. Opin. Chem. Biol.* **2000**, *4*, 199.
- [37] B. Giese, *Top. Curr. Chem.* **2004**, *236*, 27.
- [38] B. Giese, *Curr. Opin. Chem. Biol.* **2002**, *6*, 612.
- [39] G. B. Schuster, *Acc. Chem. Res.* **2000**, *33*, 253.
- [40] F. D. Lewis, R. L. Letsinger, M. R. Wasielewski, *Acc. Chem. Res.* **2001**, *34*, 159.
- [41] M. Bixon, J. Jortner, *J. Am. Chem. Soc.* **2001**, *123*, 12556.
- [42] M. Bixon, J. Jortner, *J. Chem. Phys.* **2002**, *281*, 393.

- [43] J. Jortner, M. Bixon, T. Langenbacher, M. E. Michel-Beyerle, *Proc. Natl. Acad. Sci. U. S. A.* **1998**, *95*, 12759.
- [44] B. Giese, M. Spichty, *Chem. Phys. Chem.* **2000**, *1*, 195.
- [45] E. Sim, *J. Phys. Chem. B* **2005**, *109*, 11829.
- [46] J. Stubbe, D. G. Nocera, C. S. Yee, C. Y. Chang, *Chem. Rev.* **2003**, *103*, 2167.
- [47] M. Ekberg, S. Potsch, E. Sandin, M. Thunissen, P. Nordlund, M. Sahlin, B. M. Sjöberg, *J. Biol. Chem.* **1998**, *273*, 21003.
- [48] U. Rova, A. Adrait, S. Potsch, A. Graslund, L. Thelander, *J. Biol. Chem.* **1999**, *274*, 23746.
- [49] M. C. Y. Chang, C. S. Yee, D. G. Nocera, J. Stubbe, *J. Am. Chem. Soc.* **2004**, *126*, 16702.
- [50] M. R. Seyedsayamdost, C. S. Yee, S. Y. Reece, D. G. Nocera, J. Stubbe, *J. Am. Chem. Soc.* **2006**, *128*, 1562.
- [51] C. Aubert, M. H. Vos, P. Mathis, A. P. M. Eker, K. Brettel, *Nature* **2000**, *405*, 586.
- [52] Y. F. Li, P. F. Heelis, A. Sancar, *Biochemistry* **1991**, *30*, 6322.
- [53] T. Carell, L. T. Burgdorf, L. M. Kundu, M. Cichon, *Curr. Opin. Chem. Biol.* **2001**, *5*, 491.
- [54] J. H. A. Nugent, *Eur. J. Biochem.* **1996**, *237*, 519.
- [55] E. W. Schlag, D.-Y. Yang, S.-Y. Sheu, H. L. Selzle, S. H. Lin, P. M. Rentzepis, *Proc. Natl. Acad. Sci.* **2000**, *97*, 9849.
- [56] S.-Y. Sheu, E. W. Schlag, D.-Y. Yang, H. L. Selzle, *J. Phys. Chem.* **2001**, *105*, 6353.
- [57] E. W. Schlag, S.-Y. Sheu, D.-Y. Yang, H. L. Selzle, S. H. Lin, *Angew. Chem.* **2007**, *119*, 3258.
- [58] R. A. Malak, Z. Gao, J. F. Wishart, S. S. Isied, *J. Am. Chem. Soc.* **2004**, *126*, 13888.
- [59] H.-B. Kraatz, I. Bediako-Amoa, S. H. Gyepi-Garbrah, T. C. Sutherland, *J. Phys. Chem. B* **2004**, *108*, 20164.
- [60] I. Bediako-Amoa, T. C. Sutherland, C.-Z. Li, R. Silerova, H.-B. Kraatz, *J. Phys. Chem. B* **2004**, *108*, 704.
- [61] I. Pujols-Ayala, C. A. Sacksteder, B. A. Barry, *J. Am. Chem. Soc.* **2003**, *125*, 7536.
- [62] S. S. Isied, M. Y. Ogawa, J. F. Wishart, *Chem. Rev.* **1992**, *92*, 381.
- [63] D. R. Striplin, S. Y. Reece, D. G. McCafferty, C. G. Wall, D. A. Friesen, B. W. Erickson, T. J. Meyer, *J. Am. Chem. Soc.* **2004**, *126*, 5282.
- [64] S. A. Serron, W. S. Aldridge III, C. N. Fleming, R. M. Danell, M.-H. Baik, M. Sykora, D. M. Dattelbaum, T. J. Meyer, *J. Am. Chem. Soc.* **2004**, *126*, 14506.
- [65] B. Giese, M. Napp, O. Jacques, H. Boudebous, A. M. Taylor, J. Wirz, *Angew. Chem. Int. Ed.* **2005**, *44*, 4073.
- [66] M. Napp, Dissertation thesis, University of Basel (Basel), **2004**.
- [67] E. Meggers, M. E. Michel-Beyerle, B. Giese, *J. Am. Chem. Soc.* **1998**, *120*, 12950.
- [68] E. Meggers, D. Kusch, M. Spichty, U. Wille, B. Giese, *Angew. Chem. Int. Ed.* **1998**, *37*, 460.
- [69] J. H. Horner, E. Taxil, M. Newcomb, *J. Am. Chem. Soc.* **2002**, *124*, 5402.
- [70] E. Taxil, L. Bagnol, J. H. Horner, M. Newcomb, *Org. Lett.* **2003**, *5*, 827.
- [71] K. Bernhard, J. Geimer, M. Canle-Lopez, J. Reynisson, D. Beckert, R. Gleiter, S. Steenken, *Chem. Eur. J.* **2001**, *7*, 4640.
- [72] M. Faraggi, M. R. Defelippis, M. H. Klapper, *J. Am. Chem. Soc.* **1989**, *111*, 5141.
- [73] E. Meggers, A. Dussy, T. Schäfer, B. Giese, *Chem. Eur. J.* **2000**, *6*, 485.
- [74] E. Hasler, A. Hörmann, G. Persy, H. Pletsch, J. Wirz, *J. Am. Chem. Soc.* **1993**, *115*, 5400.
- [75] J. Wirz, *Pure Appl. Chem.* **1984**, *56*, 1289.
- [76] E. Leyva, M. S. Platz, G. Persy, J. Wirz, *J. Am. Chem. Soc.* **1986**, *108*, 3783.
- [77] A. Harriman, *J. Phys. Chem.* **1987**, *91*, 6102.
- [78] R. H. Schuler, P. Neta, H. Zemel, R. W. Fessenden, *J. Am. Chem. Soc.* **1976**, *98*, 3826.
- [79] A. Vassilian, J. F. Wishart, B. Vanhemelryck, H. Schwarz, S. S. Isied, *J. Am. Chem. Soc.* **1990**, *112*, 7278.
- [80] P. O'Neill, S. Steenken, D. Schulte-Frohlinde, *J. Phys. Chem.* **1975**, *79*, 2773.
- [81] N. Ichinose, T. Tanaka, S. Kawanishi, T. Suzuki, *J. Phys. Chem. A* **1999**, *103*, 7923.
- [82] D. Chiapperino, S. McIlroy, D. E. Falvey, *J. Am. Chem. Soc.* **2002**, *124*, 3567.
- [83] A. Zweig, W. G. Hodgson, W. H. Jura, *J. Am. Chem. Soc.* **1964**, *86*, 4124.
- [84] S. Dileesh, K. R. Gopidas, *Chem. Phys. Lett.* **2000**, *330*.

- [85] P. Jacques, X. Allonas, M. von Raumer, P. Suppan, E. Haselbach, *J. Photochem. Photobiol. A* **1997**, *111*, 41.
- [86] S. Yasui, M. Tsujimoto, K. Itoh, A. Ohno, *J. Org. Chem.* **2000**, *65*, 4715.
- [87] T. A. Gadosy, D. Shukla, L. J. Johnston, *J. Phys. Chem. A* **1999**, *103*, 8834.
- [88] D. Dauzonne, R. Royer, *Synthesis* **1987**, 399.
- [89] R. Glatthaar, M. Spichty, A. Gugger, R. Batra, W. Damm, M. Mohr, H. Zipse, B. Giese, *Tetrahedron* **2000**, *56*, 4117.
- [90] A. Marx, P. Erdmann, M. Senn, S. Körner, T. Jungo, M. Petretta, P. Imwinkelried, A. Dussy, K. J. Kulicke, L. Macko, M. Zehnder, B. Giese, *Helv. Chim. Acta* **1996**, *79*, 1980.
- [91] K. Kim, K. Parang, O. D. Lau, P. A. Cole, *Bioorg. Med. Chem.* **2000**, *8*, 1263.
- [92] F. M. Bautista, J. M. Campelo, A. García, D. Luna, J. M. Marinas, A. A. Romero, *J. Chem. Soc. Perkin Trans. 2* **2002**, 227.
- [93] U. Nagel, *Angew. Chem.* **1984**, *96*, 425.
- [94] M. Tagaki, K. Yamamoto, *Tetrahedron* **1991**, *47*, 8869.
- [95] A. Gugger, Dissertation thesis, University of Basel **2000**.
- [96] S. Kakinoki, Y. Hirano, M. Oka, *Polym. Bull.* **2005**, *53*, 109.
- [97] I. Z. Steinberg, W. F. Harrington, A. Berger, M. Sela, E. Katchalsky, *J. Am. Chem. Soc.* **1960**, *82*, 5263.
- [98] J. Engel, *Biopolymers* **1966**, *4*, 440.
- [99] B. J. Stapley, T. P. Creamer, *Protein Sci.* **1999**, *8*, 587.
- [100] Z. Shi, K. Chen, Z. Liu, N. R. Kallenbach, *Chem. Rev.* **2006**, *106*, 1877.
- [101] A. Berger, J. Kurtz, E. Katchalsky, *J. Am. Chem. Soc.* **1954**, 76.
- [102] P. M. Cowan, S. McGavin, *Nature* **1955**, *176*, 501.
- [103] B. Schuler, E. A. Lipman, P. J. Steinbach, W. A. Eaton, *Proc. Natl. Acad. Sci.* **2005**, *102*, 2754.
- [104] L. Stryer, R. P. Haugland, *Proc. Natl. Acad. Sci. U. S. A.* **1967**, *58*, 719.
- [105] D. G. McCafferty, D. A. Friesen, E. Danielson, C. G. Wall, M. J. Saderholm, B. W. Erickson, T. J. Meyer, *Proc. Natl. Acad. Sci. U. S. A.* **1996**, *93*, 8200.
- [106] R. Huisgen, in *Methoden der Organischen Chemie (Houben-Weyl)*, Vol. 3 (Ed.: E. Müller), Georg Thieme Verlag, Stuttgart, **1955**, pp. 139.

Curriculum Vitae

MEIKE CORDES

PERSONAL INFORMATION

Date/Place of birth April 19, 1980 in D-Mülheim/Ruhr
Nationality German

EDUCATION

10/2004 – 04/2008 **PhD** work at the University of Basel (CH), Departement of Chemistry, *How Do Amino Acids Transport Electrons Through Peptides?*, supervisor: Prof. B. Giese
11/2005 – 11/2007 Distance learning: **Specialised Journalism** (Deutsche Fachjournalisten-Schule)
08/2004 **Diploma (Chemistry)**
01/2004 – 08/2004 **Diploma thesis**, supervisor: Prof. M. Bröring (Philipps Universität Marburg, D), *Mn(IV)corrols with σ -Aryl-Substituents*
08/2002 – 01/2003 **Exchange student** at Stockholms Universitet, Sweden
10/2001 **Vordiplom**
08/1999 – 08/2004 **Chemistry studies** at Philipps-Universität Marburg
18.05.1999 **Abitur** (Gymnasium Broich, Mülheim/Ruhr, D)

SCHOLARSHIPS

03/2005 – 03/2007 Kekulé-grant for PhD students (Stiftung Stipendien-Fonds, Verband der Chemischen Industrie)
04/2002 – 08/2004 Online-grant e-fellows.net (current status: Alumnus)

TEACHING

10/2006 – 01/2008 Lecture assistance: basic lectures in organic chemistry
04/2005 – 07/2006 Laboratory teaching assistant in organic chemistry for 2nd year biology and pharmacy students; participation in the reorganisation of the course due to increasing number of students
04/2004 – 07/2004 Laboratory teaching assistant for 1st year biology students
10/2001 – 06/2002 Laboratory teaching assistant for 1st year medicine students

PUBLICATIONS

Bröring M, Cordes M, Köhler S: **Manganese(IV) Corroles with σ -Aryl Ligands**. *Z. Anorg. Allg. Chem.* 2008, 125.

Bröring M, Link S, Cordes M, Brandt C: **Oxidative Pyrrole Exchange and meso Pyrrolylation - Unexpected Reactions of Open-Chain Tetrapyrrolic 2,2'-Bidipyrins**. *Z. Anorg. Allg. Chem.* 2007, 211.

Cordes, M., Köttgen, A., Jasper, C., Jacques, O., Boudebous, H., Giese, B.: **Development of a Model System for the Study of Long Distance Electron Transfer in Peptides**, *Adv. Synth. Cat.*, in press.

Cordes, M., Köttgen, A., Jasper, C. Jacques, O., Boudebous, H., Giese, B.: **Influence of Amino Acid Side Chains on Long-Distance Electron Transfer in Peptides: Electron Hopping via "Stepping Stones"**, *Angew. Chem. Int. Ed.* 2008, 47, 3461.

Eidesstattliche Erklärung

Ich erkläre, dass ich die Dissertation "How Do Amino Acids Transport Electrons Through Peptides?" nur mit der darin angegebenen Hilfe verfasst und bei keiner anderen Universität und keiner anderen Fakultät der Universität Basel eingereicht habe.

Basel, 11.03.2008

Meike Cordes